UNIVERSIDADE TÉCNICA DO ATLÂNTICO
INSTITUTO DE ENGENHARIA E CIÊNCIAS DO MAR

WEST AFRICAN SCIENCE SERVICE CENTRE ON CLIMATE CHANGE AND ADAPTED LAND USE

Master Thesis

GRAVITATIONAL ENERGY POTENTIAL AND MULTI-CRITERIA ASSESSMENT OF MARINE GRAVITATION ENERGY SITES IN CABO VERDE

HAFEEZ OPEYEMI OLADEJO

Master Research Program on Climate Change and Marine Sciences

São Vicente
2021

UNIVERSIDADE TÉCNICA DO ATLÂNTICO
INSTITUTO DE ENGENHARIA E CIÊNCIAS DO MAR

WEST AFRICAN SCIENCE SERVICE CENTRE ON CLIMATE CHANGE AND ADAPTED LAND USE

Master Thesis

GRAVITATIONAL ENERGY POTENTIAL AND MULTI-CRITERIA ASSESSMENT OF MARINE GRAVITATION ENERGY SITES IN CABO VERDE

HAFEEZ OPEYEMI OLADEJO

Master Research Program on Climate Change and Marine Sciences

Supervisor | Dr. Gael Alory

São Vicente
2021

UNIVERSIDADE TÉCNICA DO ATLÂNTICO
INSTITUTO DE ENGENHARIA E CIÊNCIAS DO MAR

WEST AFRICAN SCIENCE SERVICE CENTRE ON CLIMATE CHANGE AND ADAPTED LAND USE

Gravitational Energy Potential and Multi-criteria Assessment of Marine Gravitation Energy Sites in Cape Verde

Hafeez Opeyemi Oladejo

Master's thesis presented to obtain the master's degree in Climate Change and Marine Sciences, by the Institute of Engineering and Marine Sciences, Atlantic Technical University in the framework of the West African Science Service Centre on Climate Change and Adapted Land Use

Supervisor

DR. GAEL ALORY
Toulouse, LEGOS

São Vicente
2021

UNIVERSIDADE TÉCNICA DO ATLÂNTICO
INSTITUTO DE ENGENHARIA E CIÊNCIAS DO MAR

WEST AFRICAN SCIENCE SERVICE CENTRE ON CLIMATE CHANGE AND ADAPTED LAND USE

Gravitational Energy Potential and Multi-criteria Assessment of Marine Gravitation Energy Sites in Cape Verde

Hafeez Opeyemi Oladejo

Panel defense

President

_____

Examiner 1

_____

Examiner 2

_____

São Vicente
2021

Financial support

The German Federal Ministry of Education and Research (BMBF) in the framework of the West African Science Service Centre on Climate Change and Adapted Land Use (WASCAL) through WASCAL Graduate Studies Programme in Climate Change and Marine Sciences at the Institute for Engineering and Marine Sciences, Atlantic Technical University, Cabo Verde.

Dedication

This work is dedicated to people facing energy challenge especially those from the Sub-Saharan part of Africa experiencing constant interrupted electricity supply.

Acknowledgements

All praise and thank belong to the Creator for the grace and mercy throughout my life, the era of the pandemic, and the completion of my master's program.

Special thanks to my supervisor, and to Professor Vladimiro Miranda for their support, dedication, guidance, and intuitive reasoning, and ideas that are put into this work.

Also, I would like to thank all the data providers for this research starting from the I-Atlantic group including Dr. Rui Freitas, Irene Perrez, and Vikki Gunn for the high-resolution bathymetry data, and also Dr. Jonathan Gula for the high-resolution ocean current data.

I can't thank the director of my master's program enough for her support, motherly advice throughout this program.

I appreciate the advice, support, and guidance of our scientific coordinator.

To all WASCAL Cabo Verde staff, I really thank you all.

To all my colleagues, I appreciate sharing the strength and courage we give one another, especially over these past difficult periods.

To my family, I'm appreciative of your motivation, love, and support throughout my life.

Resumo

Neste estudo, foi avaliado o potencial de Armazenamento de Energia Gravitacional Marinha (MGES), e o conceito de análise de decisão multicritério foi adotado para classificar as águas de Cabo Verde em zonas aptas para dois casos de instalação de MGES. O presente estudo começou-se por analisar o estado energético de Cabo Verde, dando especial atenção à energia eólica. Uma variedade de conjuntos de dados, incluindo sensoriamento remoto, *in-situ*, saídas de modelo, provedores de dados demográficos e publicações de pesquisa foram combinados. Esta análise evidenciou que o consumo de energia eólica está diminuindo ao longo dos anos, enquanto as emissões de CO_2 e o consumo de combustíveis fósseis estão aumentando, devido curtailement, intermitência e ineficiência da rede, resultando em preços de eletricidade altos e instáveis, desperdício de energia e impactos negativos na economia. Cabo Verde possui uma enorme capacidade para outras energias renováveis marinhas e terrestres, mas muitas delas são caracterizadas por intermitência temporal. Vários locais no oeste, centro e sul de Cabo Verde são adequados para o sistema *offshore* com uma alta capacidade de armazenamento de 6 a 11 kWh. A maioria das ilhas também possui porções de suas águas circundantes adequadas para o sistema conectado em terra, variando de 4 a 7 kWh e podendo chegar a 8 kWh ao redor da cadeia de ilhas na região sul. As ilhas com maior população já detêm turbinas eólicas instaladas e também correspondem a ilhas com maior potencial para MGES. Assim, o empilhamento estratégico de várias massas poderia atender a capacidade atual de consumo de energia em Cabo Verde, e o investimento em tecnologias de armazenamento como o MGES irá melhorar a penetração de energias renováveis, reduzir as emissões de CO_2 e dependência de combustíveis fósseis, melhorar a estabilidade da rede e atingir a meta do governo cabo-verdiano de se tornar uma nação 100% renovável.

Palavras-chave: multicritério, redução, intermitência, aptidão, MGES

Abstract

In this study, the Marine Gravitational Energy Storage (MGES) potential was evaluated, and the concept of multi-criteria decision analysis was adopted to classify Cabo Verde's waters into zones of suitability and quantify the storable energy for two cases of MGES installation. We started by first analyzing the energy state of Cabo Verde with a special attention on wind energy. We combined a variety of datasets including remote sensing, in-situ, model outputs, demography data providers, and research publications. This study highlighted that wind energy consumption is declining over the years while CO_2 emission and fossil fuels consumption are increasing due to energy curtailment, intermittency, and grid inefficiency, and consequently resulting in high and unstable electricity prices, energy waste, and negative impacts on the economy. Cabo Verde possesses an enormous renewable capacity for other marine and land-based renewables but many of them are characterized by temporal intermittency. Several locations in the western, central, and southern Cabo Verde are sites that are optimally suitable for the offshore system with a high storage capacity of 6 to 12 kWh per ton of mass. Similarly, most of the islands have portions of their surrounding waters optimally suitable for the onshore-connected system ranging from 3 to 7 kWh and can reach 8 kWh around the South Island chain. Many of the highly populous islands with installed wind turbines also correspond to islands possessing the greatest potential for MGES. Thus, stacking up several masses strategically could meet the current capacity of energy consumption in Cabo Verde, and investment in storage technologies like MGES will improve renewable penetration, reduce CO_2 emission and reliance on fossil fuels, improve grid stability, and achieve the goal of Cabo Verdean government of becoming a nation with 100% renewable.

Keywords: Multi-criteria, Curtailment, Intermittency, Suitability, and MGES

Abbreviations List

AHP	Analytical Hierarchy Process
ARES	Advanced rail energy storage
BE	Buoyant Energy
CAES	Compressed Air Energy Storage
CC	Canary Current
CC	Canary Current
CVFZ	Cabo Verde Frontal Zone
DOGES	Deep ocean gravitational energy storage
DTM	Digital Terrain Model
EEST	Electrical energy storage technologies
ESS	Energy storage system
FES	Flywheel energy storage
GD	Guinea Dome
GES(T)	Gravity energy storage (technology)
GHG	Greenhouse gas
GPM	Gravity Power Module
GWh	Gigawatt-hours
ITCZ	Intertropical Convergence Zone
MC	Mauritanian Current
MCDA	Multiple-criteria decision analysis
MES	Mechanical Energy Storage
MESS	Mechanical energy storage system
MGES(T)	Marine Gravity energy storage (technology)
MGH	Maritime Green Horizon
MWh	Megawatt-hours
NEC	North Equatorial Current
NEC	North Equatorial Current
NECC	North Equatorial Counter-Current
NEU	North Equatorial Undercurrent
ORES	Ocean Renewable Energy Storage

OTEC	Ocean Thermal Energy Conversion
PSH = PHES	Pumped-storage hydropower
PV	Polyvoltaic
RERs	Renewable energy resources
RES	Renewable energy source
SIDS	Small island developing states
SST	Sea surface temperature
UOSS	Underwater Ocean Storage Systems
UWCAES	Underwater compressed air energy storage

General Index

Figure Index

Table Index

1. Introduction

Renewable energy technologies have offered humanity a principal solution to unsustainable energy consumption. Since the intense civilization and industrialization over the past few decades have brought a total reformation to the contemporary society to the levels that the importance of energy in engaging in every form of daily activity cannot be overemphasized, secured and constant availability of energy is predominant for the preservation of human's civilization (Hall and Klitgaard, 2011; Yergin *et al*., 2013). Hence, effective, and new ways of harnessing our planet's abundant energy resources are necessary to meet a new era of energy utilization that is coupled with an ever-rising energy demand of this century (International Energy Agency, 2014). For decades, fossil fuels such as oil, coal, and natural gas have been heavily relied upon to power the rapidly growing society (Ahuja and Tatsutani, 2009). However, they are finite, non-renewable, non-reliable, unhealthy, and unsafe (Nye, 2011; Htut *et al*., 2014; Mardiana and Riffat, 2015; Marrasso *et al*., 2019). They are also responsible for global warming through the CO_2-induced greenhouse effect (IPCC, 2017; Allen *et al*., 2018). Further, these resources are rapidly depleting and increasingly difficult to extract with most major reserves now located far offshore (Krishan and Suhag, 2018). The diverse nature, environmental-friendly, sustainability, and broad utilization of renewable energy sources (RES) offer the best approach for energy production (Ren *et al*., 2017; Mahmoud *et al*., 2020).

In the 1990s, as nations started to acknowledge the urgency and benefits of investing in renewable energy resources (RERs), there was a global rise in the number of developed land-based renewables and hydropower stations Amirante *et al*., 2016; Ajanovic, 2020). Despite such a trend and recent ones, the strong variability of many RERs has been a barrier to overcome the traditional energy sources from fossil for mass production (Cheng, 2005; Catalano *et al*., 2011; Amirante and Tamburrano, 2015). For instance, some RERs with great potential such as wind and solar are largely unpredictable and stochastic (Ren *et al*., 2017; Krishan and Suhag, 2018). Additionally, demand and supply often do not align, resulting in inefficient and inadequate energy available for direct consumption because energy is over-produced and wasted at low demand (Amirante *et al*., 2016; Yang *et al*., 2017). Energy resource waste can be translated into significant losses for the economy in the energy industry (Marques, 2018). The cost of achieving a sustainable and secured energy system is to critically consider

and incorporate the missing ingredient; the capacity to store, regulate, and control the amount of the generated energy (Ibrahim, 2008; Singh, 2016).

While renewable deficiencies are still a major concern at the moment, the industry of renewable technologies is expected to grow in the future to the extent that the whole world will almost be completely powered by RERs (I. E. A and World Bank 2014, IRENA, 2016). According to International Renewable Energy Agency 2016, the total electricity generated by renewables will equal that of coal and natural gas in 2040. Several emerging and new technologies have already been developed in this field (Guney and Tepe, 2017). Thus, the investment and development of efficient and cost-effective energy storage technologies is a necessity to keep pace with the tremendous growth of renewable energy technologies and the increasing demands for electricity arising from continued growth in population and productivity (Union, 2014; European Commission 2017; Klar, *et al*., 2017; Com, 2018; Botha and Kamper, 2019). Further, in isolated or weakly connected power systems such as offshore platforms, and islands, the maximum exploitation of renewable intermittent energy sources can be obtained by means of cost-effective storage technologies making an energy storage system a principal factor as to whether RES technology should be accepted or not (Cazzaniga *et al*., 2016). Generally, they can also enhance the grid stability, reliability, and efficiency by providing services in power quality, bridging power, and energy management (Römer 2012; Com 2016; Ozdemir 2017; European Commission 2017; Krishan and Suhag, 2018).

The basic principle behind Energy storage is to capture energy produced at one time for use at a later time using energy carriers (Øvergaard, 2008; Aneke and Wang, 2016; Mukhedkar, 2019). On one hand, storing energy in its primary form is the most common and stable form of storage as seen when crude oil is stored in tanks before transported to refineries for processing or coal stored in large piles either in coal-fired power stations or industrial plants prior to use (Geometrica 2008; Lovell, 2013; Schüth, 2013; Nakagawa, 2013; Freeport LNG 2014). On the other hand, primary energy forms such as renewables are not easily storable in their natural form and must be converted to secondary forms such as work, heat, or electricity (Øvergaard, 2008; Aneke and Wang, 2016; Mukhedkar, 2019). Work in its form is also not storable but must be converted into a more stable and storable energy form with the intent of transforming it back to electricity when needed (Aneke and Wang 2016; Mukhedkar, 2019). The technologies responsible for the whole process of back-forth electricity transformation are the

Electrical energy storage technologies (EEST) and can be categorized as mechanical, chemical, electrochemical, and thermal based on their properties (SBC, 2011; Zakeri *et al*., 2015; World Energy Council, 2016; Guney and Tepe 2017; Gür TM 2018). Each of these subdivisions has several technologies tailored for specific applications (SBC, 2011; Aneke and Wang, 2016).

The traditional form of Energy storage is chemical storage in batteries which has fewer advantages than disadvantages (Hai Alami, 2014). It led research focus into exploring alternative forms of energy storage that can normalize sharp surges between energy production and demand (Hai Alami, 2014). One such promising approach is the mechanical energy storage systems (MESS) that can convert electrical energy into forms of easily storable energy (Aneke and Wang, 2016), and are among the most efficient and sustainable energy storage systems (Mahmoud, *et al*. 2020). Under this category is the Gravity energy storage technologies (GEST) comprising the most mature and widely used large-scale energy storage technology to date known as Pump hydro electrical storage system (Rehman *et al*., 2015; Guezgouz *et al*., 2019). Other Mechanical and GEST includes Dry gravity, Flywheel, Compressed air, Underwater compressed air, and Deep-ocean gravitational energy storage (Cazzaniga *et al*., 2017; Gür 2018; IRENA 2017). Generally, GEST depends on depth or height for energy conversion (Klar *et al*., 2017; Aneke and Wang, 2016) with a wide range of applications and advantages including non-degradable capacity after each cycle, and decoupled power capacity from energy capacity (Morstyn *et al*., 2018). The focus of this study is one of the GEST termed Marine Gravitational Energy Storage Technology (MGEST).

Cabo Verde is among the Small Island Developing States (SIDS) in the Sub-Saharan part of Africa with huge and diverse renewable energy resource potential but heavily relied on fossil fuel for energy generation (Alves *et al*., 2000; Gesto, 2011; The African Development Bank, 2014; Sawin, 2018; Nordman *et al*., 2019). Cabo Verde has no oil refining capacity, having no known crude oil or gas reserves on any of its islands or their surrounding coastal waters, thus has to import all its petroleum products (REEEP, 2012; UNEP, 2017). The lack of indigenous fossil energy resources and low renewable energy penetration have made Cabo Verde a net importer of energy, and also place it in a fragile position continuously threatened by the volatility of international oil prices (Duić 2008; Tavares *et al*, 2019). Some energy proposals were made but most could not be implemented because they didn't address the energy curtailment and intermittency of RERs in Cabo Verde especially in a cost-effective manner

(Segurado *et al*., 2011; Heck *et al*., 2013; Segurado *et al*. 2015). Recently, a 20 MW off-stream Pumped Storage Hydropower was chosen to be installed on three sites in Santiago (Barreira *et al*., 2017), and a hydraulic battery storage was stated to be in the final stages of completion to be installed on the same island (Lusa, 2021). Nevertheless, more is needed to be done to meet the growing energy needs, improve renewable penetration, and reduce fossil fuel consumption.

As previously mentioned, energy storage systems (ESS) should be an integral part of energy production and distribution because of their role in the energy supply chain (Hai Alami, 2014; Dehghani, 2019; Ajanovic *et al*., 2019). Several electrical forms of ESS are currently being developed (Luo *et al*., 2015; European Commission 2017). However, no single storage technology is neither applicable to all RERs due to diversity, nor establishes a clear solution to overcome the associated deficiencies as the rate of penetration of RERs onto existing electricity grids increases. The application of storage technologies is based on factors including storage properties, energy challenges, and technological and financial capacity (Andrijanovits, 2012). We critically considered these major factors in proposing MGEST for Cabo Verde. MGEST is an emerging and new storage technology that can take advantage of the huge available depth of the marine environment to lift masses and store a large amount of energy (Toubeau, 2020). The implementation can be possible in diverse locations from the nearshore to the offshore region. The technology can also offer flexible integration into existing or newly developed intermittent energy sources or can serve as a standalone technology. It is environmentally friendly with a little required level of sophistication. The materials of construction such as concrete, reels, and pulleys are widely available and less costly (Brancato, 1992).

In this study, we adapted an operational research decision concept known as Multiple-criteria decision-making (MCDM) or multiple-criteria decision analysis (MCDA). MCDA evaluates multiple conflicting criteria in decision-making. The goal is not only to propose a storage technology or analyze derivable resources but to examine ways of minimizing implementation cost while applying the technology in a secured and safe location. Much is yet to be known about MGES, and this research will add to the dearth of information on MGES. Also, this will the first study applying the MCDM principle to identify potential sites for energy storage systems. Thus, we developed our own strategy to conduct the study and utilized the MCDA concept. We considered two cases, a situation where we want to store energy and stay connected to the grid onshore; an Onshore-connected system, and a situation where we want

to consume our stored energy offshore such as offshore installation, and oil platform; an Isolated system. For the first case, the three conflicting criteria include resources as a function of depth, cost as a function of distance to shore taking a maximum distance of 20 km, and security as a function of underwater current. While we considered resources, and security as the major two criteria for the isolated systems since the stored energy is to be consumed offshore such as in a desalination plant, or during offshore installations, and offshore mariculture practices.

1.1. Problem Statement

The major setbacks facing most renewable energy resources are their intermittency and the challenge to synchronize demand with supply which makes them unreliable for steady energy supply (Amirante *et al*., 2017; Ren *et al*., 2017; Yang *et al*., 2017). For instance, Hove 2017 reported that 46% of wind-generated electricity in Cabo Verde was wasted in 2017, and directly ascribed this power curtailment to the lack of energy storage. Energy storage offers the best solution to overcoming the asynchronous nature of energy demand against production (Ibrahim, 2008; Singh *et al*., 2016). Thus, it is essential to intensify scientific research into systems of energy storage that can improve production efficiency and reduce or prevent the need to burn fossil fuels.

In comparison, the level of investment, research, development, and the installed capacity of intermittent renewable energy far exceeds available storage at present (Dragoon, 2012). A typical example is Cabo Verde where much research has been conducted on both land and offshore renewables including their diverse nature, yet less are known about storage systems. However, the most promising way of transforming renewable energy resources RERs into reliable and steady energy sources is integration with energy storage systems indicating the role of advancing efforts both locally and globally to research and development of energy storage especially in a country like Cabo Verde which is one of the SIDS aiming for 100% electrification from RERs (Sawin *et al*., 2018).

Cabo Verde is home to one of the largest land-based and marine RERs due to its tropical climate, strong winds, surrounded by the vast Atlantic, and blessed with the longest coastline in West Africa (World Atlas, 2021; Gesto Energy, 2011; African Development Bank, 2014;

Sawin *et al*., 2018; Nordman *et al*., 2019). Despite the huge renewable potential, fossil fuel dominates the energy supply of Cabo Verde. For example, Cabo Verde generated 82.2% and 87 % of its electricity in 2017 and 2015 respectively through thermal power plants (AFREC, 2015). Tavares *et al*., (2019) linked the electrical energy generated in 2017 from imported fossil fuels to energy resource underutilization and highlighted the need for diversifying energy offers and investing in renewable energy infrastructure. However, energy storage systems possess the capacity to rescue renewables from their associated deficiencies including unpredictability, stochastic nature, and response to demand variations, and as a result improve their penetration (Ajanovic *et al*., 2020).

Some the negative effects of fossil fuel consumption are the associated impacts of emitting more quantity of greenhouse gas (GHG) and other air pollutants into the environment. Although, it should not be regarded as an advantage for countries that have, but Cabo Verde has no known fossil fuel reserves and has to import all its consumed fuels. The price of importation coupled with the volatility of the resource price position its economy to be highly susceptible to the impacts of oil crises (African Development Bank 2014). A typical example is fluctuations in oil prices that usually parallels frequent changes in electricity price (Tavares *et al*. 2019).

Lastly, the electricity cost in Cabo Verde is very expensive reflecting the price of imported oil. The average price of electricity in 2017 was 0.26 €/kWh (Electra, 2018), a price higher than the European average of 0.2113 €/kWh (Eurostat, 2018) which calls for investment in renewable energies such as marine-based renewables, and energy storage and energy storage to diversify the energy supply and make the energy market a more competitive one.

1.2. Aims and Objectives

This study aims to evaluate Marine Gravitational Energy storage resource potential and develop a multi-criteria model that identifies the best locations to site the technology around the coastal waters of Cabo Verde while maximizing resources and cost, and the specific objectives are:

i. Highlight the energy state including energy sources, demands, utilization, potential, and fossil fuel emissions under a growing population and climate change regime in Cabo Verde;

ii. Quantification of the amount of marine gravitational energy around the islands of Cabo Verde based on depth and mass;

iii. Zoning, classification, and identification of places with their maximum individual energy storage potential based on depth, mass, distance from shore, and the effect of current for the Isolated system;

iv. Zoning, classification, and identification of places with their maximum individual energy potential based on depth, mass, and the effect of current for the Onshore connected system;

v. Estimation of CO_2 emission that will be prevented with the implementation of this technology.

1.3. Structure of the work

This research work is divided into nine sections. We have highlighted the background of this study including the problems that have led to this research in the introductory session. We have also stated our aims and objectives. The rest of this study is organized as follows:

Section two describes the demography, climate, and oceanographic characteristics of the study area to have a brief overview of those major environmental factors that are related to this research either the energy situation portion of the underwater storage system. It further introduces energy storage systems but focuses on mechanical type, MGES, and their state of the art.

Section three highlights the characteristics of the sets of data used in this study, and the processing methodology adopted. Here, we detailed the approaches we used, our assumptions, and the rationale behind those methods.

Section four is split into two, first part presents the result related to the energy situation in Cabo Verde including electricity prices, renewable energy potential, wind consumption, and related cost with the amount of CO_2 avoided, while the second part shows the results related to MGES including resource potential, ocean current analysis results, and suitability maps imbedded into resource potential map.

Section five discusses the result, and the final Section concludes this work. Then, the articles cited for this work were shown in Section seven, and lastly, the Appendix section shows some additional results.

2. Literature review

This Section is used to review the geographic settings, demography, and oceanographic settings of the study area to better understand the depth variation, underwater features, climate, and the nature of circulation in the study area. We also highlight some important concepts such as energy storage systems, their benefits and characteristics, and some of the technologies used at the moment with a focus on MESS, GEST, and MGEST. A brief review of MCDA is also presented in this Section.

2.1. Demography and Geomorphology

The Republic of Cabo Verde is an archipelago (Figure 1) of islands and islets situated in the subtropical region of the Atlantic Ocean between 17° 12'15''N and 14° 48'00''N and 22° 39'20''W and 25° 20'00''W. Nine out of the ten major islands are inhabited (Figure 1a and 1b) but all the islets are uninhabited. The islands are all volcanic in origin at an approximate distance of 400 km off the coast of Senegal and organized in a west-facing horseshoe disposition (Ramalho, 2011). Cabo Verde has a total land area covering 4033 square kilometers with a significant coastline spanning 1020 km^2 approximately (DGA, 2004).

The archipelago can be divided into the Windward Islands at the north and the Leeward Islands at the south as shown in Figure 1a. Whilst the islands of Santo Antão, São Vicente, Santa Luzia (uninhabited island), São Nicolau, Sal, and Boa Vista constituted the Windward Islands, the Leeward Islands are made up of the islands of Maio, Santiago, Fogo, and Brava. Santiago is the largest island dominating a total of 991 km^2 while Santa Luzia is the smallest covering just 35 km^2. The distance between islands varies from 8 km between São Vicente and Santa Luzia to 270 km between Maio and Santo Antão (Ramalho, 2011).

There are several features revealed by the bathymetry of Cabo Verde but two structures stand out. The first structure is the northern chain consisting of islands from Santo Antão to São Nicolau in a west-east orientation and characterized by shallow depths between them (Figure 1a and 1b). The second structure is composed of islands from Sal to Santiago formed by two detached edifices oriented in a north-east–southwest disposition (Figure 1a and 1b; Ramalho, 2011). Another important feature is the João Valente bank, a very shallow area

situated between Maio and Boa Vista Island with the highest summit of about 14m depth (Figure 1a; Ramalho, 2011).

Cabo Verde has a total estimated population of 550,000 inhabitants with a population growth rate of about 1.8% p.a (Instituto Nacional de Estatistica, 2016). A large portion of the population is concentrated in Santiago, especially in the capital city of Praia as shown in Appendix 1. Generally, 62% of the total population lives in cities (Instituto Nacional de Estatistica, 2016).

The archipelago has an arid and rugged terrain with little vegetation. Boa Vista, Maio, and Sal have long beaches and flat surfaces, but other islands are majorly mountainous. The weather condition is characterized by prevailing northeast trade winds occurring throughout the year (Appendix 2). These winds influence the intensity and direction of surface currents. Higher wind intensities are more frequent in the Leeward Islands than in the Windward Islands (DGA, 2004).

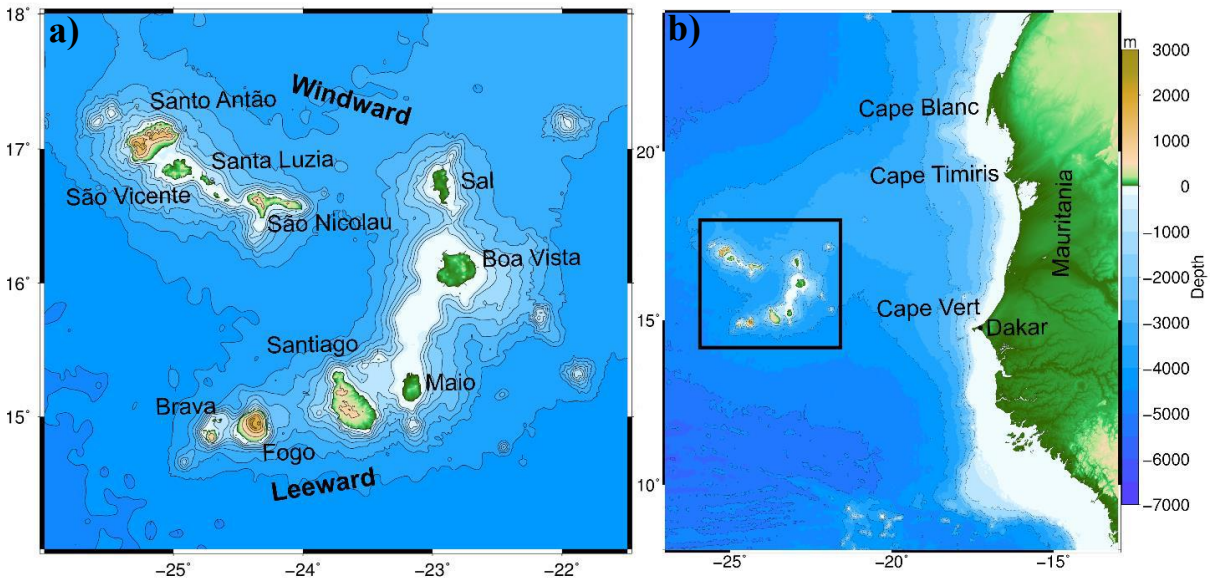

Figure 1. (a) Bathymetry and Topography of the Cabo Verde islands, showing the grouping and identification of the islands. Isolines have a 500 m interval, (b) Regional setting of the archipelago, with the identification of the main coastal features. Isolines have a 1000 m interval (Data from GEBCO).

2.2. Climate and Oceanographic setting

This subsection presents the climatic regime as well as the predominant ocean currents and water masses that can be found in the study area. Some other associated physical properties and dynamics such as sea surface temperature (SST) and eddies are also presented.

2.2.1. *Major currents and Climate*

Cabo Verde is located at the southernmost tip of the Canary current (CC) in the eastern boundary of the North Atlantic subtropical gyre (Fernandes *et al*., 2005). This area falls within a zone of large-scale interactions (Figure 2) between the North Equatorial Counter-Current (NECC), the North Equatorial Current (NEC), the CC, and the seasonal Mauritanian Current (MC) (Mittelstaedt, 1991). This large-scale surface circulation varies seasonally as a response to the meridional migration of the Intertropical Convergence Zone (ITCZ) (ITCZ; Stramma and Schott, 1999). The prevailing northeast trade winds directly affecting this region throughout the year have a higher intensity during winter and spring of 9.5 m s^{-1} maximum mean speed as shown in Appendix 2a and 2b (Lázaro *et al*., 2005; Varela-Lopes and Molion, 2014).

As highlighted, one of the prominent oceanic features influencing circulation patterns in Cabo Verde is the Canary Current (CC), transporting cold water off the coast of Africa from the north to the south, then migrating south-westward near Cabo Blanc where it joins the North Equatorial Current (NEC) (NEC; Mittelstaedt, 1983, 1991; Stramma *et al*., 2005). CC is stronger near the African coast in summer, and stronger west of the Canary Islands in the winter (Stramma and Siedler, 1988). The NEC has a mean speed of 10–15 cm s^{-1} in a dominating west/northwestward direction (Stramma and Siedler, 1988; Zhang *et al*., 2003), with a weakening in winter and maximum speed during summer (Arnault, 1987) as highlighted in Appendix 2 bottom panels.

As for the NECC, it is generally located between latitudes 5- and 10-N with an eastward mean flow speed of approximately 42 cm s^{-1} (Fratantoni, 2001). It also exhibits seasonality, being strong when the ITCZ reaches its northernmost position (Lázaro *et al*., 2005) corresponding to early autumn, and summer (Arnault, 1987; Mittelstaedt, 1991). During this time, the zonal flow can extend over the whole of Tropical Atlantic (Mittelstaedt, 1991;

Stramma & Siedler, 1988) and can influence the Cabo Verde archipelago (Fernandes *et al*., 2005).

The Mauritanian Current (MC) is another prominent feature around the west African coastal water that might not be directly impacting circulation around Cabo Verde (Figure 2) but contributing to the large-scale circulation in this region, as it has been documented to be partly responsible for the suppression of the regional coastal upwelling (Mittelstaedt, 1991). This narrow northward flowing current flowing forms as a result of the interaction of the NECC with the Africa coast transporting warm equatorial water to the eastern tropical Atlantic and can reach 14° N during winter/early spring (Appendix 2e and f), and ~20° N during summer/early autumn (Appendix 2g and h).

Lastly, there exists the Guinea Dome (GD) southwest of Cabo Verde formed as a part of the large-scale near-surface flow fields associated with the NEC, the NECC, and the North Equatorial Undercurrent (NEU) (Siedler *et al*., 1992). This permanent cyclonic geostrophic is developed by divergent wind-stress curl (Richardson, 1983; Siedler *et al*., 1992).

Different water masses meet around Cabo Verde typically in the large-scale frontal system formed between Cabo Blanc and the northernmost Cabo Verde Islands termed Cabo Verde Frontal Zone (CVFZ) (Zenk *et al*., 1991). This thermohaline front (Zhang *et al*., 2003) separate the cooler, fresher South Atlantic Central Water from the warmer saltier North Atlantic Central Water (Mittelstaedt, 1983, 1991; Pérez-Rodríguez *et al*., 2001; Meunier *et al*., 2012).

2.2.2. Eddies

Oceanic eddies are ubiquitous rotating water bodies moving across the ocean, either cyclonic or anticyclonic with a typical horizontal scale of about 50 km - 500 km and time scale of a few days to hundreds of days. Eddies are characterized by considerable kinetic energy in the peak of the ocean kinetic energy spectrum, and they can directly influence the distribution of current speed, the thermohaline structure, and also transport heat and momentum, and can strongly influence the physical properties of the upper ocean. (Li *et al*., 2012).

Canary Current Upwelling System is a major regional upwelling system situated off Northwest Africa, and is associated with several mesoscale features including filaments that

can stretch out from the adjacent coast to hundreds of kilometers offshore (Van Camp *et al*., 1991; Kostianoy and Zatsepin, 1996; Lange *et al*., 1998); and eddies (e.g., Karstensen *et al*., 2015; Löscher *et al*., 2015; Fiedler *et al*., 2016; Schütte *et al*., 2016a; 2016b), with both having a profound effect on the regional oceanography. The part of this upwelling system in close proximity to Cabo Verde is the Northwest Africa upwelling system which even though it is situated in waters relatively close to the coast, the associated eddies and filaments, and the propagation of Rossby waves could lead to the impact of this cold SST to be felt 300 to 600 km offshore, or other regions elsewhere (Mittelstaedt, 1991).

The diverse physical mechanisms in the ocean that can induce eddy generation are: the effect of topography (Barkley, 1972; Heywood *et al*., 1990; Alpers *et al*., 2014); ocean-atmosphere interaction (Calil *et al*., 2008; Jiménez *et al*., 2008; Couvelard *et al*., 2012; Hogg *et al*., 2016); current shear (Chelton *et al*., 2011; Schütte *et al*., 2016a), or even eddy-eddy interaction (Sangrà *et al*., 2009; Chelton *et al*., 2011), and the island-induced processes (Cardoso, *et al* 2020). The majority of these features are present around the archipelago and are influencing the dynamics of this area.

Much theoretical evidence has supported the shadow effect induced by the topography of the island in the lee of all major islands when weaker winds detach from the sides of strong winds. This mechanism has now been fully established to be capable of fueling the generation of anticyclonic and cyclonic eddies in the island(s) wake (Calil *et al*., 2008; Jiménez *et al*., 2008; Yoshida *et al*., 2010; Jia *et al*., 2011; Couvelard *et al*., 2012; Caldeira *et al*., 2014). According to Varela-Lopes and Molion 2014, the wind shadowing effect may be responsible for the nearly permanent anticyclonic eddy south-southwest of the islands of Cabo Verde, which was found to be more pronounced during the periods of strongest wind intensity. Caldeira *et al*., 2014 also confirmed that the islands of Cabo Verde are exposed to a remarkable number of far-field eddies from the western African coast that interact with the islands and local eddies, and at such, it is difficult to discern the major eddy generating mechanism.

2.2.3. SST

This region experiences one of the largest SST cycles in the tropics (Faye *et al.*, 2015). The SST variation has a considerably lower amplitude in offshore waters than in coastal waters, a fact that is conspicuously related to the coastal upwelling seasonal cycle (e.g., Mittelstaedt, 1991; Van Camp *et al.*, 1991; Marcello *et al.*, 2011). In the area of Cabo Verde Islands, maximum values (29 ºC) are found from July to November – coincidently with higher chlorophyll pigment concentrations near Cabo Verde (Fernandes *et al.*, 2005) –, whilst minimum values (21 – 22 ºC) are conversely seen between December and May (DGA, 2004).

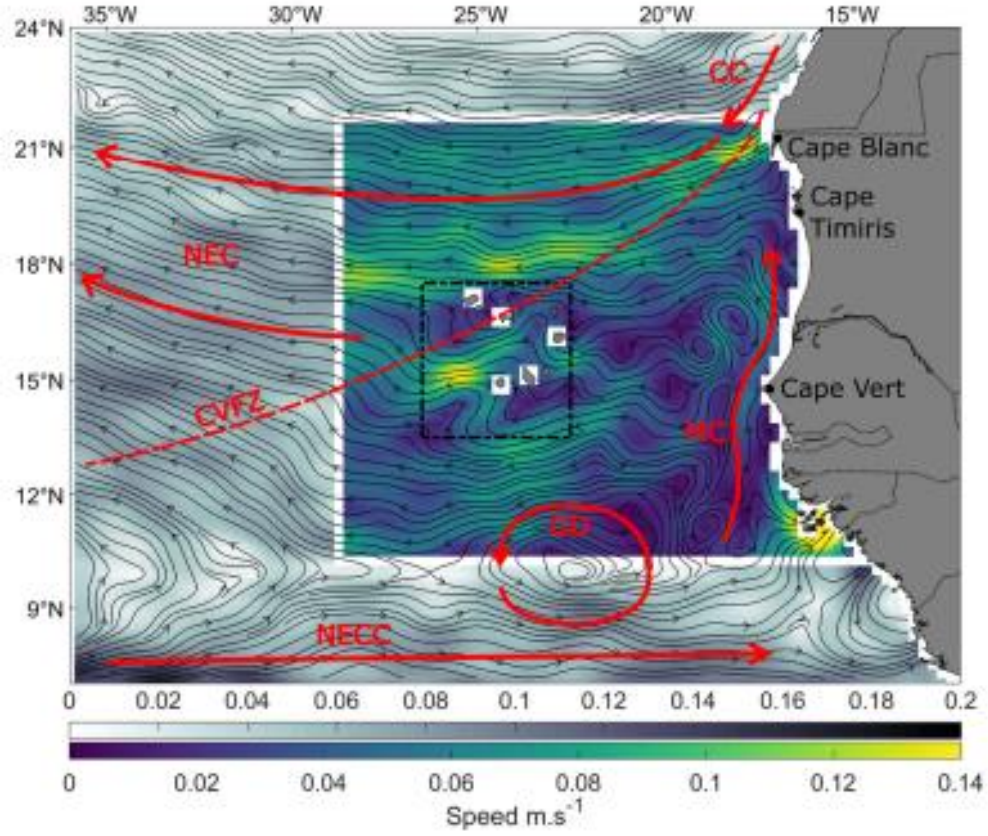

Figure 2. Mean surface ocean currents and features: CC – Canary Current; NEC – North Equatorial Current; NECC – North Equatorial Counter Current; MC – Mauritania Current; GD – Guinea Dome; CVFZ – Cabo Verde Frontal Zone. The dotted area represents the represents the near-field CV) area. The grey and coloured colour maps (with different scales) represent the exterior and interior of the study area, respectively adapted from Cardoso, *et al* 2020.

2.3. Energy Storage and State of the Art of ESS

This subsection describes the logic behind storage systems and MESS and their state of the art. Electrical energy storage technologies are designed to directly absorb electrical energy produced at a time (act like increased demand) and release it as electrical energy (act like a generator) at a later time (Aneke and Wang, 2016). The process of absorbing the energy is termed the charging phase while that of giving out the energy is the discharging phase (Jonathan 2013; Klar *et al*., 2017). Different materials known as energy carriers as indicated in figure 3 are used in the process of storing the energy (Aneke and Wang, 2016). The whole scheme of energy generation and transmission from an intermittent energy source to the grid is depicted in figure 4, illustrating one of the major roles of energy storage system to store and control energy.

2.3.1. Benefits of Energy Storage

The benefits associated with ESS are enormous (Krishan and Suhag, 2018; Dehghani, 2019; Mahmoud *et al*., 2020). They can function as a key player in the energy supply chain and thus have to be considered as an essential component of energy production and distribution (Hai Alami, 2014; Dehghani, 2019; Ajanovic *et al*., 2019). Adding to the storage of excess energy, some of their key advantages include:

i. Energy management

Energy storage systems are essential in energy management as they help to reduce energy wastage through peak demand reduction, and serve as a backup, and increase the energy utilization efficiency, and power quality (Chan *et al*., 2013; Abedin and Rosen, 2012). The storage of secondary forms of energy such as work, electricity, and heat, helps to reduce the quantity of primary energy forms (ie. fossil fuels) consumed to generate them. Consequently, this lowers the emissions of CO_2 and other greenhouse gas, and associated global warming (Mahlia *et al*., 2014).

ii. Transmission, distribution, and Micro-grid applications

Energy storage helps in voltage support, power system planning, operation, and frequency regulation (Tan X *et al*. 2012, Chen H. *et al*., 2009). Other functions include

maintaining stability in energy systems, managing grids, renewable integration, grid enhancement, synchronizing demand with supply (Tan *et al*., 2013; Castillo and Gayme, 2014; Ibrahim *et al*., 2008), and load shifting (Kousksou *et al*., 2014).

iii. Major Energy player

Energy storage can also be a major player in increasing the rate of penetration of green, clean, renewable, and intermittent energy resources to the grid including solar energy, wind energy, and offshore energy resources such as marine waves, and tidal current (Zhou *et al*., 2013; Plebmann *et al*., 2014; Pardo *et al*., 2014; Castillo and Gayme, 2014).

Figure 3. Operation of Energy Storage Systems (ESS). Adapted from Jonathan (2013).

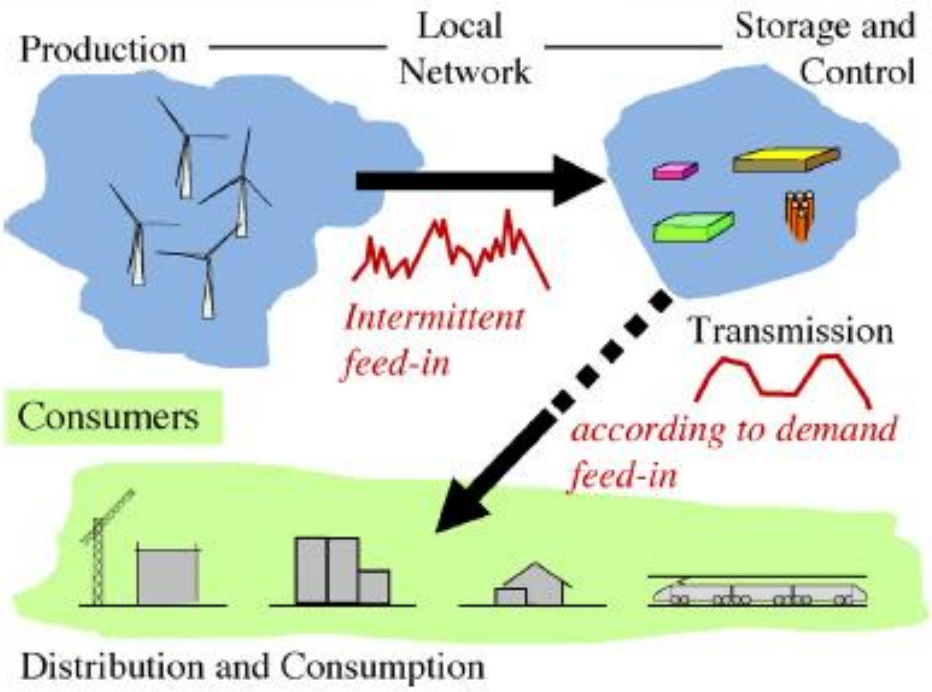

Figure 4. Mode of Operation of ESS 2. Adapted from Klar *et al*. (2017).

2.3.2. Energy Storage State of the Art

A range of energy storage technologies exist, each with different trade-offs for particular applications (Morstyn *et al.*, 2019). Several storage systems are under development and compete with each other. Figure 5 shows one of the major classifications of the electrical storage system and Appendix 3 highlights the differences and similarities among them. The focus of this Section is those that are exclusively marine-based.

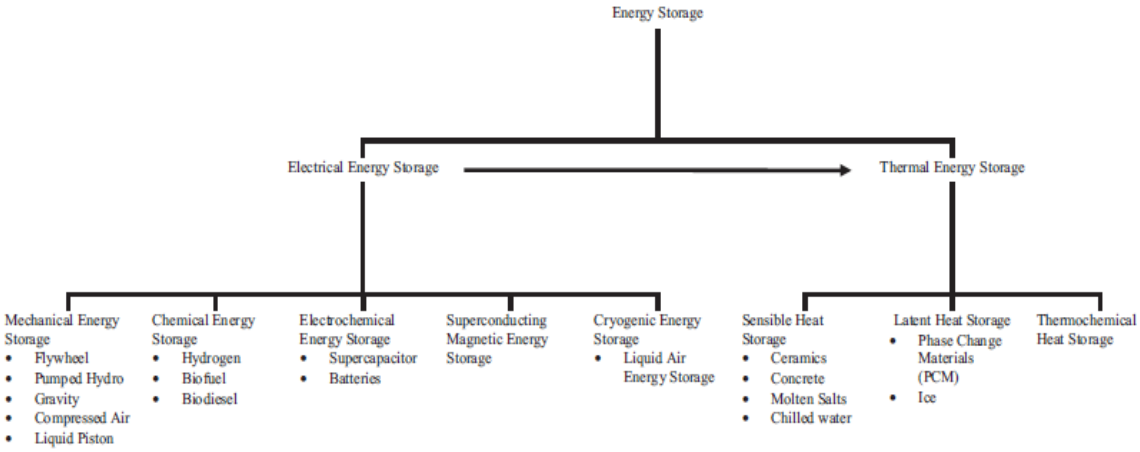

Figure 5. Classification of ESS. Adapted from SBC (2011).

Before going into the state of the art of the energy storage systems under study, it is important to understand some factors characterizing energy storage systems. According to Aneke and Wang (2016), and Castillo and Gayme (2014), the fundamental attributes to evaluate any storage system are the following:

- ❖ Energy storage capacity and duration – Refers to the amount of energy that can be stored and the duration that said energy can be stored.
- ❖ Energy/power density – The power density (Wm^{-3}) is the output power per unit volume, and the energy density (Whm^{-3}) is the amount of energy that can be stored per unit volume of the system.
- ❖ Lifetime – Measured in years or total charge/discharge cycles, it is the functioning life span of the storage technology

- ❖ Charge/discharge and response time – The amount of time required for the storage system to become fully charged or discharged. Response time is the time required to start providing rated power output.
- ❖ Roundtrip efficiency – Also called the AC-to-AC efficiency, this is defined as percentage ratio of Output-Energy to Input Energy per one charge/discharge cycle.
- ❖ Capital Cost – This is the upfront costs of a storage technology per unit of energy or power discharged.

Some of the major Mechanical energy storage systems are presented below:

i. Pumped-storage hydropower (PSH) technology

PSH is a robust, most used, and most mature large-scale energy storage technology (Aneke and Wang, 2016). The storage system has high efficiency of around 85-90% (Cazzaniga *et al*., 2017), with an unlimited storage period. The global capacity for pumped storage in 2015 is 144 GW (World Energy Council, 2016), and by the end of 2017, nearly 96% of the total installed electrical energy storage capacity across the globe, with over 183 GW, was in the form of PHES (Gür, 2018; IRENA 2016), with a lifetime of about 30 to 50 years.

This traditional energy storage system that was also called the Pumped Hydroelectric Energy Storage (PHES) by many authors (Pickard, 2011; Mahlia 2014; Plebmann *et al*., 2014; Castillo and Gayme, 2014) is based upon the principle of the gravitational potential to store energy by utilizing the energy produced by a power plant (intermittent sources) during off-peak periods to pump water into a reservoir at a high elevation from a lower reservoir (figure 6a and 6b). The water flows back to the lower-altitude basin through the same pump to generate electricity during the high energy demand period. The pump act as a generator during pumping and turbine during discharge. The power capacity of the system is proportional to the head (height difference between the upper reservoir and the turbine) and flow rate.

The major limitations are the huge capital cost (600 to 2000 $/kW), and heavy reliance on the morphological feature of a site such as two basins at different elevations (Rehman *et al*., 2015). Hence, it is only applicable in certain regions. For example, the possible application of this technique near the sea was explored under the condition of an available high elevation water basin near the coastline. The advantage of the seawater pumped storage plants includes

lower civil construction and power distribution costs due to the proximity to steam turbine power plants although corrosion resents another technical challenge (Yang *et al*., 2011).

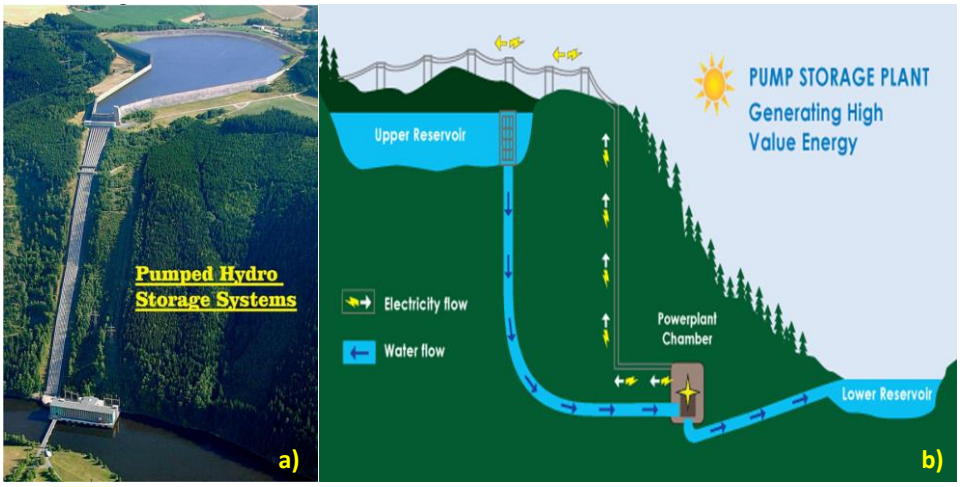

Figure 6. Pumped Hydro Storage System Mode of Operation: (a) Adapted from Cazzaniga *et al*. (2017), (b) Adapted from Aneke and Wang (2016) (underground version).

ii. Compressed Air Energy Storage (CAES)

The working principle of CAES is similar to that of the conventional gas turbine technology where the elastic potential of compressed air is used for storing the energy (Succar and Williams, 2008, Huang *et al*., 2018). CAES system harnesses off-peak electricity to compress air and store it in a reservoir such as salt caverns, depleted gas fields, aquifers, aboveground pipes, underground caverns, and vessels (Akhil, 2013). This air is released during peak periods, heated, expanded, and used in a turbine generator to produce electricity (Figure 7).

CAES is second to PSH from the perspective of the commercial bulk energy storage plants available today, ranging around hundreds of MW (Chauhan and Saini 2014; World Energy Council 2016). CAES has an estimated efficiency of 40 - 70% with an expected lifetime of about 40 years (Kousksou *et al*., 2014). Further properties include large storage capacity (up to 500 MW), high discharge duration (8-12 h), and quick response time (Energy Storage Association 2017; Nikolaidis and Poullikkas, 2017). There are three commercial plants using CAES for energy storage applications such as the 290 MWe Huntorf air storage gas turbine

power plant in Germany, and a 110 MWe CAES in Mclntosh, USA (Chen *et al*., 2009). There are also some plants being planned or under construction (Chen *et al*., 2009).

The limited exposure of this technology, and suitable geological locations are the prime constraints in the development of CAES technology. However, new technologies are being developed which use different working fluids to improve the thermal cycle. They include advance adiabatic CAES which re-utilizes heat released by conventional approach to improve efficiency (Luo *et al*., 2016), liquid air energy storage which converts liquefied air or nitrogen from liquid to gas to improve efficiency and energy density, and underwater CAES (Guo *et al*., 2016).

iii. Underwater CAES

Underwater compressed air energy storage (UWCAES) is a promising way to achieve isobaric storage by taking advantage of hydrostatic pressure. In the UWCAES system as shown in Figure 7, the air stream is compressed to the hydrostatic pressure present at depth in the marine environment where the air accumulators are located (Wang *et al*., 2016).

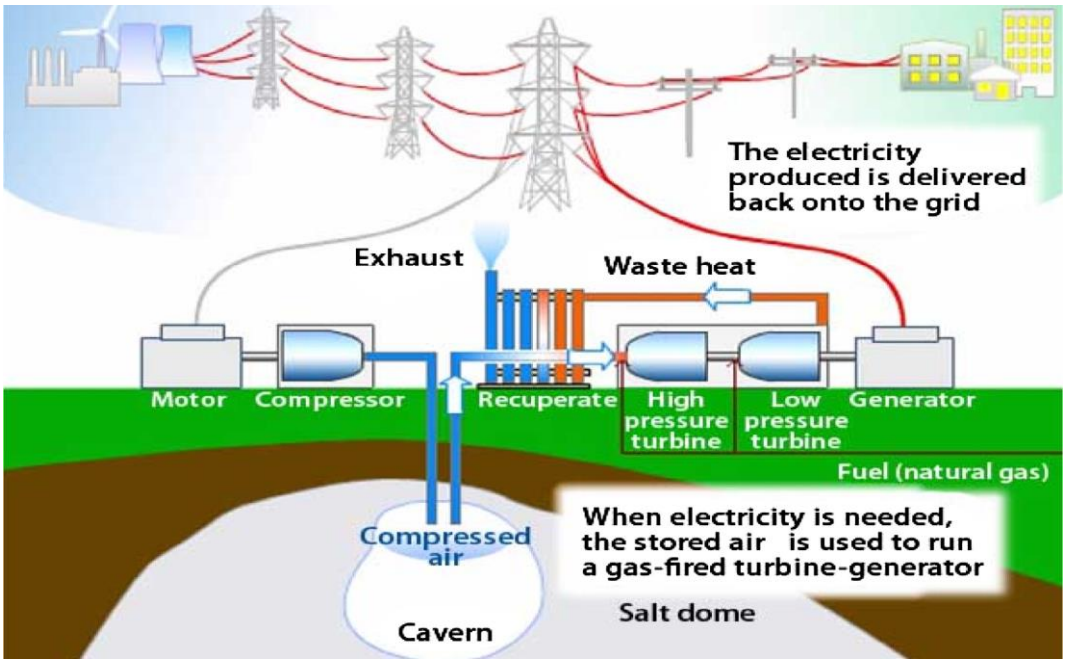

Figure 7. Compressed Air storage system mode of operation. Adopted from Argonne National Laboratory (2009).

iv. Flywheel energy storage (FES)

A flywheel is an electromechanical system that stores energy in the form of kinetic energy by utilizing the angular momentum of a rotating mass - a disc or a cylinder (Figure 8). This technology has been in existence for decades but recently draw attention for being suitable as a largescale ESS. The working principle involves storing energy during the charge phase in a rotating mass. The energy is stored by an electric machine acting as an electric motor which accelerates the rotating mass during the charge phase, and during the discharge phase, the same machine behaves like an electric generator to deliver energy to the distributed generated (DG) power system of the flywheel, thus decelerating the rotating mass (Sebastián and Alzola, 2012; Daoud *et al*., 2012).

Several approaches are used to reduce friction (Faraji *et al*., 2017; Li *et al*., 2017). The two operational designs are high speed and low-speed flywheels whose details can be found in Daoud *et al*. (2015), and Wicki and Hansen (2017).

The main advantages of FES systems include their very fast response, instant supply of a large amount of power (to the tune of MW), long useful life (up to 20 years or 105-107 cycles) irrespective of the depth of discharge (DoD), and temperature (Pena-Alzola *et al*., 2011). Besides, high efficiency (80%-99%) and not having much adverse effects on the environment are the other salient features of FES systems (Amirante R. *et al*. 2017; Cavanagh *et al*., 2015; Anonymous, 2016).

Huge cost (250-350 $/kW), and very high standing losses (self-discharge rate for complete FES system is one-fifth of the stored capacity per hour) are prominently the two major limitations of FES systems (Pena-Alzola *et al*., 2011, Lund *et al*., 2015).

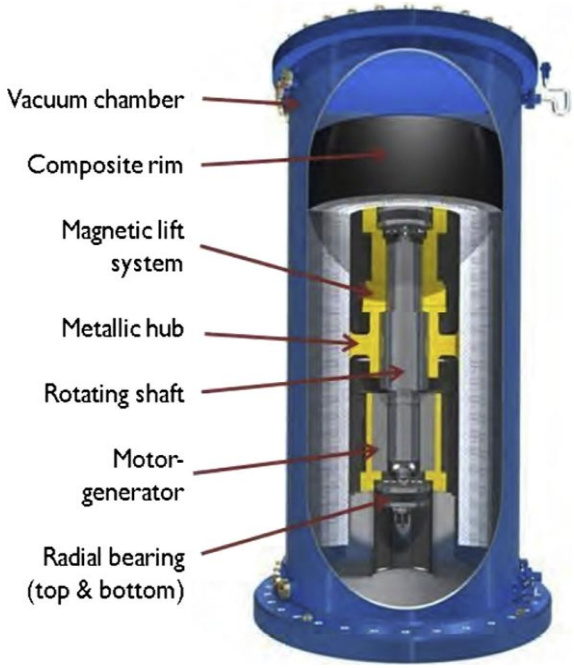

Figure 8. Flywheel system. Adapted from Faraji *et al*. (2017).

v. Dry Gravitational Energy Storage

The idea behind the gravitational energy system technologies is to store electrical energy by converting it to gravitational potential energy. The system is charged and discharged by lifting and releasing a certain mass. Amongst all the highlighted mechanical energy storage systems, pump hydro is the only storage system that uses the gravitational method of storage. Before going into Marine-based GEST besides pumped-hydro, let's briefly look at those that require no water body which are described as follows:

❖ Advanced rail energy storage (ARES)

ARES was developed by a California company (Ares, 2019). This rail-based, traction drive technology uses surplus renewable energy or low-cost electricity from the grid to move a mass in the form of concrete blocks uphill by railroad shuttles (Letcher, 2016; Ares, 2019). During the discharge phase, the shuttles are allowed to descend under gravity as shown in Figure 9. Each of the shuttle (block) weighs around 45–64 tons and travel on a 16 km trail with a slope of less than 10% (6 degrees).

Citing the pilot project located in Tehachapi in California, United States, the system has an efficiency of 78–80% with no self-discharge storage loss and a 40 years lifetime. The first commercial project is being built in Nevada: a 50 MW power system with 780 tons transport mass on a 9.3 km path generating 12.5 MWh power capacity (Figure 9a and 9b). ARES has potential for large-scale applications but has a major limitation of topographic dependence due to an altitude difference requirement for its installation (Ruoso 2019; Sandru 2012; ARES 2019). Another major disadvantage is a great amount of initial CapEx that would be required for laying rail track including the associated cost of the rail pieces in the absence of decommissioned railways (Fyke, 2019).

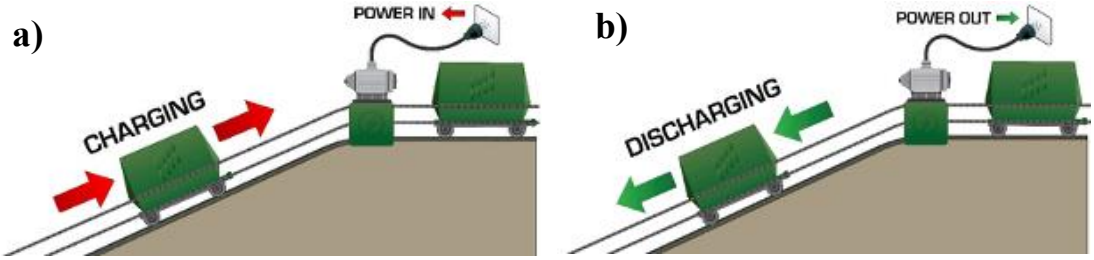

Figure 9. Traction based ARES mode of operation showing the movement of the shuttle blocks: (a) Charging phase (left), (b) discharge phase (right). Adapted from Ares (2019).

❖ Gravity energy storage proposed by Gravitricity

This storage technology (Figure 10) is based on the movement of a heavy mass vertically up and down a shaft in the ground (Blair 2016; Gravitricity n.d.). Gravitricity planned to build pistons of mass of about 12,000 tons (24 weights of 500 tons each) and shafts that can go as deep as 2000 m (Gravitricity, n.d.), using mineshafts either purposely built or existing. Similar to the hoisting systems used in cranes and mines, a system of cables, and winch is implemented to lift the masses. Each of the winches is capable of lifting its share of the weights. The system stores electricity as potential energy by raising the weights which can then be converted into power for driving a generator by lowering those weights. The design life is 50-year, efficiency is around 80–90%, the response time is around 0.5 s, and the output duration is between 15 min to 8 h. The fact that Gravitricity can readily store excess energy whenever required – either in short bursts, or very rapid, and over a long period of time are some major advantages. Gravitricity received funding in early 2018 to build a prototype with 250 kWh capacity in South

Africa (Bungane, 2018; Huisman, 2018). The major disadvantage as indicated by Botha and Kamper (2019) is the limitation of the storage capacity by both the hoisted piston mass and the system height.

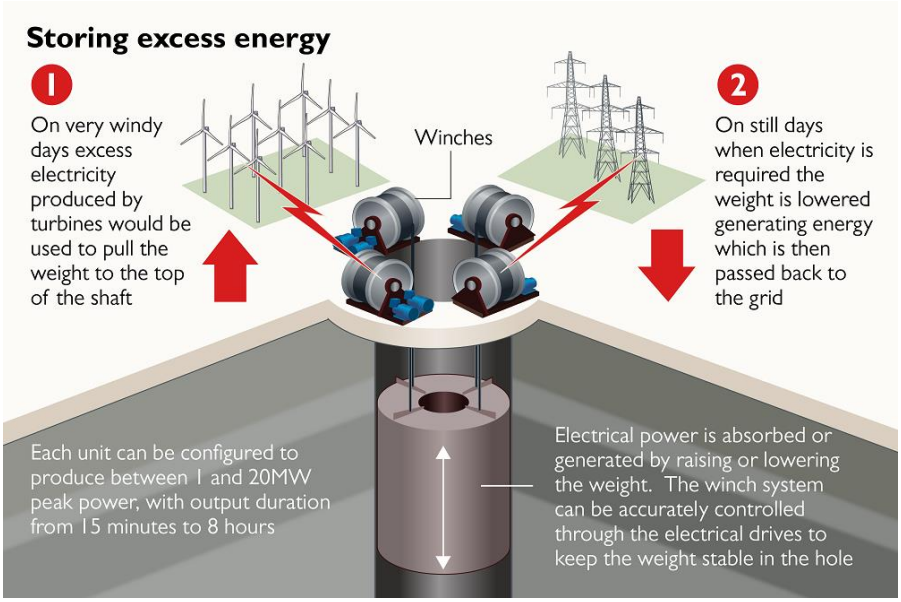

Figure 10. Concept diagram of the Graviticity energy storage system. Adapted from Gravitricity, n.d..

❖ StratoSolar GES

This proposed storage technology stores energy using winches that are driven by an electric motor/generator to raise relatively small masses (hundreds of tons) from the ground to a buoyant platform at 20 km (Figure 11a, and 11b; Appendix 4). The buoyant platform is a PV farm floating at 20 km, acting as a renewable intermittent energy source (StratoSolar, 2018). Each kilogram of weight raised stores about 54 Wh energy. Figure 11a depicts a stacked 500 tons of weight corresponding to a storage capacity of about 25 MWh. The mode of energy storage and distribution of this storage system in a simplified version, including the operation of a single winch that is raising and lowering an individual weight, is shown in Figure 11b. The winches are suspended beneath the platform modules and are not visible in Figure 11a.

As highlighted by StratoSolar (2018), this system is a highly reliable, very simple storage technology that doesn't degrade with use, and has a design life greater than thirty years with 85% round trip efficiency. Other acclaimed properties include scalability (adding platform elements and weights can increase the energy from kilowatt to terawatt), zero geographic

constraints, little environmental impact due to small weights, and low initial capital cost than any available or planned energy storage technology (approximately $125/kWh), suggesting that PV in the stratosphere combined with GES could provide a large proportion of electricity requirements at a lower market cost than fossil fuels. Some of the major challenges with this technology include the impact on feasibility and constructing and maintaining such an elevated platform.

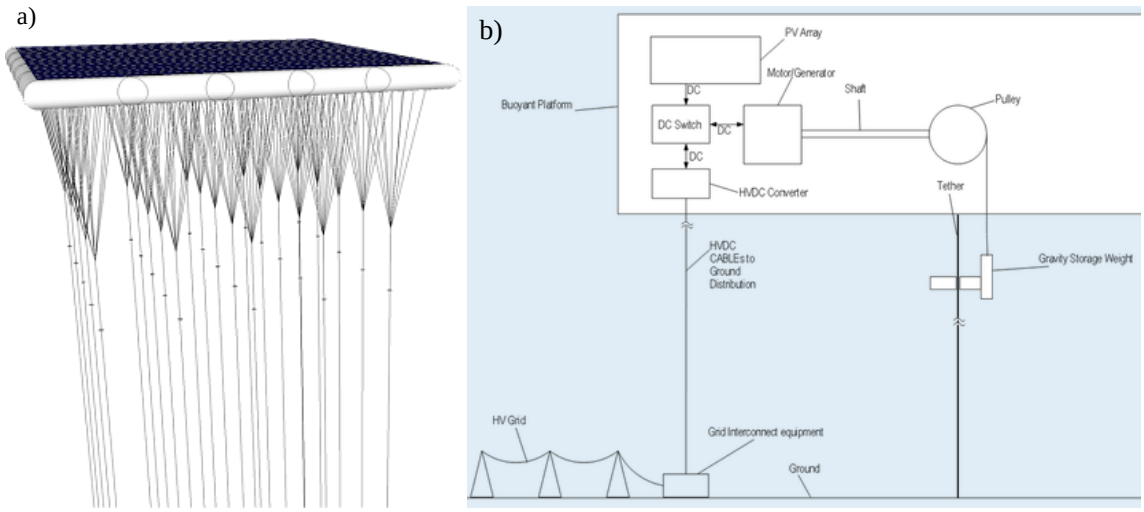

Figure 11. StratoSolar GES system: (a) PV in the stratosphere with GES, (b) Block diagram showing the connectivity of the elements of a StratoSolar Gravity energy storage system. Adapted from StratoSolar (n.d.).

❖ Energy Vault

Energy Vault is another innovative technology that applies the principle of MESS (Figure 12). The recently launched demonstration plant is a 4 MW-35 MWh aboveground storage technology (Figure 12 a – 12 e) is characterized by a six-armed crane standing like a tower in the middle of the system, vertically moving 35 tons of concrete blocks up and down over a distance of 120 m (Fyke 2019; EnergyVault, 2019). The charge phase occurs when there is excess solar or wind power. This energy is transmitted through the power electronics to rotate the electric motor, which in turn is used to raise a brick and place it on top of another stack of bricks at a higher elevation. The bricks which are neatly stacked around the crane during the discharge phase are identified in singleton by the crane's arm as directed by a complex computer algorithm and aided with a camera attached to the crane arm's trolley.

To complete the charge-discharge cycle, the bricks are again picked up by the crane and lowered, thus returning energy to the grid. During this discharge phase, the motor is driven in reverse as a generator by gravitational energy to generate electricity. The total storable energy is 20 MWH, enough to power 2,000 Swiss homes for 24 hours. In August 2019, $110 million was raised by Energy Vault to develop this storage technology. Some of the disadvantages of this system include heavy reliance on cranes, visual impact on the environment, and the influence of bad weather conditions such as high winds (Toubeau, 2020).

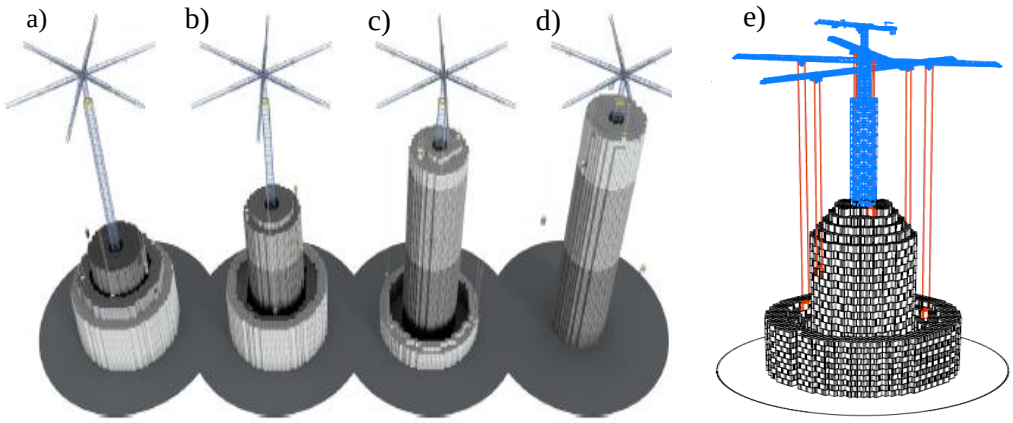

Figure 12. Energy Vault energy storage concept: (a-d) Charging and discharging cycles of the Energy Vault Tower (e) Energy Vault Tower showing the hanged masses as they move vertically. (Adapted from Fyke, 2019).

vi. Exclusively Marine GEST

The storage technologies under this category are those that are engendered as the principle of GEST is applied in the marine environment. They are as follows:

a. Deep ocean gravitational energy storage (DOGES)

Also described as Ocean Renewable Energy Storage (ORES) (Slocum *et al.*, 2013) or Underwater Ocean Storage Systems (UOSS) (Cazzaniga *et al.*, 2016), DOGES is another mechanical energy storage technology that can exploit the concept of gravity storage by reversing the storage configuration of pump hydro (Slocum *et al.*, 2013; Cazzaniga *et al.*, 2016). According to the aforementioned authors, this alternative approach to the traditional storage can be implemented wherever the intermittent energy, Photovoltaics, or wind energy production sites are on seas or oceans of sizeable depths. The operating principle is to power a

pump or turbine that forces water out of an underwater tank whenever the renewable supplies the storage system, and the external water flows back into the empty tank driving turbine on its way whenever energy is to be recovered (Figure 13).

DOGES was proposed to bypass the problems associated with UWCAES (submarine piping and compression), and PHES (topography). Presently, no utility-scale applications of ORES have been completed. According to Botha and Kamper (2019), the size or capacity of DOGES should be completely dependent on the generating unit but Cazzaniga *et al*. (2016) showed that an underwater tank at a depth of 1000 m with a volume of 360 m^3 can store 984 kWh 90% efficiency, while Slocum *et al*. (2013) presented larger scale systems around few GWh at 65–70% estimated efficiencies.

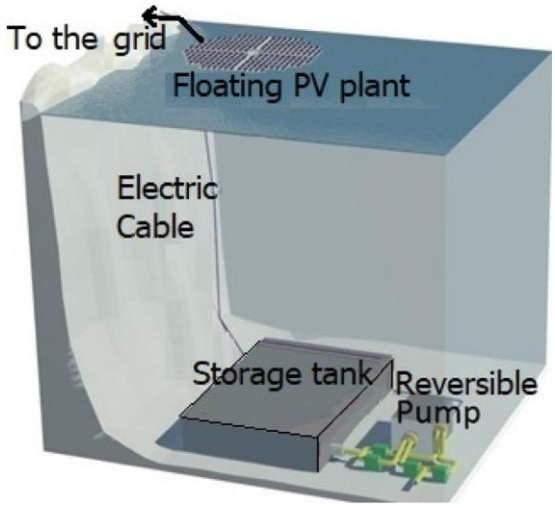

Figure 13. DOGES system adopted from Cazzaniga *et al*. (2016).

b. Buoyant Energy

Buoyant Energy (BE) is an offshore energy storage solution based on pumped-storage hydropower (PSH) technology. BE transfers the PSH key features to an offshore environment with major difference being the basic arrangement and the location of the reservoirs. While conventional PSH systems consist of an upper and a lower reservoir, BE uses a smaller reservoir (the inside space of a floating structure), located within a larger reservoir (the sea or a lake). Water can be moved from one reservoir to the other by means of pumps and turbines or a pump-turbine (Figure 14a and 14b). The required head (the height difference between an

upper and a lower water level) is defined by the mass m and the shape of the floating structure. The inside space of the structure serves as lower reservoir. Klar, *et al*. (2017) describes BE concept as a very flexible one that can be applied in "shallow" water, where wind turbines typically are bottom mounted and in deep water, where floating wind turbines are required.

The buoyant object is affixed to a cable and rigged through a pulley mounted at the bottom of the water body. The cable then passes to a surface mounted reel unit. As the reel is turned in one direction by an external force, the buoy is forced below the water surface and locked for the desired charge period. When the force acting on the reel is removed the buoy will rise and perform work on the reel. The basic buoyancy storage system is depicted in Figure 14.

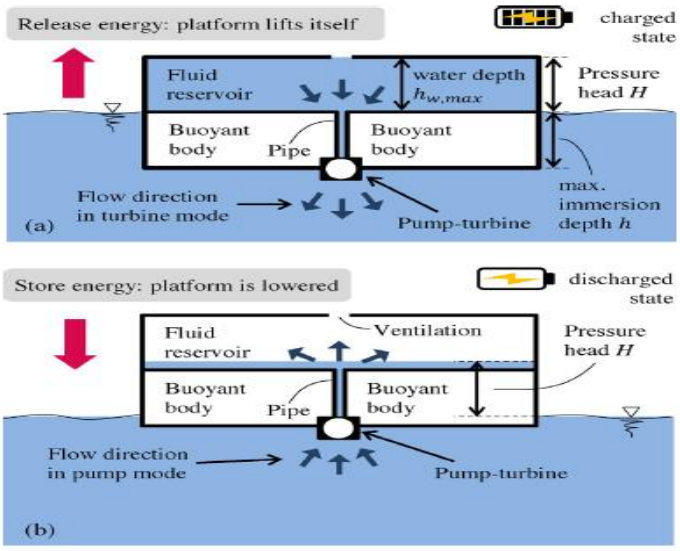

Figure 14. Basic technical concept for Buoyant Energy showing (a) Energy production, (b) Energy storage. Adapted from Klar, *et al*. 2017.

c. Hydraulic potential energy storage

This MESS uses electrical pumps to lift heavy mass hydraulically (Gravitypower, 2011; Heindl, 2014; Heindl Energy, n.d.). Initially proposed by Gravity Power LLC (Gravitypower, 2011), the heavy mass is a movable rock piston. During the charge phase (storage mode), energy from the intermittent source is used to pump water beneath the rock piston through the powerhouse, and this vertically moves the piston in the upward direction to store potential energy (Figure 15). This process also puts the water under high pressure. The downward

motion of the piston during the discharge phase (energy generation mode) releases this pressure forcing the water to power a turbine on its path and produce energy. While Figure 15a shows the working principle of hydraulic potential energy storage integrated with solar PV as energy source, 15b only gives the working principle in a schematic. The energy storage capacity is between 1 and 10 GWh with an efficiency of 80% with an investment costs ranging depending on size from 120 and 380 USD/kWh storage capacity (Heindl Energy, n.d.). According to Heindl Energy, this storage technology requires suitable geological conditions (solid bedrock), and storage capacity is a function of the fourth power of the radius of the piston while the price per kilowatt-hour of storage inversely decreases with the square of this radius.

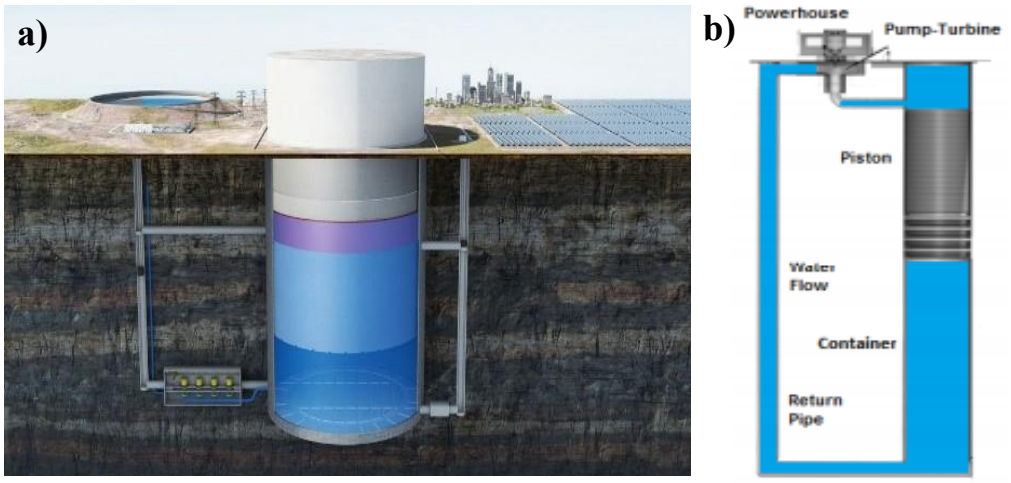

Figure 15. Hydraulic potential energy storage system: (a) Energy storage with energy source (left), (b) Energy storage schematic. Adapted from Heindl (2014).

d. MGES by Maritime Green Horizon (MGH) and SinkFloatSolutions

These two storage technologies are propositions that aimed at storing and converting potential energy by raising and lowering of masses from the ocean surface through an offshore floating platform to the seabed. The mode of operation is similar to dry gravitational energy storage systems but applied in an aquatic setting. However, this technology relies on depth instead of height, and avoids the use of mine shaft infrastructure as in some dry gravitational storage technologies.

The pending proposition by MGH (Figure 16a) is a design that uses a motorized lifting device to capture the surplus of electricity production on the land grid (renewable such as wind

or solar) to lift some weights in form of masses to the surface from the seabed thus transforming electrical energy into potential gravity energy during this ascent (storage mode) (MGH, 2015). The discharge mode occurs when energy is needed to be supplied to the terrestrial network. The weights which are now detached from the platform and attached to the generators are transferred back to the seabed, releasing the stored potential energy as electricity. The system is completely loaded (and unloaded) when all the weights get to the surface (and seabed) during ascent (and descent). A high voltage submarine power cable is used to connect the offshore platform to the power grid.

Similarly, the proposition by SinkFloatSolutions is moving concrete masses attached to floats vertically upward and downward in a marine environment with the aid of a winch that also hooks and unhooks the masses from the float. This transforms excess energy from wind or solar to potential energy during ascent, and back to electricity during descent when no energy is available. Several variants of this technology are patented by this company to reduce cost, facilitate hooking operations of masses, and increase the life of the system, but all these come with compromises (SinkFloatSolutions, n.d.). One of them is positioning floats far below the surface and stabilizing them permanently using anchoring cables to prevent the effects of winds and surface waves or even storms. The same can be done by accompanying the mass with floats during descent. Other variants include: using stabilized support to position the winch several meters below the surface; using systems like mini winches, remotely operated vehicles (ROVs), and thrusters to hang and unhook masses; and optimized design to limit hydrodynamic friction losses.

In practice, a recent work of Toubeau *et al*. (2020) investigated the techno-economic feasibility of one of the variants of SinkFloatSolutions. The system is designed to move heavy blocks (typically between 5 and 50 tons) between the bottom of the water and its surface, considering a waste material of steel making process known as steel slag as the blocks. As shown in Figure 16b, a winch can be used to connect each block to an induction machine, which acts bidirectionally as a motor, and a generator during the charging and discharging phase respectively. An automated robot hooks (and unhooks) each block to the electromechanical system that is housed in a mobile waterproof platform. A variable-frequency drive controls the speed of the induction machine. As illustrated by the author, a major constraint comes from the inability to capture a new block before the previous one ends its

travel due to lower depth considered (200 m) that does not give enough time to perform the hooking operation. Further, a robust system would consider two to three electromechanical systems to ensure the continuity of the output power and increase the number of blocks that can be simultaneously moved. The efficiency is about 80% and can change depending on the speed of float during both vertical movements, and the operation condition. This model was tested in an existing quarry with a sizeable depth of about 300m. This case study showed that 1 MW of energy is derivable from 25 tons of steel slag for this depth, and the investment cost is low at an estimated value of around 100 €/kWh with a payback period below 10 years.

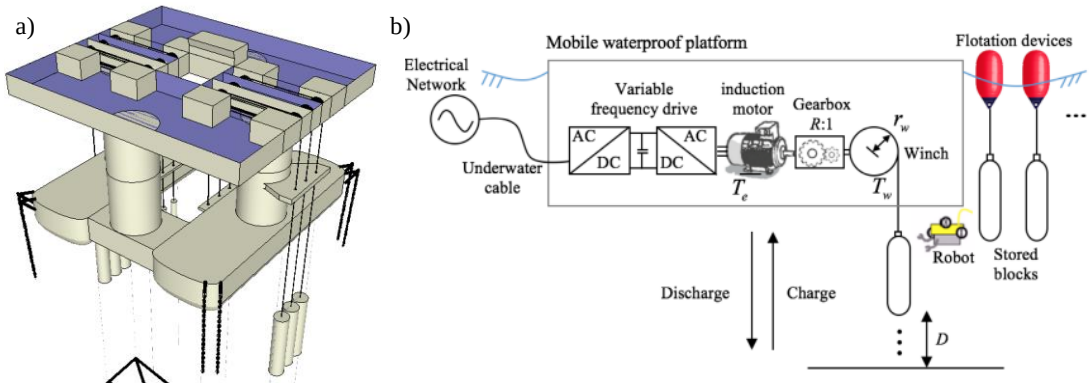

Figure 16. (a) MGH MGES storage system; Adapted from MGH (2015), (b) A typical conversion chain for a single electromechanical system of an underwater gravity energy storage (UGES) system (right); Adapted from Toubeau *et al*. (2020).

Other similar tested storage technologies worth mentioning are the work of Bassett *et al*. (2016) and (2017), and Alami (2014), but both are based on using buoyant bodies (floats and buoys) as masses that store energy as they move vertically between the surface and bottom of the aquatic medium. The whole technology is also a system of pulleys, cables, reels, and energy converters. These studies concluded that more experimental testing is required of this technology especially for quantifying the achievable round trip efficiencies for the system and utility-scale energy storage.

2.4. Multi-Criteria Decision Analysis

Multi-criteria decision analysis (MCDA) or Multi-criteria decision method (MCDM) is a group of decision-making techniques that evaluate and prioritize multifaceted, multi-

objectives, and multi-attribute problems (Estévez and Gelcich, 2015; Belton and Stewart 2002). This unique tool has been widely employed in engineering and several fields of life dealing with the issues of selection, choice, and decision making including sustainable energy planning, and suitability and choices of location, materials selections, and supply chain for the design of mechanical systems (Yoon *et al*., 1995; Wang *et al*., 2009; Huang *et al*., 2011; Zavadskas and Turskis, 2011). This method helps decision makers in segmenting the problems into smaller sections, which are analysed based upon experience and observational professionalism of the decision makers to find reasonable solutions for the issues under evaluation (Okokpujie *et al*., 2020).

MCDM is a consistent and easy tool to use encompassing several methods, including multi-attribute value theory (MAVT), entropy method, evaluation based on distance from average solution (EDAS), analytical hierarchy process (AHP), fussy AHP, data envelopment analysis (DEA), the analytic network process (ANP), the technique for order of preference by similarity to ideal solution (TOPSIS), and weighted aggregated sum product assessment (WASPA) (Fatemi and Rezaei-Moghaddam, 2019; Almeida, 2019). While the most commonly implemented MCDA approaches are AHP, MAVT, outranking, and goal programming, AHP is the most practical and well-known MCDA method (Mahdy and Bahaj, 2018; Belton and Stewart 2002).

MAVT is an approach that supports consistent and transparent decision-making among multiple alternatives in complex situations with conflicting objectives (Belton and Stewart, 2002). This method allocates a numerical value to each alternative under evaluation (Estévez and Gelcich, 2015), thus developing an order of preference for the alternatives which is based on the decision maker's value judgment (Belton and Stewart 2003). MAVT uses an attribute tree to structure the decision problems, and a central component of this technique is the generation of partial value functions (generally in the form of an additive function), which are later aggregated to deduce an overall ranking function (Von and Edwards *et al*., 1986).

AHP was proposed by Saaty (1980) for planning, resource allocation, and priority setting in operations such as transportation and military. This method is an organized process that divides the decision-making procedure into a few simple steps to generate weighted factors (Saaty, 2008). The method of AHP is similar to the MAVT approach as also based on an

additive preference function (Belton and Stewart 2002). However, AHP adopts pairwise comparisons by converting verbal statements into preference scores to evaluate the relationship between alternatives and a set of criteria, for example, how essential objective a is with respect to objective b) (Chopin *et al*., 2019). A variant of AHP is ANP which can integrate a higher level of sophistication when evaluating the interdependence of criteria, thus offering a solution to complex multi-criteria problems (Hsueh *et al*., 2015). The transparency, and simplicity of the aggregation methods of AHP and MAVT partly make them become widely used, but the same simplicity can bring about doubt regarding their validity (Harper *et al*., 2019).

There exist many different methodologies to implement multi-criteria analysis (Estévez and Gelcich, 2015), however, their theoretical formulation shares some major stages (Figure 17). The procedure is never unidirectional, and researchers have to consider one or more of the following steps for practical applications (Estévez, 2021) including:

- Decision problem formulation: This stage explores the range of values comprising the decision-making problem (Estévez, 2021).
- Developing indicators and objectives: This stage put decision-making problems into operation by converting the generated values into objectives and indicators (Keeney *et al*., 2005).
- Development of alternatives: in this stage, strategies for the achievement of objectives are explored and defined (Gregory & Keeney, 1994).
- Weights calculation: This major step in multi-criteria analysis establishes the relative importance of objectives which are generally represented as weight factors (Belton and Stewart, 2002);
- Consequences evaluation: The establishment of the potential impact of alternatives on the objectives is done in this stage with the aid of either qualitative evaluations or quantitative models, generally done by experts (Gregory *et al*., 2012).

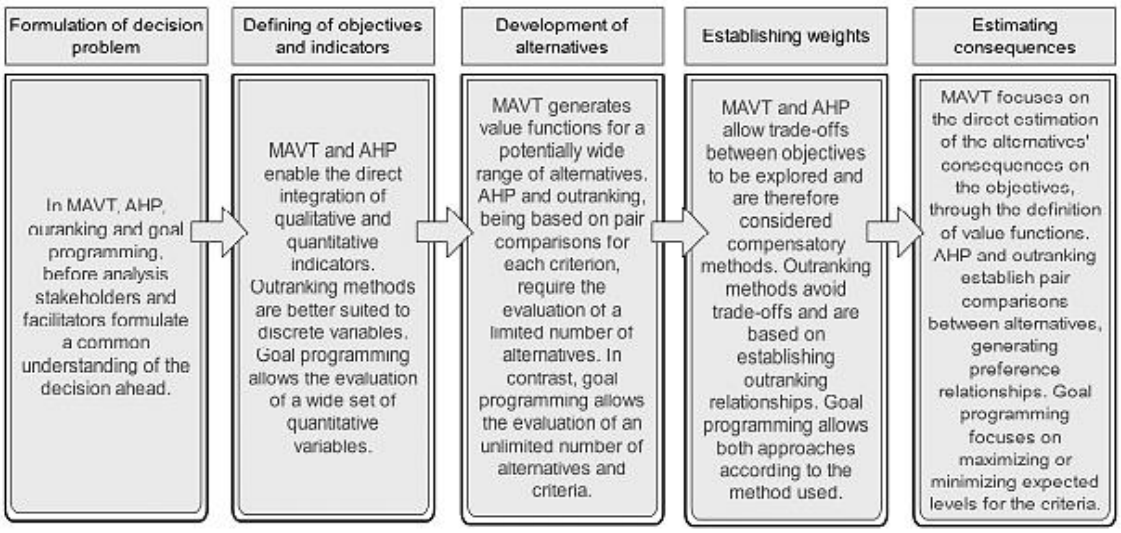

Figure 17. Stages of participation in multi-criteria decision analysis (MCDA) methodologies. Adapted from Estévez *et al*. (2021).

3. Materials and Methods

This study proposes the application of a state-of-the-art energy storage technology using gravitational potential energy form in Cabo Verde. A methodology that is used for determining the best locations for siting wind farms majorly on the continent is extended for the first time to the energy storage system, specifically an offshore energy storage system. We divided our study into sections by first evaluating the energy state of our study area. This includes electricity price, fossil fuel usage, CO2 emission, and renewable penetration where much attention was paid to the dominant energy, wind energy. We also analyzed the amount of CO2 emission prevented through wind resource utilization before briefly delving into renewable potential, and cost analysis.

The second and major aspect focused on the MGES itself and was subdivided into two systems; an isolated system and an onshore-connected system. We defined the isolated system as one that the off-peak energy is to be stored and consumed offshore without connecting to the grid onshore majorly by offshore facilities, while the onshore-connected system would be used for storing the excess generated renewable energy during off-peak period and transferring the energy to an onshore grid when needed. We have several conflicting criteria to consider for each of the two systems mainly resources as a function of depth, cost as a function of distance to the shore, and a secured location as a function of minimal impacts from currents. Thus, we are treating them separately as follows:

- **Isolated system**

This system focuses on regions with the maximum resources with little impact of underwater currents.

- **Onshore connected system**

This system focuses on all the three conflicting criteria that we want to maximize which are: resource (depth), cost (minimum distance to the coast), and security (minimum level of underwater perturbation).

Python and R are the programming languages used for data analysis and part of data acquisition. Considering the nature of this study, several datasets and processing approaches were employed. As earlier mentioned, this study is divided into energy state, and MGES.

3.1. Energy State in Cabo Verde

3.1.1. General Energy Consumption

The sources of data for this sub-section were numerous. They include several databases and past publications and annual reports such as Gesto Energy, Cabeolica (Cabeolica, 2021), Energy renewable of Cabo Verde (energiasrenovaveis, 2020), Emissions Database for Global Atmospheric Research - EDGAR (EDGAR, n.d.; Crippa *et al*., 2019 and 2020), Eurostat (Eurostat, 2018), and Electra (Electra, 2018). We conducted analysis on fossil fuel consumption, renewable penetration, wind energy usage, intermittency, and C02 emission. Further, the price of electricity in Cabo Verde was compared with other European and West African countries. Lastly, the final energy potential and their intermittency based on their sources of either renewable or non-renewable were evaluated.

3.1.2. Wind and Solar Radiation

Daily wind (10 m) and solar radiation over a surface under a clear and normal atmosphere were downloaded from Copernicus climate data[1] (Hersbach *et al*., 2018). These datasets that span between 2012 and 2020 were averaged for the entire Cabo Verde, and the annual, monthly, and hourly variations were shown. Details about the dataset will be presented under wave climate analysis.

The wind dataset comes in west-east (U) and south-north (V) velocity components which were then processed then processed using the formula:

$$Velocity = \sqrt{(U^2 + V^2)} \quad (1)$$

[1] https://cds.climate.copernicus.eu/cdsapp#!/dataset/reanalysis-era5-single-levels?tab=overview

Where U and V are the wind velocity components in the x and y direction respectively (Zhang *et al*., 2019).

3.1.3. Ocean Thermal Energy Conversion (OTEC) Analysis

The dataset used for OTEC analysis is the GLORYS12V1 reanalysis data product of the Copernicus Marine and Environment Monitoring Service – CMEMS (E.U. CMEMS, 2020). It is a homogeneous 3D gridded description of the physical state of the ocean-spanning several decades (Fernandez and Lellouche, 2018; Perruche *et al*., 2016). It is produced with a numerical ocean model constrained with data assimilation of satellite and in situ observations by means of a reduced-order Kalman filter. Nemo platform is the model component and it was driven by ECMWF ERA-Interim product and ERA5 reanalyses at the surface in the past and recent years respectively (Lellouche *et al*., 2018 and 2021). The correction of the slowly-evolving large-scale biases in the temperature is done using the 3D-VAR scheme. The Gridded daily seawater temperature (°C) model output has 50 vertical layers and 1/12 degrees in horizontal resolution (Lellouche *et al*., 2018, and 2021). We downloaded this ocean temperature product covering 12 years.

OTEC works on a principal of temperature difference between the surface and 1000 m depth (Mofor et. al, 2014). A minimum temperature gradient of 20 ºC between these two depths is necessary to achieve acceptable performance to drive turbines (Devis-Morales, *et al*., 2014). Three major types of technologies are employed for the thermal gradient ocean system namely: Close cycle, open cycle and hybrid cycle (Adesanya *et al*., 2020, Khan *et al*., 2017, Adiputra *et al*., 2020). This study adopted the approach to develop open and hybrid systems (Shadman *et al*., 2019, Khan *et al*., 2017, Adiputra *et al*., 2020) as the toxicity and availability of the working fluids for the close cycle such as ammonia, and chlorofluorocarbons, and the possible biofouling of the heat exchangers during operation are some of the major challenges facing the close system.

Using the 12 years (2009-2020) gridded daily seawater temperature data obtained from CMEMS, the total average and seasonal extractable or available power called the gross power (P gross), and the total annual and seasonal usable or output power (P net) are calculated for the 12 years period for some locations and the whole of Cabo Verde using the methodology described by Nihous, 2007, and Devis-Morales *et al*., 2014. The net power is usually 30% of

the gross power due to a considerable amount of the gross power that is exhausted to pump the large seawater flow rates through the OTEC plant (Vega and Nihous, 1994; Nihous, 2017), and it can be expressed by considering ΔT_{design} as 20 °C and the other losses presented in Nihous, 2007.

The model was constructed based on the highlighted estimations and assumptions as follow:

a. Gross Power P_g:

$$P_g = \frac{3\rho c Q_{cw} \gamma \varepsilon_{tg} (\Delta T)^2}{16(1+\gamma)T_w} \qquad (2ai)$$

(Luomi, 2014; Syamsuddin and Attamimi *et al*., 2015)

$$\gamma = \frac{Q_{ww}}{Q_{cw}} \qquad (2aii)$$

IMF (2019)

b. Net Power P_n:

$$P_n = \frac{3\rho c Q_{cw} \gamma \varepsilon_{tg}}{8T_w(1+\gamma)} \left(\frac{3\gamma(\Delta T)^2}{2(1+\gamma)} - 0.18\left(\Delta T_{design}\right)^2 - 0.12((\gamma/2)^{2.75} \left(\Delta T_{design}\right)^2 \right)$$

(2b)

(Uehara and Ikegami, 1990)

Where ρ is the density of seawater in kg/m^3, c is the specific heat of seawater, as 4000 kJ/kg K, Q_{cw} is cold water flow rate in m^3, T_w is the temperature of warm surface water in K, ΔT is the temperature difference between warm water and cold water in K, εtg is the turbine generator efficiency and γ is the ratio between warm water and cold water flow rate, ΔT_{design} is represented by the surface temperature.

3.1.4. Wave Climate Analysis

The wave dataset which was gotten from the operational global ocean analysis and forecast system of Era 5 from Copernicus climate data portal[1]. According to Hersbach *et al*. 2018, ERA5 is the output of the fifth-generation ECMWF reanalysis for the global climate and

weather over the past 40 to 70 years. It is a combination of model data with observations using data assimilation techniques into a globally consistent and complete dataset for several atmospheric, ocean waves, and land variables. The data undergoes daily updates with a latency of about 5 days. The final reanalysis product is provided on a regular grid of latitude-longitude 0.25 degrees horizontal resolution. We used 24 years (1996 -2021) wave data consisting of the significant wave height, mean wave direction, and wave period. The power density P was calculated from the significant wave height H_s and the wave energy period T_e as follows:

$$P = \frac{\rho g^2}{64\,\pi} {H_s}^2 T_e \quad (3)$$

(Nielsen, 2009)

Where ρ and g represent the seawater density (1025 kg m^{-3}) and gravity acceleration (9.806 m s^{-2}) respectively; Hs is the significant height (m), and T_e is the energy wave period (s).

This simplified expression uses deep-water approximation which fits well for most of the modeled domains as illustrated by Nielson (2009). However, some sophisticated techniques as well as in situ measurements might be required to precisely determine the shallow water wave climate as explained by the same author.

The spatial distribution of the mean wave power with its seasonal and monthly climatology was computed.

3.2. MGES Analysis

3.2.1. Bathymetry Data Choice and Analysis

Marine gravitation energy storage MGES is a technique that strongly depends on depth for its resource evaluation. Hence, the selection of the final bathymetry dataset used in this study was done after examining various bathymetry datasets. They include EMODNET, GEBCO, ETOPO1, and other in-situ sources. The output of this data is described below:

a. General Bathymetric Chart of the Oceans (GEBCO)

GEBCO's gridded bathymetric data set, the GEBCO_2020 grid is the latest global bathymetric product released by the General Bathymetric Chart of the Oceans (GEBCO) and has been developed through the Nippon Foundation-GEBCO Seabed 2030 Project[2]. This a continuous, global terrain model for ocean and land with a spatial resolution of 15 arc-seconds (450 m). The grid uses as a 'base' Version 2 of the Shuttle Radar Topography Mission (STRM) which is SRTM15+ data set (Tozer *et al*, 2019). This data set is a fusion of land topography with measured and estimated seafloor topography (Becker *et al*., 2009). It is augmented with the gridded bathymetric data sets developed by the four Seabed 2030 Regional Centers. Sources includes regional dataset, Multibeam and Single Beam Survey Data. This dataset has a good coverage but low resolution for the intended study (Figure 18).

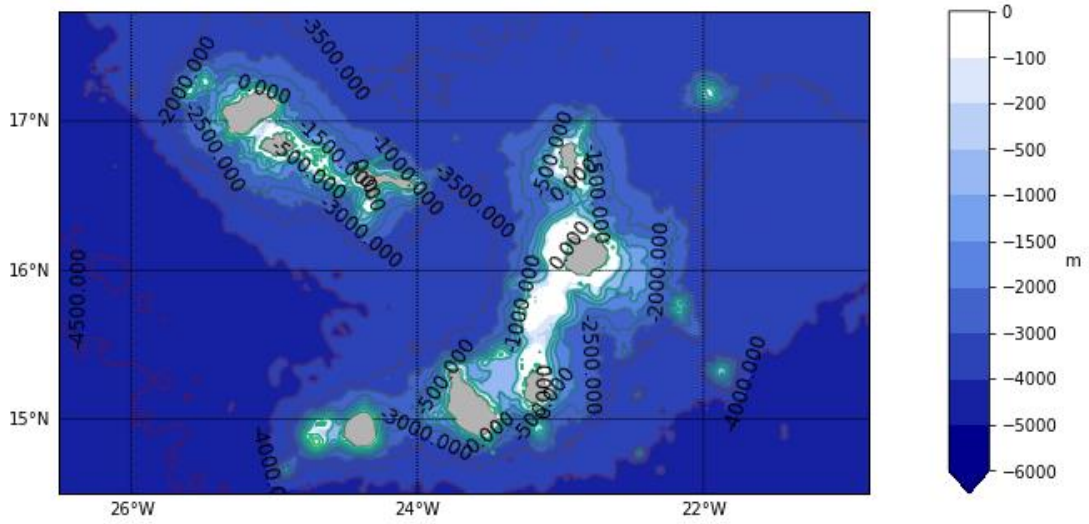

Figure 18. GEBCO Bathymetry Output (Data from GEBCO).

b. Emodnet Data

According to Emodnet Bathymetry Consortium (2018), the European Marine Observation and Data Network (EMODnet) bathymetry dataset includes survey and composite Digital Terrain Models (DTMs) collated from public and research organizations. The source data majorly constitute data from single and multibeam surveys that are delivered either as a

[2] Book, I. I. G. C., & Contributors, O. D. GEBCO_2020 Grid.

set of soundings or as a high-resolution DTM produced from a single survey. GEBCO 30 arc-second gridded data is used to complete the coverage where high-resolution data are unavailable, and this region starts from the southern part of Cabo Verde southwards. For the global coverage, the resolutions are:

- 1/8 * 1/8 arc minutes (230m) for deep sea;
- 1/16 * 1/16 arc minutes (circa 115 * 115 meters) for deep-sea and shelf, and continental margin;
- 1/32 for continental margin.

We downloaded from Emodnet data portal[3], and generated a plot for the region covered by the high resolution portion of the data (Figure 19). The high resolution does not cover south of 15 N as shown in Figure 19.

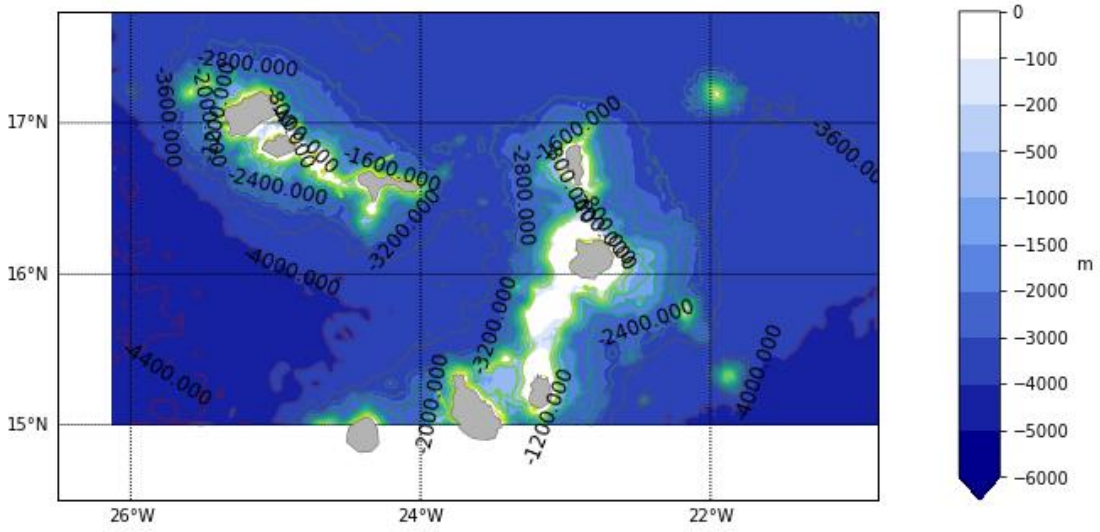

Figure 19. Emodnet Bathymetry Output (Data from Emodnet).

c. ETOPO1

ETOPO1 is a 1 arc-minute (2km) global relief model of Earth's surface that integrates land topography and ocean bathymetry (Amante and Eakins, 2009). Built from global and

[3] https://portal.emodnet-bathymetry.eu/

regional data sets, it has a higher resolution version of ETOPO2, which is a 2 arc-minute global relief model of Earth's surface. An arc-minute is 1/60 of a degree. The dataset has a good coverage but with a low resolution (Figure 20).

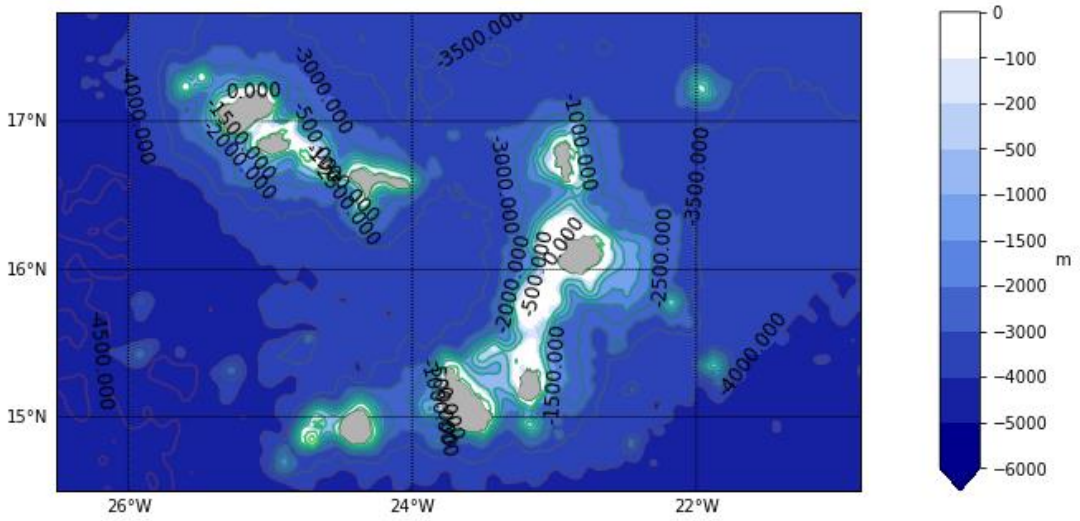

Figure 20. ETOPO1 Bathymetry Output. Data: Etopo1.

d. Survey Data

Basically, it is multibeam bathymetry and acoustic backscatter images. Multibeam bathymetry and backscatter data were collected using an Atlas Hydrosweep system on R/V *Meteor* cruise 62/3 and a Simrad EM 12 system on RRS *Charles Darwin* cruise 168. Multibeam coverage extends along both flanks of the northern island chain from São Nicolau in the east to Santo Antão in the west (Masson *et al*., 2008). For the southern island chain, the western flank of Santiago and the area around Fogo and Brava were surveyed (Figure 21). No data were collected around the eastern islands of Sal, Boa Vista and Maio. Although, places without data are filled with NASA SRTM data, we only focus on the multibeam data and filled places lacking data with zero. This dataset has a very good resolution but does not cover the whole of Cabo Verde (Figure 21).

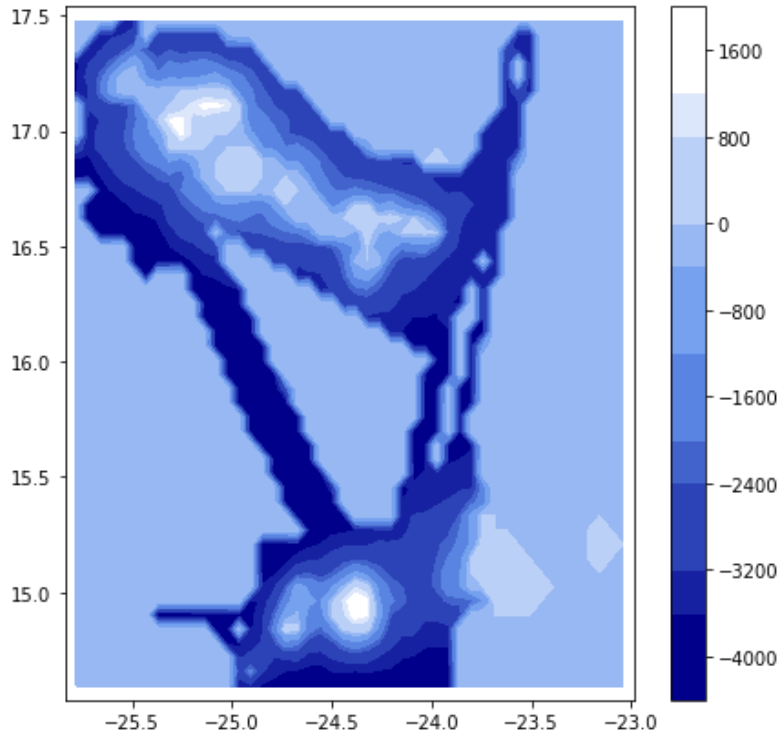

Figure 21. In-situ data Output (Masson *et al*., 2008).

e. NCEI Multibeam Bathymetry Data

NCEI is the U.S. national archive for multibeam bathymetric data and holds more than 9 million nautical miles of ship trackline data recorded from over 2400 cruises and received from sources worldwide (NOAA National Centers for Environmental Information, 2004). In addition to deepwater data, the Multibeam Bathymetry Database (MBBDB) includes hydrographic multibeam survey data from NOAA's National Ocean Service (NOS). A comprehensive list of the sources can be found in Appendix 5. More details can be found on NCEI website[4].

The high resolution of this dataset allows it to capture several features and depth variations better than other dataset presented. The coverage also spans through the whole of

[4] https://www.ngdc.noaa.gov/mgg/bathymetry/multibeam.html

Cabo Verde making it a best fit for this research (Figure 22). We selected 50 m by 50 m grid horizontal resolution which is very high.

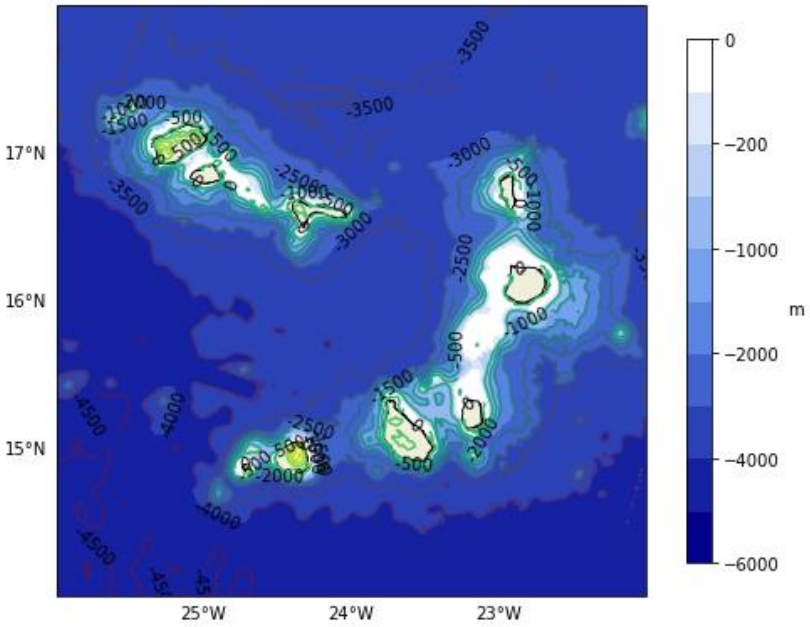

Figure 22. NCEI data Output. Data: NCEI.

3.2.2. Analysis of the Distance from coast

The distance to the coast was computed in R by adopting a function developed by Davidatlarge retrieved from the GitHub repository link that can be found in the footnote[5]. This function was developed to calculate the distance of geo points to the nearest coastline and was meant to be used for marine data. We used the more precise approach of the function to generate finer and filtered coastline with a plot output and extracted values for each of our geo-points which were later contoured. The plot output is shown as Figure 23.

[5] https://github.com/Davidatlarge/dist2coast

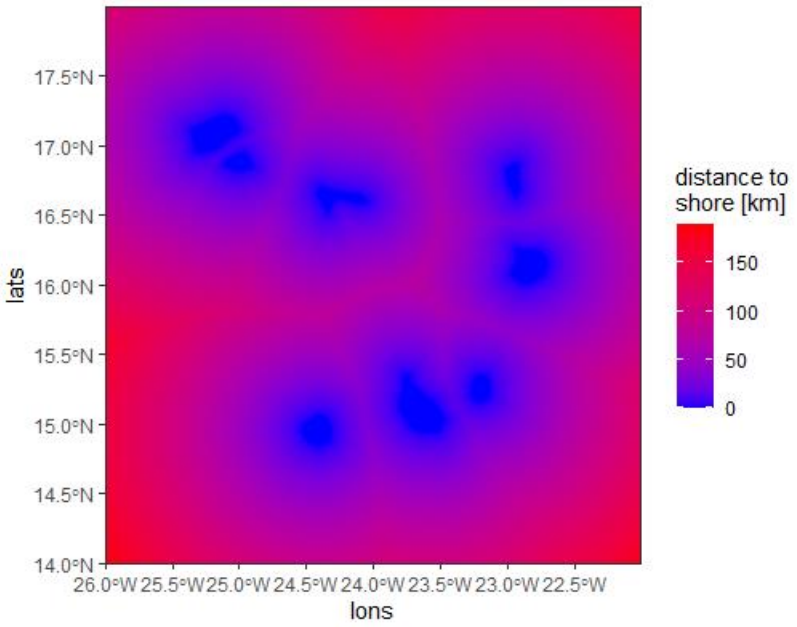

Figure 23. Distance from the coast. Data: Natural Earth[6].

3.2.3. Current Data Procurement and Analysis

The current dataset is among the output of a set of Atlantic Ocean numerical simulations performed with the Coastal and Regional Ocean Community model (CROCO). CROCO was developed based on the Regional Oceanic Modeling System (ROMS). Four sets of high resolution output have been released namely GIGATL24, GIGATL6, and GIGATL3, and the latest version and highest resolution version GIGATL1 covering the June 2008-May 2009 period which is used in this study. GIGATL1 provides hourly outputs with a resolution is <1 km in the horizontal and 100 "topography-following" vertical levels initiated from GIGATL3 simulations with boundary conditions supplied by SODA. We used the simulation with tides. The link to the data information is https://github.com/Mesharou/GIGATL/tree/v1.0.

The computed statistics for this data include: minimum, maximum, mean and standard deviation of the current amplitude for the surface, bottom and vertical mean throughout the water column. We computed from the hourly data the monthly and annual statistical variables

[6] www.naturalearthdata.com

and analyzed for the variable that can best fit our study focus since we are considering one system that can be far offshore and the other that is shore dependent.

3.2.4. Marine Gravitational Energy Storage Resource Potential

❖ **Concept**

The electrical energy derived from the intermittent renewable source at peak energy is used as an electric engine and transformed to mechanical energy that acts in lifting a number of masses (solid blocks) using systems of pulleys and winches connected to an electromechanical system acting as both a motor and a generator. As the mass rises, the potential energy increases. When the mass gets to the maximum height, the energy is then stored as mechanical potential energy, and this step is referred to as the system loading mode. The discharge mode happens when the demand for energy increases, and this is released to the descent. In this way, the motor acts in reverse, acting as an electric generator (Botha and Kamper, 2019; Morstyn, 2019; Toubeau, 2020).

❖ **System Sizing and Quantifying Resource Potential**

The marine gravitational method using potential energy from heavy masses has not been fully implemented in the marine environment, unlike the buoyancy method (another marine gravitational method), and UWCA. To determine the system's energy storage sizing and capacity, we first adopted the approach of Bassett *et al*. (2016), Botha and Kamper (2019), Morstyn *et al*. (2019), and Ruoso (2019). While Bassett *et al*. (2016) presented a theoretical and experimental validation of a wet gravitational energy storage system where the vertical (up and down) movement of a buoyant body generates potential energy, the works of Botha and Kamper (2019), Morstyn *et al*. (2019), and Ruoso (2019) focus on the dry gravitational energy storage system using suspended (heavy) masses.

We supplemented the aforementioned studies with the works of Bassett *et al*. (2017) (which showed a full theoretical system sizing of a wet gravitational potential energy using a buoyant mass), and one of the variants of the technologies patented by SinkFloatSolutions that was presented by Toubeau (2020). The reason for not fully adopting the work of Toubeau (2020) even though it also focuses on MGES of heavy masses (not buoyant bodies), and has

also been tested experimentally (a practical case study conducted in a quarry of depth 200 m), is due to the fact this presented work considers a full marine system with a potential depth that can exceed several kilometers thus giving enough time for hooking and unhooking of masses that Toubeau (2020) stated as a major challenge to this system. Further, our proposed storage system avoids both the use of robots for hooking operations, and several electromechanical systems by adopting a simple more flexible proposed solution patented by MGH[7].

Some relationships and abbreviations used in the system sizing of MGES are shown in Table 1.

Table 1. Table showing some acronyms and relationships used in MGES system sizing

Abbreviation/Acronym	Meaning and Relationship
1 W h	3600 J
1 J	$2.78 \times 10^{-4}\ Whr$
d	Diameter of mass/weight
Efficiency	Efficiency of the system
D	Total available Depth
D’	Usable depth in the marine environment to lift the weight
H	Height of the weight
h	hour
V	Volume of the weight
m	mass of the weight
ρ	density of the weight
ρ_w	density of water
F_b	Force of Buoyancy
F_d	drag force
C_d	drag coefficient
A	Area of the weight perpendicular to motion
V_c	drag velocity

The first two assumptions are that weight is composed of heavy concrete (or slag waste incorporated steel fiber-reinforced concrete (SSFRC)) with a long cylindrical shape. These two materials were considered as a result of factors like cost, environmental impacts, durability, and resistance to corrosion and chlorine penetration (Kim *et al*., 2021). According to Koyuncu (2007), streamline bodies have the lowest drag in water which is unachievable for underwater structures. Water pressure is the primal factor in determining the shape of an underwater

[7] https://youtu.be/cllRJUuJ_7s

structure. Only taking into account this factor, every underwater structure would have a spherical shape especially for hollow bodies. However, for heavy concrete or SSFRC, a cylindrical shape might be the best option as complex shapes will require customized molds which might be quite expensive and thus difficult to get. Thus, we are considering a cylindrical weight.

$$Volume\ of\ Weight = \frac{\pi d^2 H}{4} \tag{4a}$$

$$m = \rho V = \frac{\rho \pi d^2 H}{4} \tag{4b}$$

1. Defining storage potential using depth alone:

a. Consider the total potential without the efficiency of the system;

$$Energy(J) = mgD \tag{4ci}$$

$$Energy(Wh) = 2.78 \times 10^{-4} \times mgD \tag{4cii}$$

b. Inclusion of the efficiency of the system;

$$Energy(Wh) = Efficiency \times 2.78 \times 10^{-4} \times mgD \tag{4ciii}$$

$$\text{Energy (Wh)} = \frac{2.78 \times 10^{-4}\,(Efficiency \times \rho g D \pi d^2 H)}{4} \tag{4civ}$$

2. Taking account of the height of the weight;

$$Energy\ (J) = Efficiency \times mgD' \tag{4di}$$

$where\ the\ usable\ depth\ of\ the\ water\ to\ lift\ the\ weight, D' = D - H$

$$Energy\ (Wh) = \frac{2.78 \times 10^{-4}\,(Efficiency \times mgD')}{4} \tag{4dii}$$

$$m = \rho V = \frac{\rho \pi d^2 H}{4}$$

$$H = \frac{4m}{\rho \pi d^2} \tag{4diii}$$

$$D' = D - H = D - \frac{4m}{\rho\pi d^2} \qquad (4div)$$

$$Energy\ (Wh) = \frac{2.78 \times 10^{-4}\ (Efficiency \times mg(D - \frac{4m}{\rho\pi d^2})}{4} \qquad (4dv)$$

3. Efficiency

To determine the **Efficiency** of the system, we have to look at the amount of energy generated during ascent, and the amount released during descent which are a function of the system's design in general including mass used, depth of operation, shape of the mass, and energy loss due to drag, friction etc.

According to Archimedes and principle of floatation (established laws of physics), forces acting on a body fully or partially immersed in a fluid are:

i. Its weight always acting downwards;

ii. Buoyancy force always acting upward due to pressure increasing with depth making the pressure gradient force to be directed upward;

iii. Drag, acting in opposite direction to the body's motion i.e ascent or descent depending on the stage of the vertical movement.

During ascent (system loading), the tension (C) in the string or rope is a function of the weight (purple arrow in Figure 24b), and the opposing force (deep blue arrow) will only be the drag. While during descent (discharge), the opposing forces are drag and buoyancy force (Figure 24a). Thus, the tension can be expressed as the resultant force depending on ascent and descent as:

$$C = Weight \pm F_b - F_d \qquad (5a)^8$$

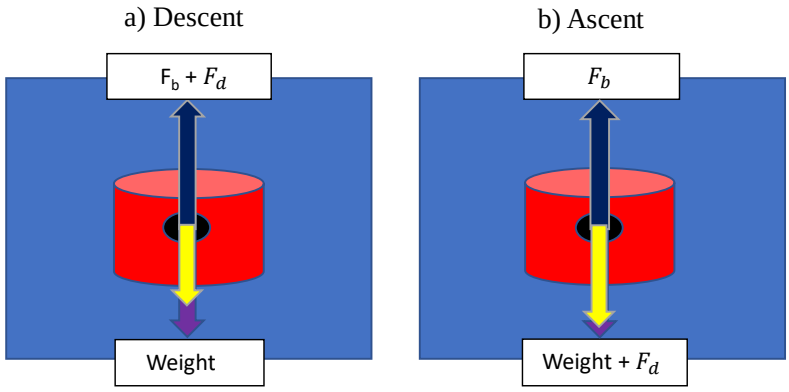

Figure 24. Schematic of the balance of all forces as a body ascend (left) and descend (right) in a fluid.

a. Buoyancy force

The magnitude of the buoyancy force is simply the weight of the fluid displaced as explained by Archimedes principle, and this is the product of the surrounding fluid density, the volume of the object, and the acceleration due to gravity. For this study,

$$F_b = \rho_w V g \qquad (5b)$$

In addition, the ambient density of water increases with depth although might not be greater than 1 to 1.5 % per 1000 and 1500 respectively.

b. Efficiency loss as a result of other factors

In addition to buoyancy force that can influence the efficiency of the storage system, other factors that are always considered during system sizing of an underwater technology that works under this principle includes the following:

[8] Equation 5a depicts that weight is always the dominant force since we are considering a heavy mass. The tension C is larger during ascent as a result of drag force complementing weight.

i. Hydrodynamic losses

The float will perform work to the fluid proportional to the hydrodynamic drag force opposing the float's motion which is proportional to the velocity. Drag force is expressed below.

$$F_d = 0.5\rho_w A {V_c}^2 C_d \tag{5c}$$

Where A is the area of float perpendicular to motion, Cd is drag coefficient, and Fd is the drag force acting opposite direction of float velocity, and Vc is charge velocity. Assumption here is the same charge and discharge velocity. Since F_d is acting against the float motion for both the charge and discharge phases, the total energy loss will be the sum of the losses for charge and discharge.

C_d is not a constant but varies as a function of flow speed, flow direction, object position, object size, fluid density, fluid viscosity, and the Reynolds number (Re), and normally be derived empirically.

$$Total\ Drag\ Energy = (F_d 1 + F_d 2)D'$$

$$= \rho_w A {V_c}^2 C_d D' \tag{5d}$$

Since Energy is the product of force and distance, and C_d equals 0.82 or 0.84 for a long cylinder or good aerodynamic shape according to Toubeau (2020) that also computed Re from linear dimension (L) of mass of 1m, speed of 1 ms^{-1}, and kinematic viscosity (μ) of 1.007 × 10^{-6} (m^2/s) as shown below:

$$\mathrm{R_e} = \frac{\mathrm{V_e L}}{\mu} = \frac{1\times1}{1.0007\times10^{-6}} \approx 10^6 \tag{5e}$$

ii. Electrical losses

When an electric motor and generator are used in connection to the reel such that electrical energy can be stored and discharged using Gravity approach, additional losses will be experienced. The power input or output from the motor unit will be proportional to system

voltage and current. The required power level and thus current can be calculated for a given float and water depth as:

$$I = \frac{CV_c}{Q} \tag{6a}$$

Where C is the tension in the string, Vc= charge velocity, I is current (amps) and Q is system's voltage (volts).

The resistive losses within the motor are related to amperage through;

$$E_{loss\_electric} = \left\{\left[\frac{CV_c}{Q}\right]^2 RT\right\} \tag{6b}$$

Where R is the total resistance of the electric motor coils, E lost is electrical loss and T is time.

Substituting t as distance/ velocity, we arrive at:

$$E_{loss\_electric} = \left\{\frac{C^2 V_c R D'}{Q^2}\right\} \tag{6c}$$

For equal charge and discharge power levels, and when charge and discharge occurs through the same electric motor (i.e. equal resistance of both charge and discharge phases), the total loss can be expressed as twice of that:

$$E_{lost\_electric\_total} = 2\left\{\frac{C^2 V_c R D'}{Q^2}\right\} \tag{6d}$$

iii. Total Round-Trip Efficiency

The total round trip efficiency of the system can be expressed after accounting for the total major losses as:

$$\text{Efficiency} = 1 - \left\{\left(E_{loss\_drag} + E_{loss\_electric}\right) + E_{loss\_upwardbuoyantforce}\right\} \tag{7a}$$

Note: We separate the energy due to buoyancy because we can incorporate it directly into the Energy Equation by using density instead of mass and deducting mass of fluid displaced from the total mass which now becomes our new equation.

Incorporating buoyancy force into the initial energy equation;

$$Energy(J) = (\rho - \rho_w)Vg\ (Efficiency\ loss\ due\ to\ drag\ and\ electric) \quad (7b)$$

$$Energy\ (Wh) = \frac{2.78\ \times 10^{-4}\ ((\rho - \rho_{w)}(D - \frac{4m}{\rho\pi d^2})g(Efficiency\ loss\ due\ to\ drag\ and\ electric)}{4} \quad (7c)$$

c. Total Round Trip Efficiency 2

Assumption for Drag losses:

The effect of hydrodynamic drag is of a significant importance as it accounts for the fundamental losses of energy due to viscous dissipation. As shown in the previous equations, drag force is governed by drag coefficient. Drag coefficient is also a function of Bejan number, Reynolds number, and the ratio between wet area and front area (shape) (Liversag and Trancossi, 2018). Drag coefficient is inversely proportional to Reynold's number but drag force and energy are directly proportional to drag coefficient. Since drag is a complicated issue that requires a detail analysis, we further adopted the concept of Bassett *et al*. (2016) for circular cylindrical bodies, and other similar studies that explained the concept of drag crisis, indicating that drag coefficient drastically decreases for high Reynolds numbers of 3×10^5 as a result of the boundary layer transition from laminar flow with a wide wake, to turbulent flow with a narrowed wake (Fluent Inc., 2016; Singh and Mittal, 2004). Bassett *et al*. (2017) analyzed ranges of speed of drag crises between the best case and worst case scenario of drag losses from 0.2 to 12 respectively, and showed that for a float moving very slowly in relation to its size, the hydrodynamic drag losses are very small compared to total energy storage capacity, and as such the efficiency range is very high.

Finally, to quantify the efficiency in other components of this system, we adopted the work of Morgan (2010), an existing patent form of gravity energy storage through buoyancy that also utilizes barges, pulleys and other system's design similar to this study. Although no specific references were presented, the patent utilized a generator efficiency of 95%, pulley efficiency of 99%, and motor efficiency of 97% in the calculation. Siemens (2016) showed that the efficiencies used by the patent for motor and generator respectively are obtainable. Further,

the maximum efficiency of pulley obtained by a research by Balance Community in 2016 is 96%. In addition, we can consider an electric motor/generator of the model W22 Magnet IR5 Ultra-Premium, manufactured by the company WEG. This motor is a synchronous type with high-performance permanent magnets and has 97% efficiency (Ruoso *et al*., 2019).

Putting everything together,

$$\eta_{roundtrip} = \eta_{motor} \times \eta_{generator} \times \eta_{charge} \times \eta_{discharge} \times \eta_{pulley}$$

$$\eta_{roundtrip} = 0.97 \times 0.95 \times 0.97 \times 0.97 \times 0.96 = 0.86 \qquad (7d)$$

The computed roundtrip efficiency of 86% in Equation 7d is reasonable as also highlighted by Toubeau (2020) that the round-trip efficiency in MGES can be higher than 80%. In this regard, our equation becomes:

$$Energy\ (Wh) = \frac{2.78 \times 10^{-4}\ (\rho - \rho_w)\left(D - \frac{4m}{\rho\pi d^2}\right) g \times 0.86}{4} \qquad (7e)$$

❖ **Reel and pulley anchorage**

Since we are considering depth around 800-1000m or more, a fixed structure might not be feasible, thus a floating platform should be considered. The required foundation mass that can support the floating system will be proportional to factors including the volume of the mass, ambient fluid velocity, and design safety factor. For zero ambient fluid velocity, the required foundation mass can be expressed as:

$$M = \frac{2C\{S_f\}}{g} \qquad (8)$$

Where C is the tension in the cable without drag (ρV_c g - mg), and S_f is the safety factor, a dimensionless quantity that gives a wholesome of the amount of mass the foundation mass can support.

3.2.5. Developing Multicriteria Model and Generating Energy Storage Suitability Maps

The last subsection was used to quantify the resources. This subsection is showing the approach adopted to identify the best locations and develop a suitability map using MCDA

concept. MCDA is a widely used tool in proposing sites for wind farms and generally in wind spatial planning. Some of the major criteria they consider for onshore wind are wind speed-factor, distance to roads, and the proximity of farms to built-up areas, whereas water depth and wind speed are the major factors under consideration for offshore indicating MCDA is problem orientated. Based on this, we developed our own criteria tailored to our problem and identified our criteria for each of our focus. According to Salty (2008), one of the best ways to solve a multiple criteria problem is to study the problem and its characteristics, then arrive at specific conclusions. We have already highlighted that we are focusing on two systems, Onshore-connected and Isolated, and we have identified our criteria for each. The approached we used is shown in Figure 25.

After problem definition that we have already done, we set a weight of one. Weight in this regard is used to establish the relative importance of each of the criteria that are used in our model as explained by Belton and Stewart (2002). However, we are considering all the criteria to be of equal significance. After rescaling the model output, and creating a refined scale, the final suitability map has five indices namely; optimally suitable, most suitable, moderately suitable, least suitable, and not-suitable. Our major focus is highlighting the optimally suitable zones and quantifying their storable energy. However, zones with great storage potential falling under the category of the most suitable class is also of high importance to this research. Refining the scale allows us to filter the major areas of our focus especially the optimally suitable zones. A detailed procedure of how we adopt the concept of MCDA and generate our suitability models is presented next.

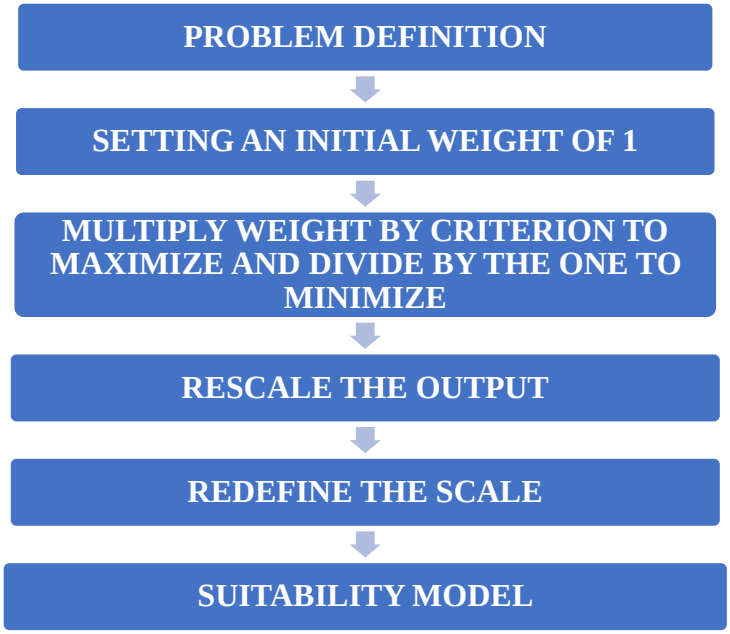

Figure 25. Flow-chart for generating suitability model.

❖ Economic Interest Zone

A part of the previous subsections was used to describe the principle behind MGES, the choice of data for this study, the procedure we used to quantify the resource potential including the storage system's efficiency, and all the associated assumptions. To determine the best locations to site this technology in Cabo Verde that we termed **Economic Interest or suitable zones**, we split our analysis into two as stated in the introductory zone. The first system (Isolated system) is majorly concerned with the maximum derivable resources, hence, the factors under consideration are just both resources and minimal current impact. In the second system (Grid or Onshore Connected system), the focus includes maximizing resources (depth), minimizing distance to the nearest coast, and minimizing the impacts of ocean current.

a. Economic Interest Zone1 with resources

For isolated system, the bathymetry was first filtered to remove any associated land dataset. We incorporated the current data into our model. We generated a suitability map. We delineated the three best suitability indices into the resource map.

b. Economic Interest Zone2 with resources

For the onshore-connected system, we first filtered the land bathymetry out. The second part is divided into two: we only considered the resource (~depth) and the closest distance from the shore for the first one, then generate the suitability map and delineate the best three suitability indices in our resource map. This is to give an understanding of the effect of switching criteria or the influence of a certain criterion. The second case includes all the three criteria (depth, distance, and ocean current). We generated our suitability model and map, and finally delineate the three best suitability indices in our resource map. Another critical factor we considered is a maximum distance of 20 km for this system for achieving a realistic output.

4. Results

4.1. Energy Situation in Cabo Verde

This sub-Section highlights the need for engaging in energy storage research by analyzing the energy situation in Cabo Verde, the resource strength and intermittency of the available renewables, the portion of fossil fuel and renewables in the total energy mix, the high and fluctuating electricity price, and some renewables option with their huge potential.

4.1.1. Thermal Plants, Electricity price and Renewable Energy Penetration in Cabo Verde

The three major consumed energy sources in Cabo Verde are wind energy, fossil fuels, and solar energy (Figures 26, 27, and 28; Appendix 6). There is at least an installed thermal plant on each island as shown in Figure 26. In 2015, the islands with the minimum number of thermal plants are Maio, Sal, São Nicolau, and Brava, having one thermal plant each. Santo Antão, Fogo, and the island of São Vicente have two thermal plants each. The most populous island has the largest number of thermal power plants of five (Figure 26). In 2018, a large fraction (ninety percent) of the locally consumed energy in Cabo Verde comes from fossil fuels (Appendix 6).

Similar to the number of thermal plants, the share of fossil fuels also varies for each island. Boa Vista is the only island that consumed less than fifty percent electricity from fossil fuel in 2012. The island of Sal generated electricity of close to fifty-five percent from fossil fuel, while Santo Antão, Santiago, and São Vicente consumed more than seventy percent of electricity from this same source in 2015. São Nicolau, Brava, Fogo, and Maio run completely on fossil fuels for electricity generation.

Renewable energy sources represent approximately twenty, eighteen, and seventeen percent of the consumed energy in Cabo Verde in 2018, 2019, and 2020 respectively shared between wind and solar energy, with solar taking approximately two, three, and three percent of this share within those respective periods (Appendix 6; Table 2). A significant rise in the consumption of renewables was witnessed between the period of 2011 and 2012, a trend that extended till 2014 though at a reduced rate of increase. After the first and second peaks

achieved in 2014 and 2018, the electricity consumption from renewables always undergoes a decline phase, with a minimum in 2017 (Figure 28).

The trend in the consumption of renewables for electricity generation is clearly illustrated in the pattern of wind usage for electricity generation in Cabo Verde. Between the periods of 2010 to 2019, both wind and total renewable show similar trends of increase and decrease although the manner of increase witnessed in the total renewable between 2017 and 2018 is far beyond that of wind consumption. Five out of the nine inhabited islands have electricity power plants running on wind energy in 2015 (Figure 26). They are Santo Antão, São Vicente, Boa Vista, Sal, and Santiago. Only Sal and Santiago generate electricity from solar power for that year indicating that these two islands have the most diverse energy mix of any islands in Cabo Verde.

The comparison of the price of electricity in Cabo Verde with other countries clearly expresses the impact of heavy reliance on fossil fuels on price fluctuation (Figure 27). Except for Angola, Zimbabwe, China, and Japan, all other countries experienced a price change within an interval of just three months. The price change corresponds to an increase in electricity prices for all the countries. Ireland, New Zealand, and Cabo Verde are some of the countries that experienced a very high change in price between these three months period which can be strongly linked to higher fuel prices as a result of fuel supply constraints or disruptions or an increase in price on the world market. Out of these three countries, Cabo Verde and New Zealand witnessed the highest change having undergone a price change of 0.05 and 0.06 United States dollars per kilowatt-hour of electricity respectively (Figure 27).

In June and September 2020, Cabo Verde ranked fourth out of the 19 countries whose prices of electricity were studied (Figure 27). Germany, Bermuda, and Denmark are the three countries whose citizens pay a higher fee than Cabo Verdeans to purchase electricity. The price of electricity in Cabo Verde is far higher than in some of the advanced countries including the USA, Japan, and Italy. A more detailed illustration would highlight that Cabo Verdeans pay more than twice the price paid by a USA citizen for this period over the same or similar commodity. Regionally, the price of electricity is higher than in other studied countries in West Africa and Africa. Approximately, it doubles that of Sierra Leone and Mauritius while it is in a five-fold multiple for countries like Nigeria and Ghana, as depicted in Figure 27.

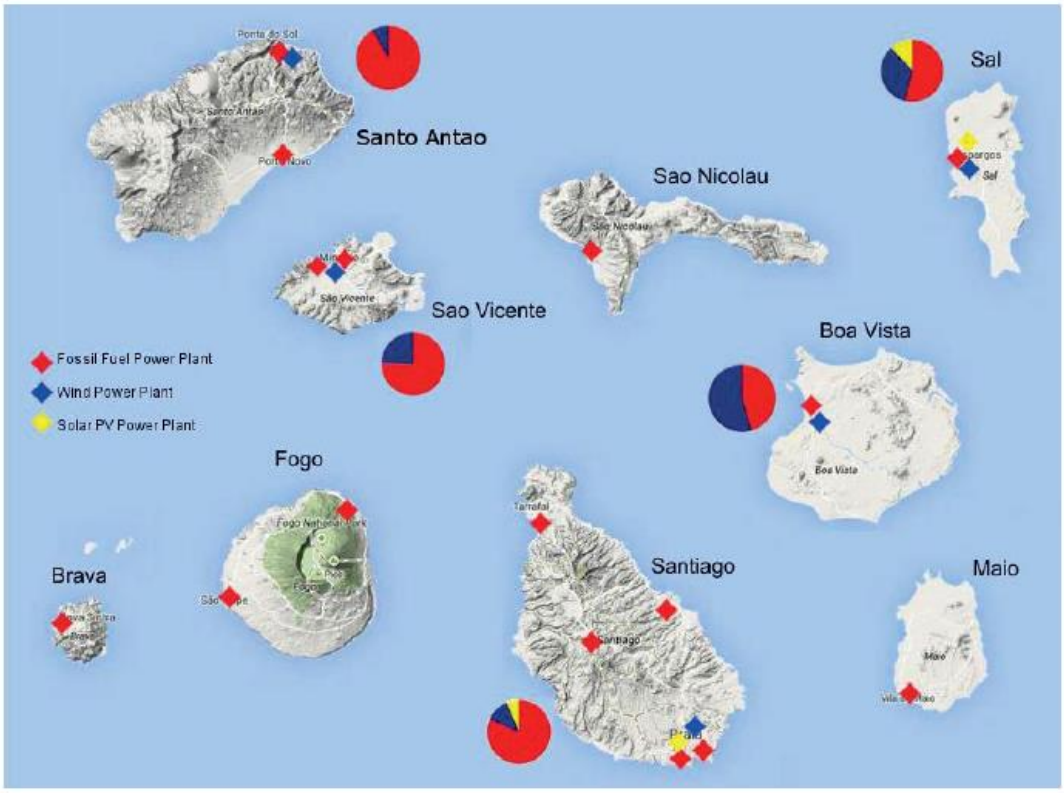

Figure 26. Cabo Verde Islands, and the locations of electricity generation and shares of capacity among selected Islands in 2012 (UNIDO; ECREE, 2010) and (Electra, 2013) Note: Not drawn to scale

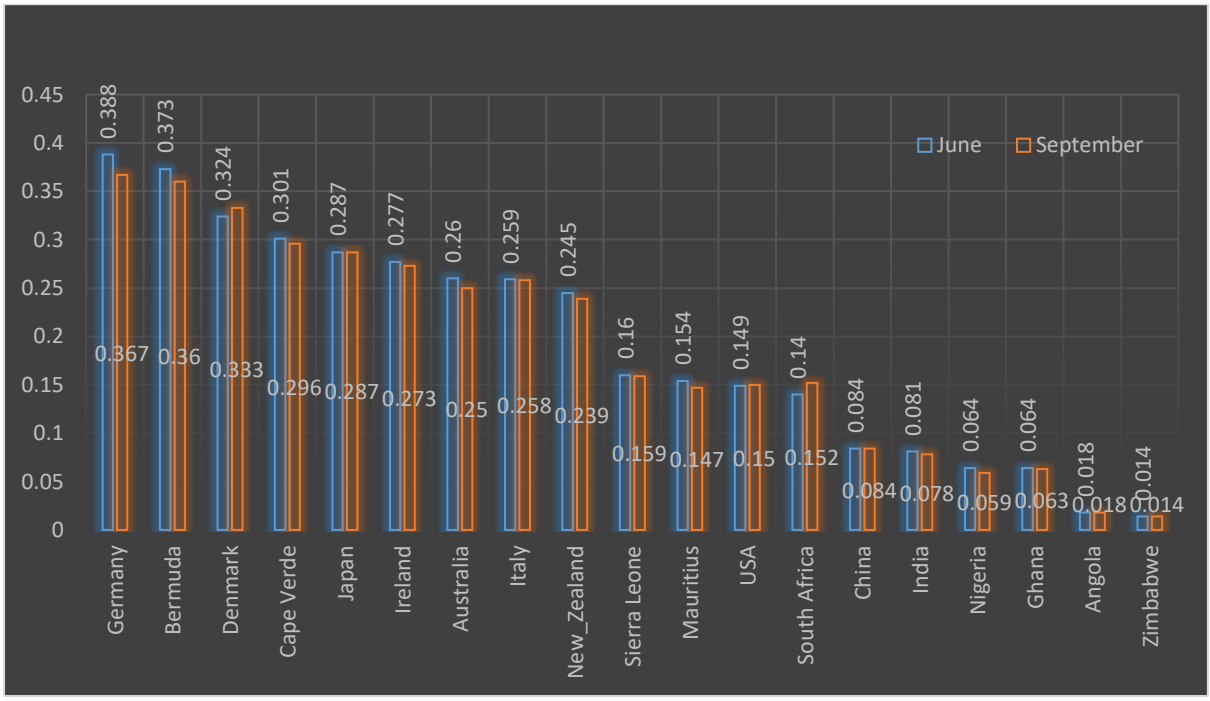

Figure 27. Comparison of Electricity Prices (KWH/$) in June and September -2020 Data: Energypedia.com

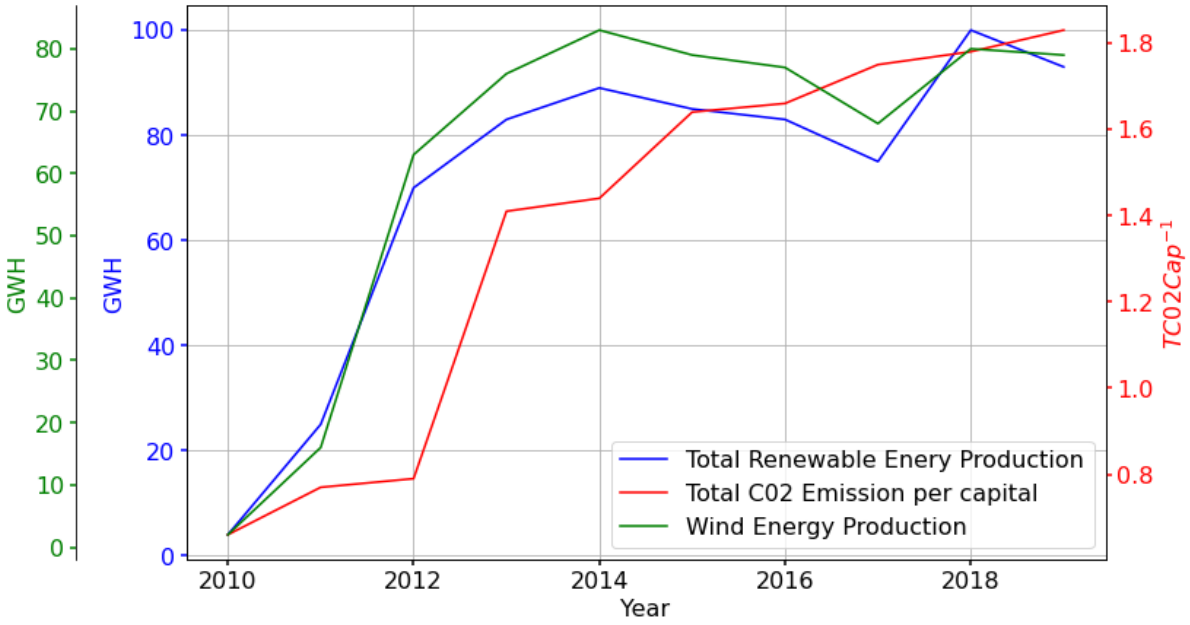

Figure 28. Wind, Total Renewable and CO2 Emission in Cabo Verde. Data: Edgar (2020); Cabeolica (2021)

4.1.2. Harnessed Wind Resources, Cost and Resource Curtailment

The installed wind capacity in the archipelago has been almost constant since 2012. To date, wind plants are installed on only five of the islands of the archipelago: Santiago, São Vicente, Boa Vista, Santo Antão, and Sal as shown in Table 2 and Appendix 6. Note, Table 2 considers data from Cabeolica which focuses on four of the islands while Appendix 6 focuses on the Total Renewable on all the islands. Thus, all the four most populous islands constituting more than eighty percent of the total population have installed wind on them (Appendix 1). However, this does not ignore the fact that the renewable penetration on those islands is also a bit low (Table1, Appendix 6).

The ratio of the consumed to the generated wind energy (Consumed/Generated in Table 2) for wind is generally low. This indicates that the total amount of energy that the wind power plants are supposed to produce from the available wind resources is low, thus generating less than its actual potential, a term that is usually referred to as **energy curtailment.** This reduction in potentially generated wind energy is generally high in Cabo Verde and varies from thirty-four percent in 2012 to twenty-two percent in 2019 as can be deduced from Produced/Available

in Table 2[9]. Although, the result shows an improvement in curtailment over the years. Yet, it has been fluctuating by year and the maximum over the years was recorded in 2019 with a seventy-eight percent (Generated/Available), thus twenty-two percent curtailment[9]. Among islands, Santiago has the highest percentage of produced to available while the lowest is experienced on Sal Island. A great improvement of 24% occurred within the period of study in Sal which improved the overall annual penetration rate in the country. The improvement on other islands is approximately 9.6.

Similar to the resource, the sum of money paid for wind purchase changes per year but the minimum has been 8.5 million Euros while the maximum is ~11 million Euros. Judging from this cost, ~2.9 million euros worth of wind energy was wasted as a result of energy curtailment in 2012, and ~4 million euros was lost in 2016. However, although other factors including wind speed, grid efficiency, and cost of management could also play some roles. The amount of produced energy from wind also grows within the span of 2012 to 2019 by 7.9 % approximately. The year with the highest production is 2018 with a significant value of 85.154 GWh.

The estimated rate of penetration – ERP (ratio of the amount of electricity consumed from wind to the total electricity consumed in the country) has been unstable since 2012. The maximum penetration rate occurred in 2014 (24%) while the minimum occurred in 2019 (15%) indicating a decline of approximately 38% over these two periods. However, the penetration rate has never been above the third quarter of the total percentage. Another thing worth mentioning is that the maximum penetration rate does not occur in the year with the maximum production. Among islands, the estimated rate of wind penetration varies from low in Santiago to high in Boa Vista according to the statistic from Table 2. Among islands, the estimated rate of wind penetration is always lowest on Santiago island and highest on Sal and recently with Bao Vista although everything keeps changing per year.

[9] Curtailment = 100 – (Generated/Available) in Table 1

Table 2. *Wind Energy consumption in Cabo Verde (Source: Cabeolica 2012-2020).*

Indicator/Year	**2012**	**2013**	**2014**	**2015**	**2016**	**2017**	**2018**	**2019**	**2020**
Average wind speed	8.3	8.6	9.1	9	9.1	8.9	9.4	9	8.5
Installed capacity (MW)	25.5	25.5	25.5	25.5	25.5	25.5	25.5	25.5	25.5
Average (Produced/Available) %	66	74	74	73	72	75	76	78	68
Production (GWh)	61 643	75 197	80 878	77 153	75 426	75 352	85 154	78 575	64 926
Estimated Penetration rate (ERP) (%)	18	23	24	21	20	17	18	15	14
Average/ERP - Santiago (%)	NA	NA	NA/16	NA/16	95/15	98/13	99/16	99/12	97/13
Average/ERP - São Vicente (%)	NA	NA	NA/33	NA/28	63/25	70/25	69/27	66/24	61/21
Average/ERP - Boa Vista (%)	NA	NA	NA/27	NA/27	77/31	79/21	78/23	81/18	56/23
Average/ERP - Sal (%)	NA/23	NA/31	NA/32	NA/32	53/27	54/27	59/29	69/22	47/23
Cost (Euros)	8,454,641	9,983,055	10,474,073	10,516,731	10,485,074	10,500,497	11,000,084	10,100,000	10,629,561
Equivalent CO2 avoided (tons)	42,439	51,633	55,381	52,688	51,429	51,514	58,168	53,692	44,440

4.1.3. Renewable Energy Resource Potential and their Intermittency

i. Wind and Solar Power

Wind is a dynamic variable that varies according to the time of the day, year, and season (Table1, Figure 22a, 22b, and 22c). The wind speed with the maximum yearly average was recorded in 2018 as revealed in Table 1. The yearly average wind speed varies from a minimum of ~8.3 ms^{-1} in 2012 to a maximum of ~9.4 ms^{-1} in 2018, and the annual average is closer to 9 ms^{-1} or beyond as also depicted in Table 1.

The hourly wind-speed data for the whole of Cabo Verde shows that the wind velocity can be as high as 14 ms^{-1} in some hours of the day and as low as about 1.5 ms^{-1} in another (Figure 29a). Some other trends can also be deduced from the wind plot to illustrate the dynamic nature of wind over time. For instance, the highest values over a certain time period generally reduce between 2009 to 2021, illustrating a reduction in the maximum extractable wind resources over this period (from around 14 ms^{-1} in 2000 to 11 ms^{-1} in 2020). However, the lowest value remains almost the same over this period. Also, most of the data fall within the range of 5 ms^{-1} to 9 ms^{-1}. Intuitively, this result supports the previous one highlighted in the last paragraph from a different data source (Cabeolica in Table 1) by just averaging over the years.

The result of the monthly wind velocity averaged over the period of 2009 to 2020 (Figure 29b) illustrates the peak months to be occurring from December to around May. A minimum of ~7.5 ms^{-1} throughout this period is achievable. Despite this, the monthly average is never below 5 ms^{-1} even for the months with the lowest values, July and August. Generally, the period of June to October has the lowest wind speed below an approximate value of 6.5 ms^{-1}. One thing that can also be noted, the stochastic level of the wind resource is clearly revealed across the months, although that will be discussed in the later section. Figure 29c gives the result of wind velocity averaged over the hours of the day for the study period. This figure reveals that, unlike the monthly average, the hourly average has a small range. The maximum speed range occurs between the hours of 9 to 12. Almost 18 out of the 24 hours of the day has a velocity above 6.8 ms^{-1}.

Solar energy has a more regular pattern than wind (Figure 30a, 30b, and 30c). The hourly amount of solar insolation falling on a surface averaged for the entire Cabo Verde range from 0 to 3.5 kWm^{-2} during a typical day[10] (Figure 30a). The major sets of highs occur at ~2.8 and ~3.3 kWm^{-2}. Figure 23b reveals the monthly average of the solar insolation. It indicates that the months of April through August have the highest amount of solar insolation. These values are quite low in comparison to the hourly average (Figure 30c) and hourly dataset (Figure 30a) which is majorly due to computing average over a complete cycle of when solar energy is available such as daytime to few hours beyond mid-day, and when it is not available, such as during the night-time. Conversely, the hourly average only averages for a specific hour of the day as illustrated in Figure 23c. Thus, the minimum values for the monthly average are always above the hourly and hourly average, a value above 0.8 kWm^{-2}.

The hourly average of solar radiation (Figure 30c) illustrated that the amount of energy received in the first 8 hours, and the last 4 hours of the day is zero. This coincides with the early morning when the sun is yet to be out or when it starts to rise, and the latter part of the day when the sun is setting. The amount that is greater than 1 kWm^{-2} occurs within 10 to 18 hours, while above 3 kWm^{-2} from 12 to 17 hours which is the time the sun is reaching its peak. The window continues to shrink as the values get higher.

[10] Figure 30a is a 12 year period hourly data and the data is stacked up that the figure does not depict the plots as it reduces to zero.

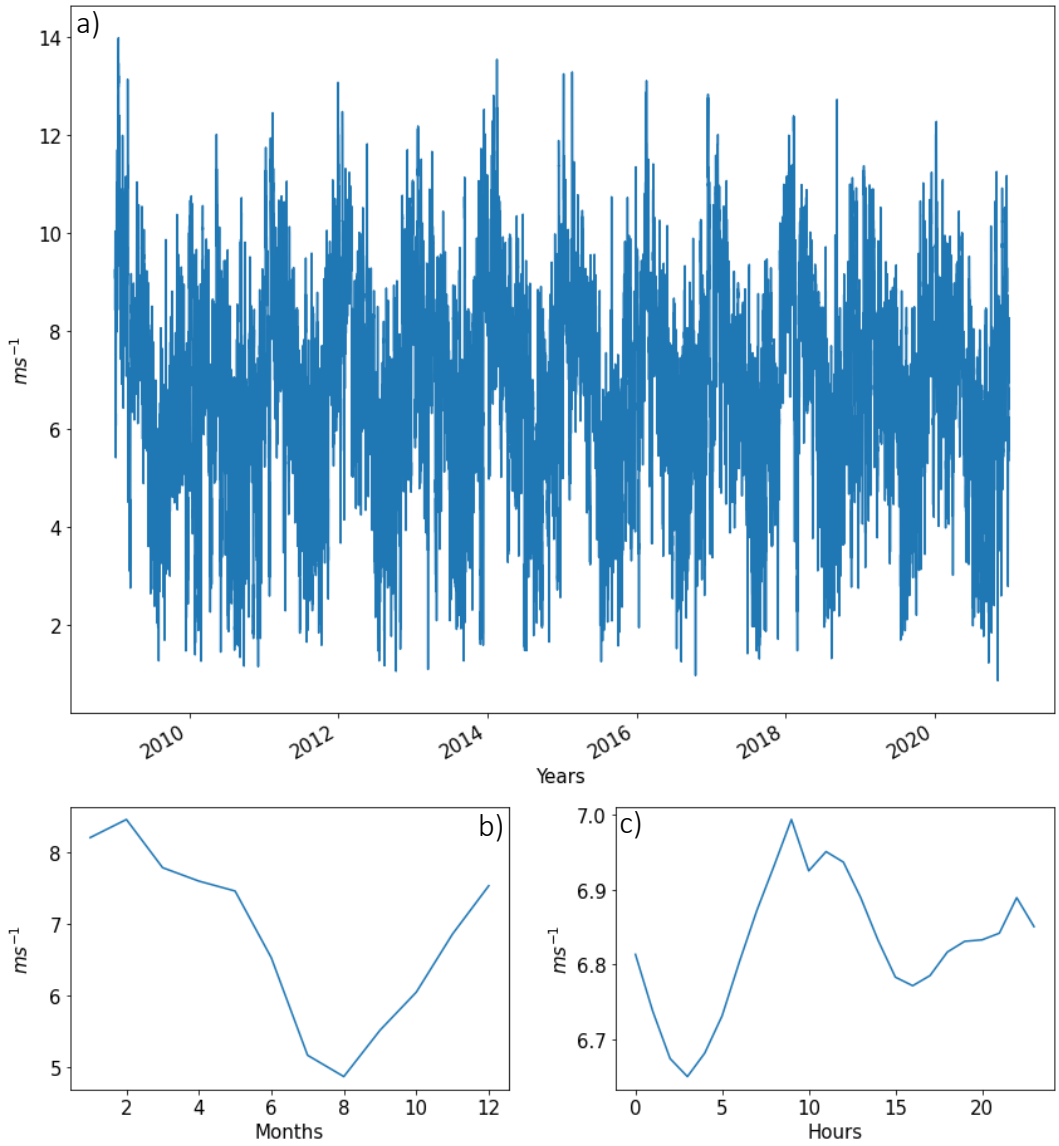

Figure 28. Wind speed output: (a) 2009-2021 Hourly, (b) 2009-2021 monthly average and (c) 2009-2021 hourly average. Data: Era5.

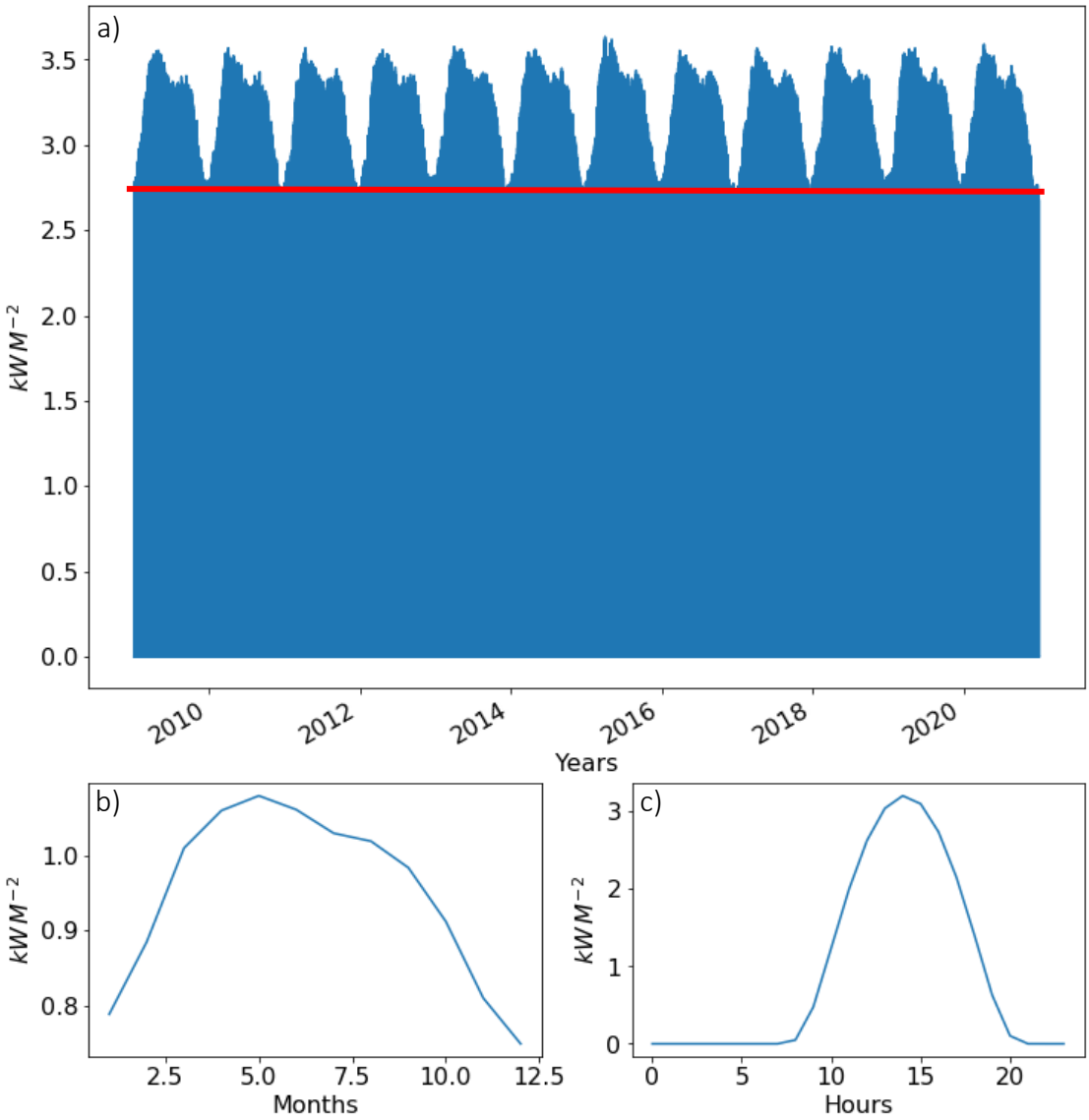

Figure 29. Solar power output: (a) 2009-2021 Hourly, (b) 2009-2021 monthly average, and (c) 2009-2021 hourly average. Data: Era5.

ii. Wave, and OTEC Power

The mean wave power in Cabo Verde ranges between 8 kwm^{-1} to above 18 kwm^{-1} (Figure 31). Places within the islands generally have low potential especially the southern part of São Vicente, and Santiago, and the south-western Boa Vista. There is a massive potential in the northern part of Santo Antão, Sal and the northern Cabo verde as a whole. A potential of 14.4 kwm^{-1} is derivable in these zones which is extendable to about 18 kwm^{-1}. The southern islands have less potential, and the target area would be few kilometers outside of the island in the western and eastern direction. About 16 kwm^{-1} is also derivable in these regions (Figure 31).

OTEC runs on temperature difference between the warm surface and deeper part of the ocean. At such, the southern islands generally have higher potential for OTEC power than other parts of Cabo Verde (Appendix 10). The average annual net power, Pnet and Pgross from OTEC (Table 3) extracted for some seemingly promising locations and averaged for the whole of Cabo Verde depicts some places with very great potential. A net power of 9 MW is generally available while 10 MW can be found at some locations. The average for the whole Cabo Verde is also around 9 MW. From the seasonal statistic (Figure 32), 13 MW and above are derivable in the summer months while this value can become 6 to 8 MW in the winter months. Similar to solar and wind, Wave power and OTEC potential also have an imbedded intermittency according to season (Figure 32, Appendix 9). While OTEC has a high potential in the summer months, wave power has a higher potential in the winter months as it is primarily driven by winds which are stronger in the winter periods, and OTEC is driven by temperature which is higher in summer months. Specifically, the amount of energy is high starting from July to November and very low from February to April (Figure 32). While wave power is high from December to March, and low from June to September (Appendix 9).

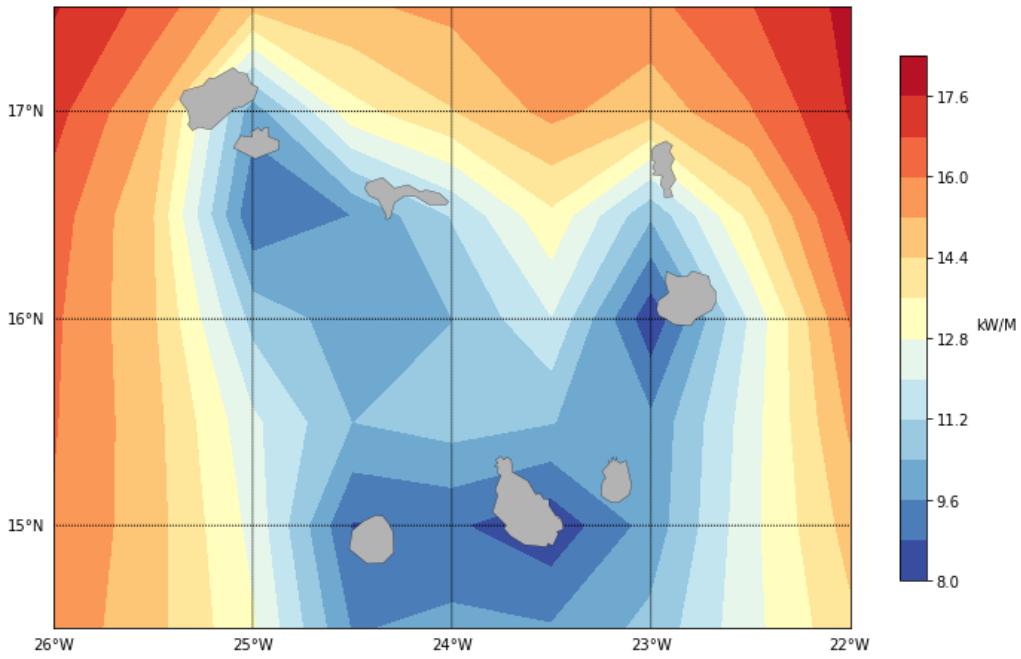

Figure 30. 1996-2021 average mean wave power. Data: Era5.

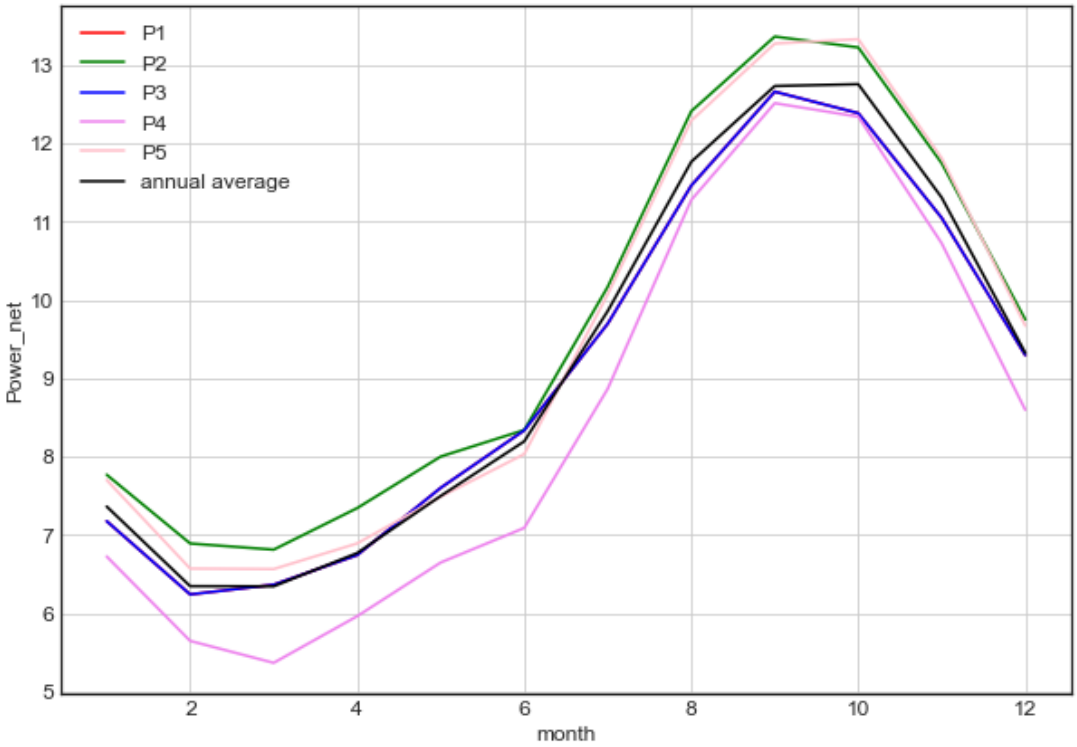

Figure 31. 1996-2021 Average OTEC Net power Analysis. Data: GlorysV1 from CMEMS.

Table 3. OTEC power Analysis

Positions	Latitude	Latitude	Longitude	ΔT(C)	Pnet	Pgross
P1	16.42	16.42	-25.17	19.022612	12.711532	9.083171
P2	14.83	14.83	-24	19.45475	13.274162	9.650813
P3	16.42	16.42	-25.17	19.022612	12.711532`	9.083171
P4	16.42	16.42	-22.58	18.529104	12.11218	8.478738
P5	15	15	-23	19.309198	13.099067	9.474057
Whole CV				19.077564	12.815277	9.187364

4.1.4. C02 Emission, C02 avoided with Wind usage in Cabo Verde

The total amount of CO_2 released in Cabo Verde has been on the rise since 2003 (Figure 28 and 33, Appendix 7). There were many steep and falls witnessed before this period particularly the decline between 1980 and 1982 as shown in Figure 33 and Appendix 7. Buildings and other industrial combustion activities took the largest proportion in the past (Appendix 7). Currently, both the transport and power industry release the largest quantity of CO2 into the atmosphere in Cabo Verde (Appendix 7).

The amount of C02 released per capital (total emission of a country divides by its population in tons per capital), and the total amount of released CO2 (in million tons) increases annually with a strong steep witnessed between 2012 and 2013, at ~43% increase (Figure 28, Figure 33, Appendix 7). A 12.5% increase was also witnessed between 2014 and 2015 although far lower than the previous one. Within the periods 2010 to 2019 and 2010 to 2017, there has been an approximate 1.8-, and 3.9-fold multiple in the quantity of released C02 per capital, and total released CO2 per year as presented in Figure 28 and Figure 33 respectively [11]. Several million tons of CO2 have been released over the past few years (Figure 33). Precisely, 4.64 million tons were released between 2010 and 2017 alone (Figure 33). At the same time, the

[11] The calculations involving Figure 28 and Figure 33 were done by summing the values in both over any stated time period and computing proportion of increase.

installed wind has avoided the release of ~0.8 million tons into the atmosphere (Table 1). This corresponds to ~17% of the total C02 that would have been burnt during this period[12].

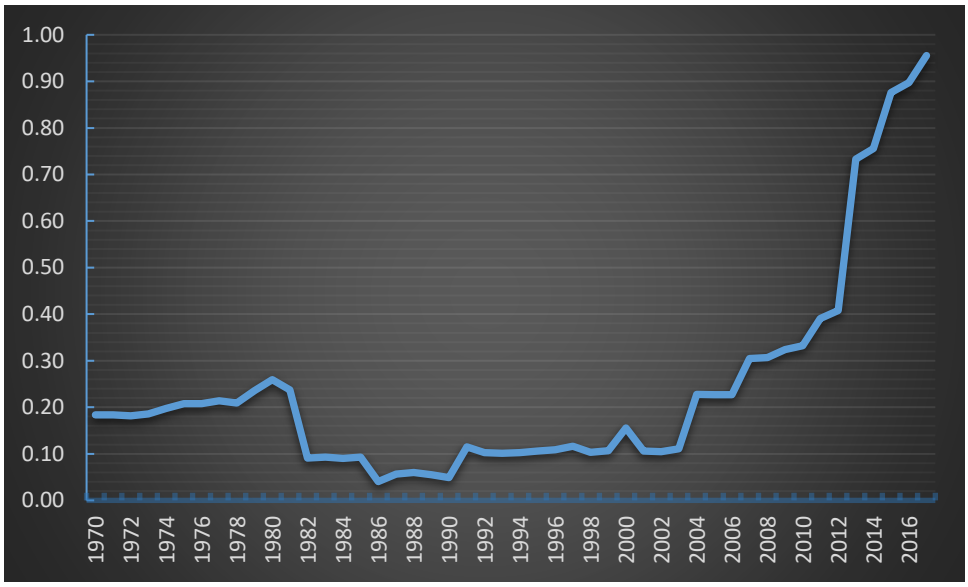

Figure 32. Yearly total CO_2 emission in Cabo Verde (Million-tons-co_2yr^{-1}). Source: EDGAR 2020.

4.2. Marine Gravitational Energy Storage Analysis

The focus of this research is not only to quantify the amount of energy that is storable by implementing this storage technology but also investigate the best locations to site this storage system considering factors such as cost, and the potential impacts of subsurface currents. We have analyzed and selected the best bathymetry data, computed the distance to the coast (Figure 23, Appendix 8), and determined the sizing and efficiency of the storage system for resource potential computation. The next step before developing the suitability model is to choose the ocean current variable to include in the model.

[12] This continues the previous calculation by dividing by the amount of co2 avoided and calculating the percentage.

4.2.1. Ocean Current Analysis

Ocean current is another important physical parameter that has the potential of impacting underwater structures such as the storage system we are proposing. Before developing a suitability model and incorporating ocean current data as one of its criteria, we are starting by investigating some ocean current variables to determine the one that can give a good representation of the places we are trying to avoid (those impacted by strong currents). This analysis is also important because the proposed storage system will be oscillating vertically in the water column and can sometimes either stay closer to the surface or the bottom, thus liable to be subjected to the effects of currents at any time. The variables under consideration include:

a. The monthly and vertical mean of the daily standard deviation of the current amplitude (Uv_mstd)

Uv_mstd produces a similar pattern from January to December. The Uv_std is stronger in between the islands which is pronounced between the islands of Santo Antão, São Vicente, and São Nicolau, and also, between Boa Vista and Maio extending to Santiago as the months progresses (Figure 34). The computation of the average is done as the name implies from the daily standard deviation over the whole water column for the whole month. In respect to this, it gives a representation of the effects of tidal currents as the major oceanic process changing on a daily basis.

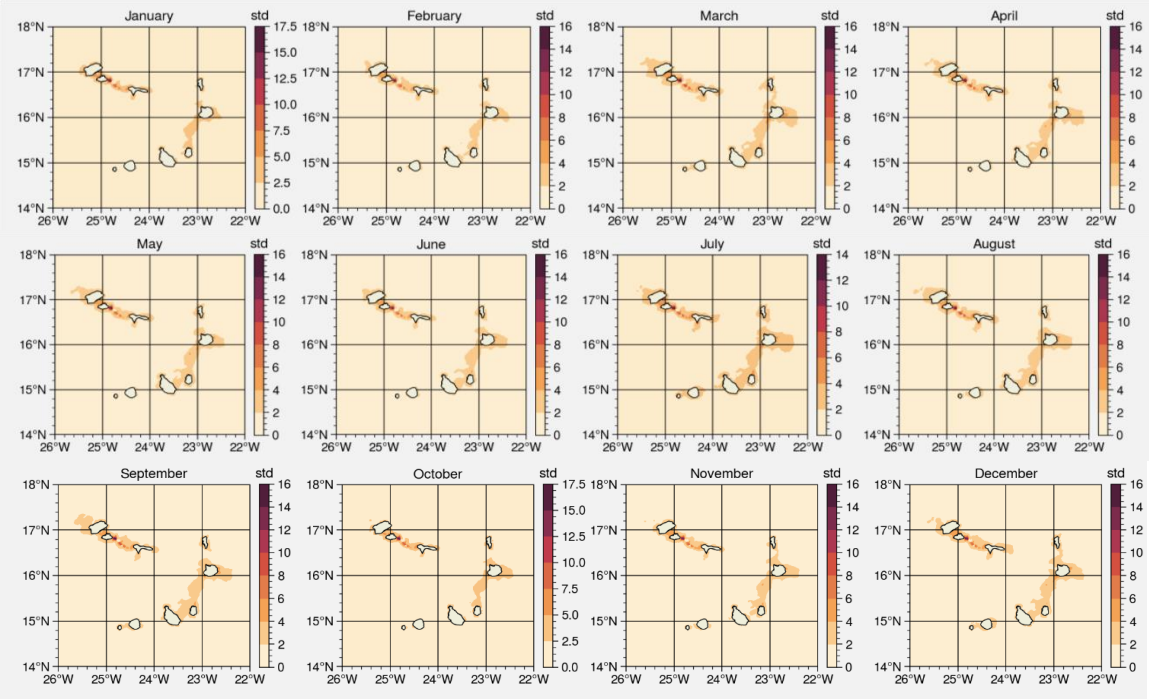

Figure 33. One year monthly and vertical mean of the daily standard deviation of the current amplitude. Data: GIGATL1.

b. The monthly and vertical maximum of the current amplitude (Uv_max)

Similar to Uv_mstd, Uv_max also gives a general monthly pattern especially in between the north-western island group from Santo Antão to Sao Nicolau although not as pronounced as Uv_mstd. Also, the currents are stronger between the islands. Months with the highest magnitude where the impacts of the currents are felt at several locations include July, August, and September. Unlike Uv_mstd that captures daily mostly daily variability, Uv-max accounts for the strongest current throughout the whole water column in that month. One major discernable feature throughout the months is the amplitude greater in the northern part with a signature of eddies showing as high values along the perimeter of moving circles (e.g. around 18°N, 24°W in April on Figure 35).

c. The monthly maximum of the current amplitude at the bottom and surface Uv_max_bot, and Uv_max_0

These two variables are representing th ocean current with the highest magnitude at the bottom (Uv_max_bot) and the surface (Uv_max_0) for each of the months. Uv_max_bot has

a similar amplitude, signature and pattern as Uv_max (Figure 35 and 36) except that the signature of eddies have disappeared, indicating that they are not found near the bottom. The patterns are distinct especially in the months of April, July, and September. Uv_max_0 has similar monthly pattern from January to December (Appendix 11). The current amplitude is half of the bottom (Uv_max_0) and vertical maximum (Uv_max).

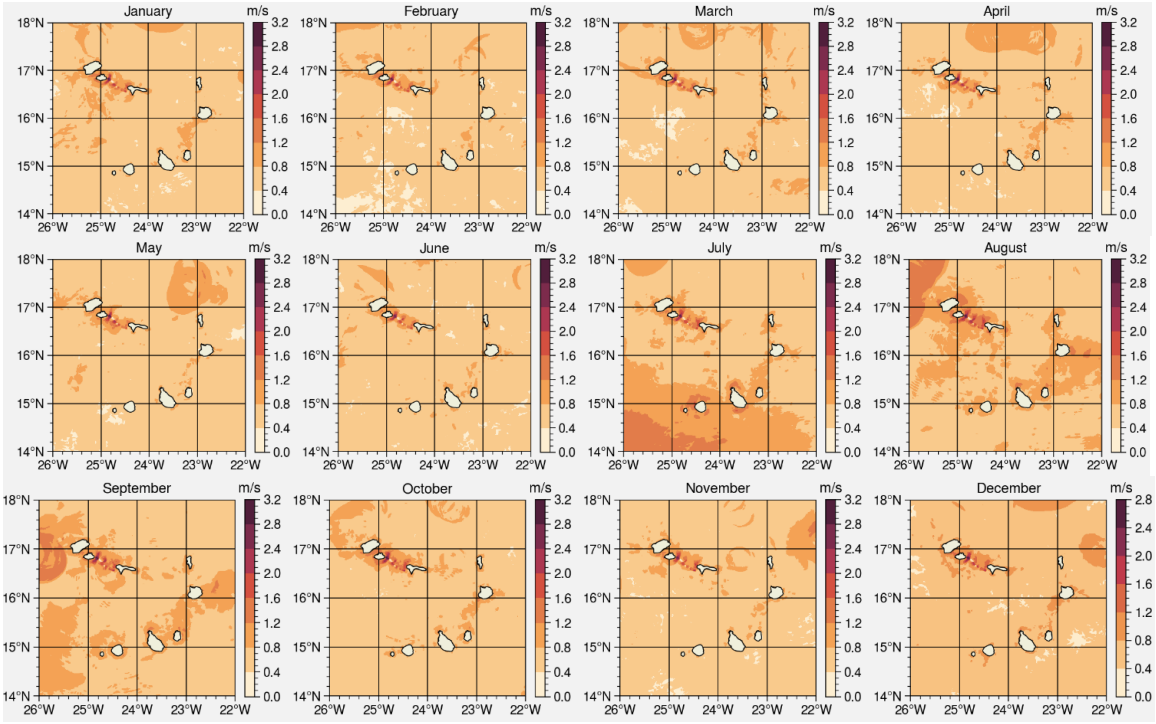

Figure 34. One year monthly and vertical maximum of the current amplitude. Data: GIGATL.

4.2.2. Conclusion on the current variable to use

The goal is to determine the ocean current where the ocean currents would have the least overall impacts on the energy storage system. Among variables associated with the maximum ocean current namely Uv_max, Uv_max_0, and Uv_max_bot, Uv_max_0 has the smallest maximum amplitude and thus it is unsuitable for this work. Uv_max bottom and Uv_max both give a qualitative representation of the current with reasonable amplitude while Uv_mstd obviously overestimates the amplitude of the current. Additionally, Uv_max_bot and Uv_max both have a larger monthly variability than Uv_mstd does. Although, Uv_mstd captures the daily variations of the current associated with tides.

In summary, it is quite difficult to choose the most suitable variable especially for a structure that oscillates vertically. However, Uv_max probably best capture the overall impacts of current, either at the surface, or bottom, or in-between, and also includes both impact of tides, eddies, and other currents as shown in figure 37.

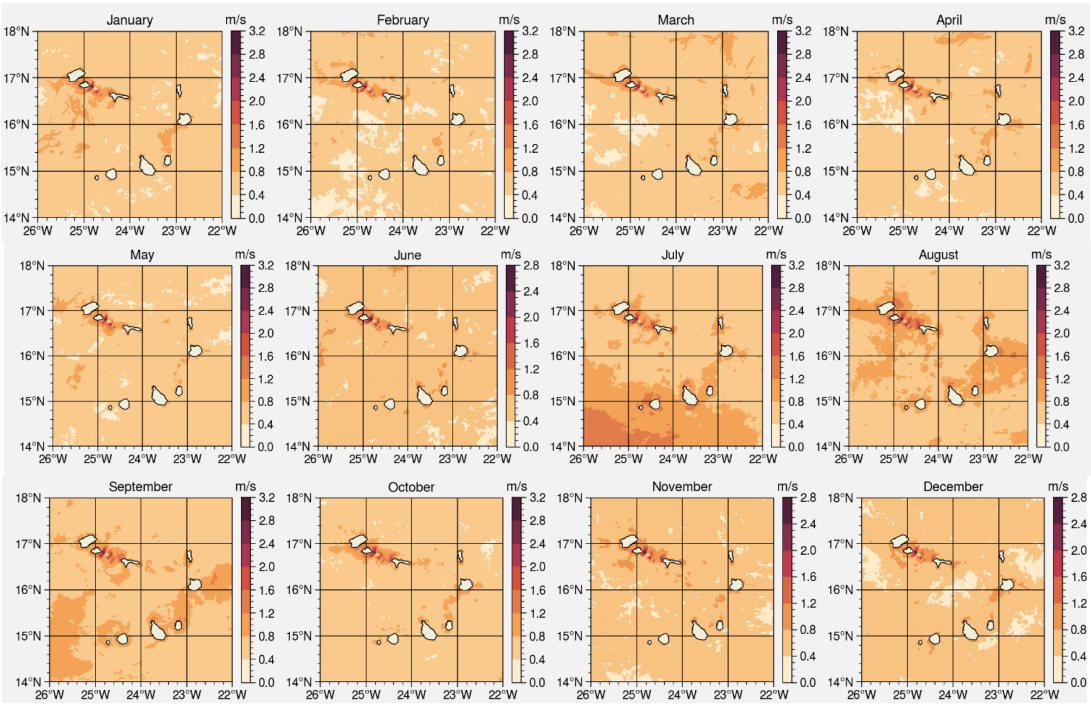

Figure 35. One year monthly maximum of the current amplitude at the bottom. Data: GIGATL1.

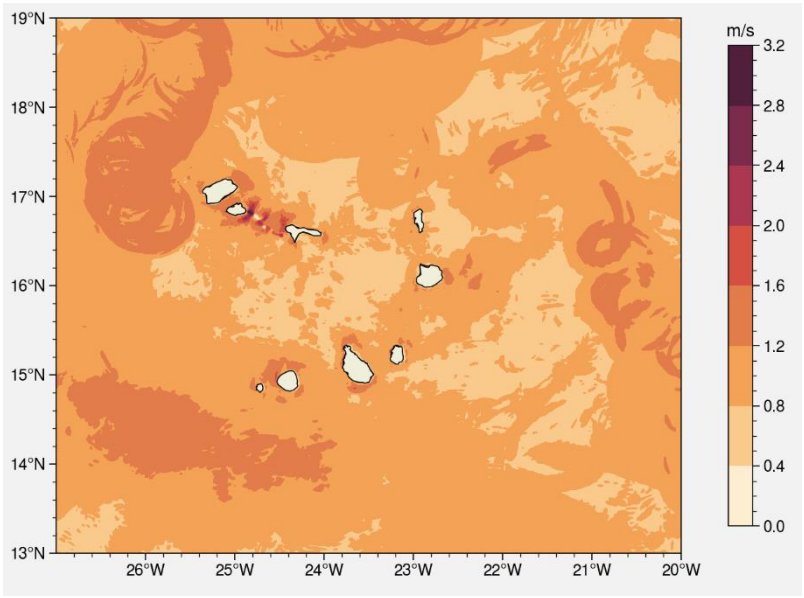

Figure 36. One year average of the vertical maximum of the current amplitude. Data: GIGATL1. The impact of eddies are pronounced in the north-west Cabo Verde and far east. Also, high current are situated in the south west.

4.3. Marine Gravitational Energy Storage Resource Potential

We considered a mass of 1 ton having a cylindrical shape. The resource potential as depicted in Figure 38 is clearly a function of depth thus increasing and decreasing with depth. Generally, locations with smaller depths such as places closer to the coast have low storage potential while places farther from the coast have high storage potential. The northern and eastern parts of Cabo Verde have low capacity in comparison to the western and southern part of Cabo Verde (Figure 38). While 8kWh is derivable in the northern part of Cabo Verde waters which can reach 9 kWh, 9 to 10 kWh is achievable in the western region and can go up to 12 kWh (Figure 38). However, 10 kWh is generally available in the southern Cabo Verde waters that can also increase to 12 in the south west, yet the trend in the eastern side typically follows the northern portion. The waters situated in the central Cabo Verde also follows the same trend as the northern and eastern with a potential of about 8 to 9 kWh per ton of mass (Figure 38).

The resource potential also varies across the islands (Figure 38). The south western side of Santo Antão, São Vicente and São Nicolau are some distinct areas with good potential close to the shore with an approximate storage capacity of 5 to 7 kWh. The immediate waters close to Sal, Maio, and Boa Vista has low potential for the development of this technology ~2-5 kWh. However, north of Sal is also a promising location as it is closer the northern offshore waters with a potential that can reach 7 to 8 kWh. But, considering a 20 km distance from the shore, the value can reduce to 5-7 kWh (Appendix 12). The southern part of Santiago, Fogo, and Brava has an energy storage value of ~9 kWh at a reasonable distance from the coast.

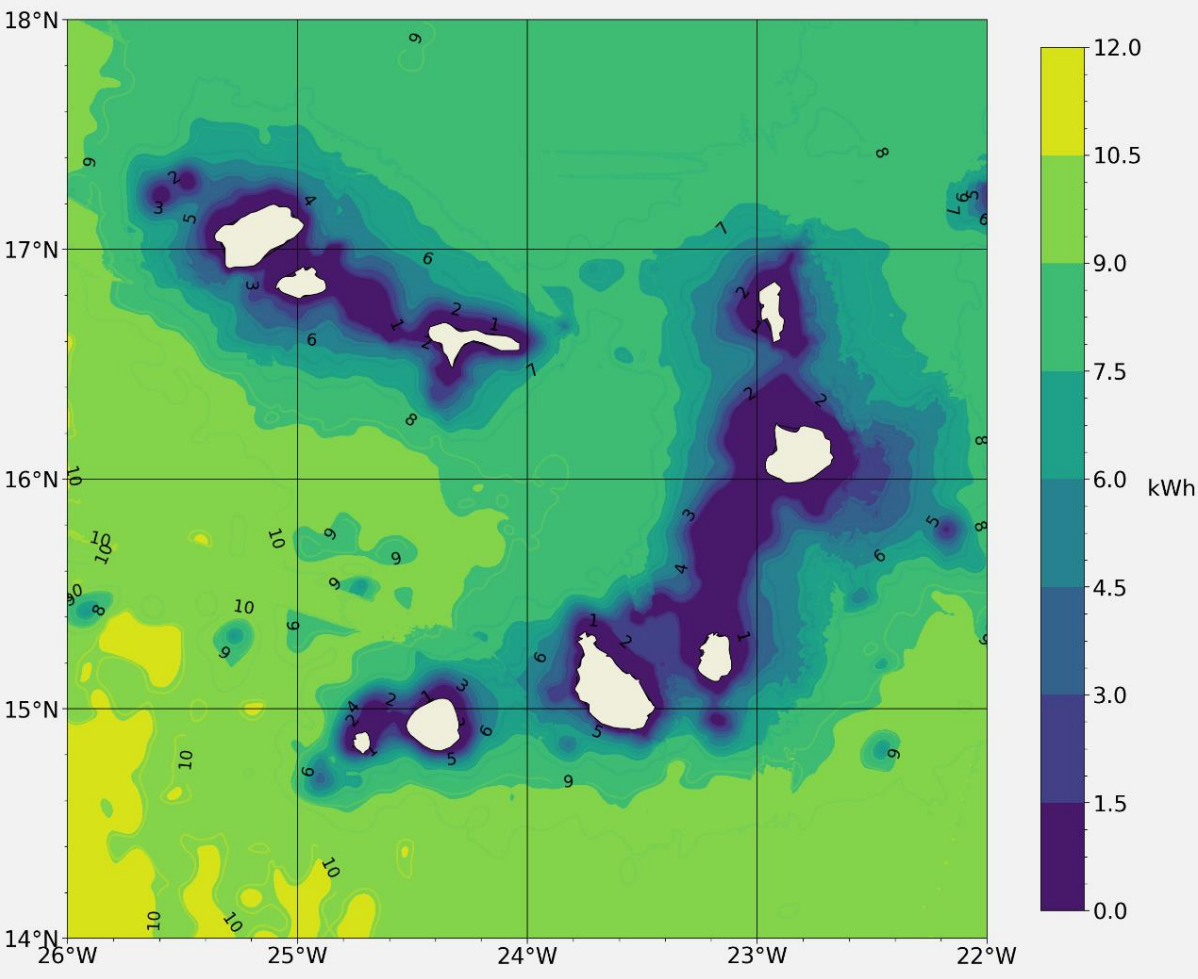

Figure 37. Marine gravitational energy storage resource potential per ton of mass for Cabo Verde. The version showing isolines (1000m, and 10, 15, and 20km distance from coast) can be found in Appendix 12.

4.4. Economic Interest (Suitable Energy) Zone 1 - Isolated System

The first thing worth noting is that we employed five indices of suitability in mapping the waters of Cabo Verde for both Isolated and Onshore connected systems as explained in the methodology section. This classifies the waters in a hierarchical manner to depict the best site(s) to install any of the two systems under consideration. We have already revealed the storage resource potential using Figure 38. The motivation for generating suitability models is to find a trade-off between the energy storage resource potential and other factors that have to be considered before such a technology can be brought to life including cost, and the dynamics of the marine environment. In this regard, the best class termed optimally suitable zone does not imply zones with the maximum resource potential, but the best zones to install the storage system after identifying and analyzing all the relevant factors associated with that system.

As pre-defined, the proposed isolated system consumes the stored energy offshore without transferring the energy onshore. Hence, the focus is on maximizing resources and minimizing oceanic processes such as strong currents that can threaten and negatively impact underwater structures. The result of classifying the Cabo Verde's waters based on suitability is presented first before incorporating it into the resource map.

4.4.1. Suitable Energy Storage Zones for Isolated System

The zones with the optimal suitability for the Isolated system (deep red: index>5.5) majorly lie in west-central Cabo Verde, east southern, and some locations in the northern, and central Cabo Verde as shown in Figure 39. The second index of suitability (most suitable: 4.5<index<5.5) has a similar pattern with an extended range as it falls mostly in a wider area immediately beyond the first class. The other classes are not our major focus for this system under study but they are also worth mentioning. The third index of suitability (moderately suitable: 3.0<index<4.5) covers a large part of the northern and southern waters away from the islands while the fourth classification (least suitable: 1.5<index<3.0) is just a little extension of the fifth class. The waters of Cabo Verde lying next to the coast are the spots not suitable (fifth class: 0<index<1.5) under this criteria, and as shown in Figure 39, most of this area falls within the 20 km maximum distance from the coast.

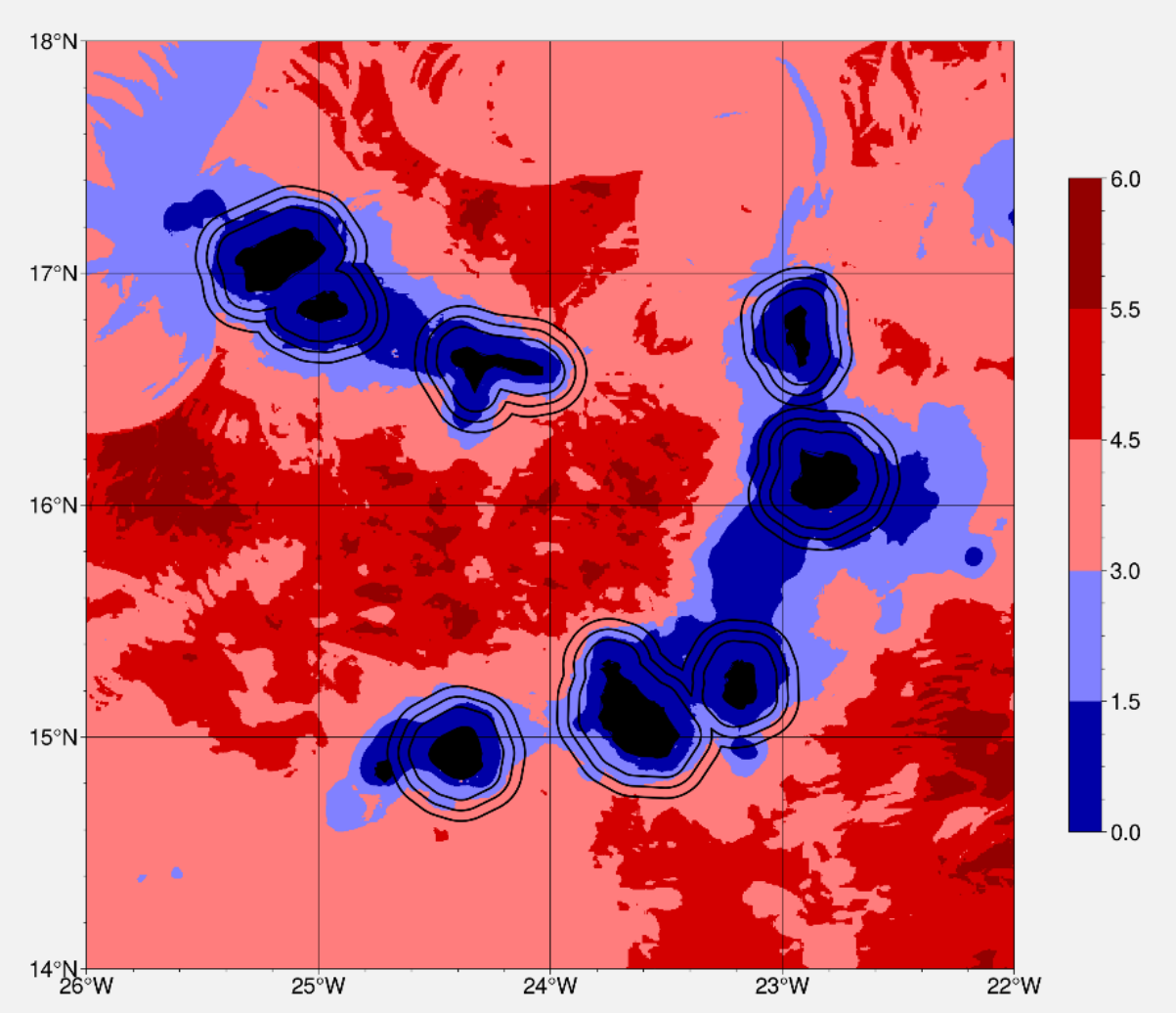

Figure 38. Marine gravitational energy storage suitability map for the offshore system for Cabo Verde. The scaling is non-uniform and gets thinner as the zoning gets higher (0-1.5, 1.5-3, 3-4.5, 4.5-5.5, 5.5-6). The three black isolines represent 10, 15, and 20 km distance from the coast.

4.4.2. Suitable Energy Storage Zones with Resources for Isolated System

We have incorporated the three best classes into our resource map by delineating them with areas falling into red, orange, and white in descending order of suitability as revealed in Figure 40. Under the system under consideration (Isolated system), the amount of storable energy resource for the optimally suitable zones (in red) are mostly above 8 kWh and could go to 11 and 12 kWh at some locations especially west-central Cabo Verde (Figure 40). The optimal zones that fall in the northern and central Cabo Verde are mostly 7 and 8 kWh. However, the second class (most suitable in orange) that falls in the western and southern part of Cabo Verde also ranges between 8 and 11 kWh. The storable energy for the third class

(moderately suitable), although not really the major focus when considering this isolated system ranges between 1 kWh when closer to the islands to 6 kWh in the northern part of Cabo Verde.

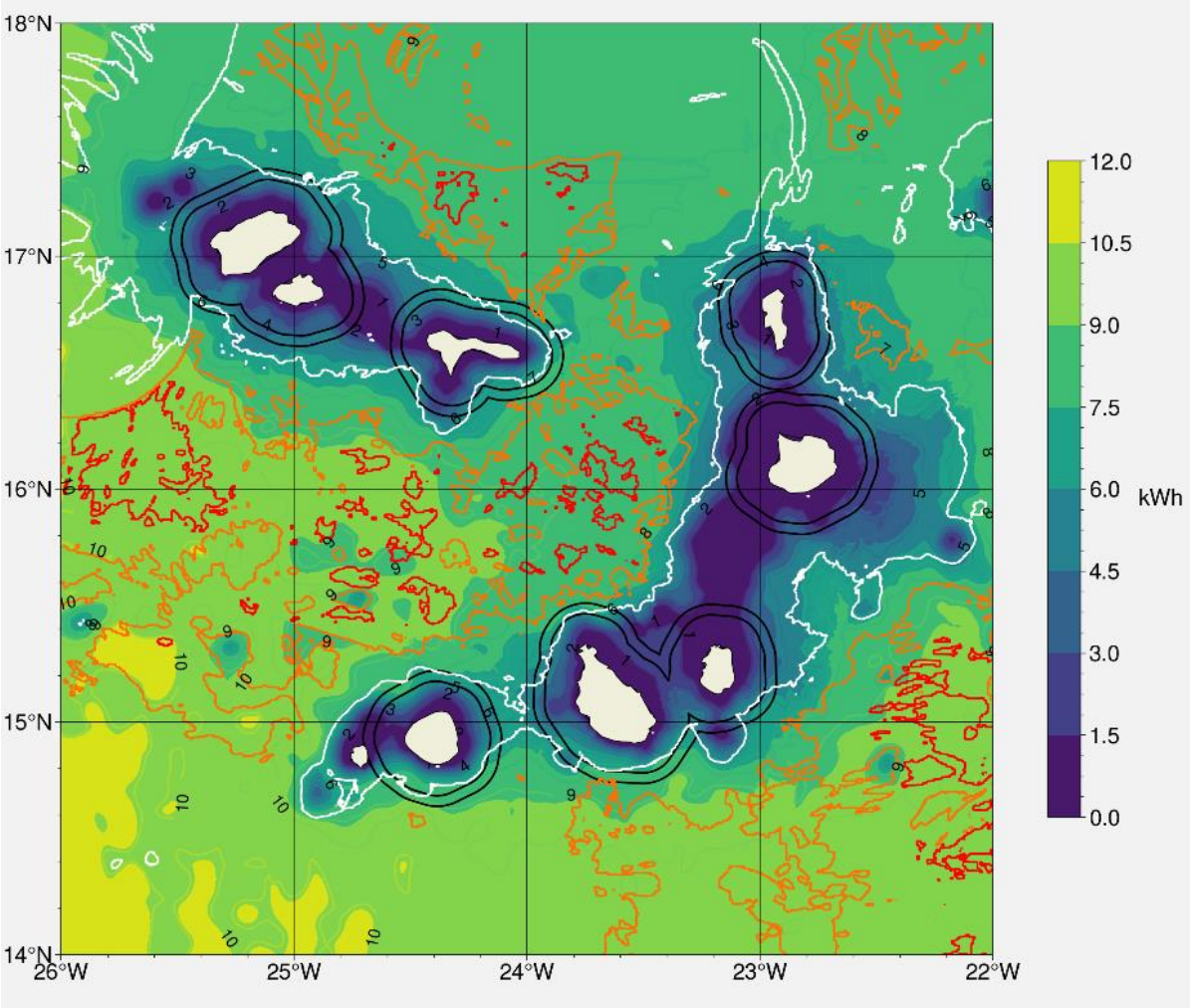

Figure 39. Marine gravitational energy storage resource potential per ton of mass showing the optimally, most, and moderately suitable for offshore system for Cabo Verde. Note: Areas encircled in the deep-red, orange and white are the zones representing optimally, most, and moderately suitable zones for energy storage. The two black isolines represent 15 and 20km distance from the coast respectively.

4.5. Suitable Energy Storage Zones for Onshore connected System

This aspect that aims at sending the stored energy onto the grid onshore tackles the problem from two different perspectives. The first case is developing a two criteria model that tries to set a balance between optimizing energy storage resources and cost. For the second

case, all the three criteria (cost, resources, and potential effects of currents) are considered and incorporated into the model.

4.5.1. Suitable Energy Storage Zones for Onshore Connected System (Case 1): Considering Resource (~Depth), and Cost (~closest distance)

To begin, a distance of 20 km is set as the maximum for all cases of onshore connected system (both two and three criteria models) since these systems will transmit the energy via cable to the grid onshore. The output of our two criteria model (Figure 41) shows that the optimally suitable zones include a portion of north and south of Santo Antão, south of Santa Luzia not far from the coast, an almost circumscribed São Nicolau, south-tip of Sal, and some areas of its north. Further, it also includes a tiny part in northern Boa Vista, south of Maio, a large portion of the immediate waters of Santiago, almost the whole water surrounding Fogo, and south part of Brava. The second and third best index of suitability follow similar pattern with broader span as shown in Figure 41.

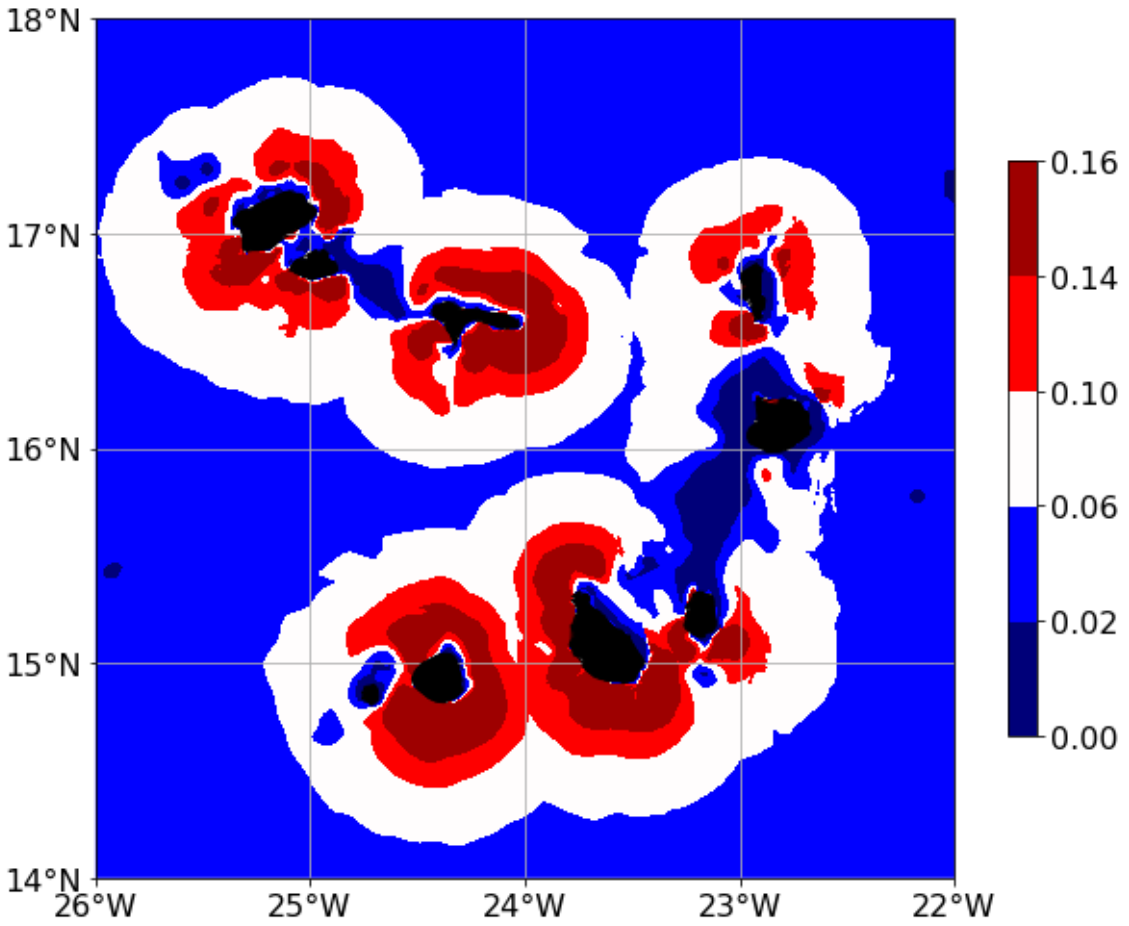

Figure 40. Marine gravitational energy storage suitability map for the two criteria model onshore connected system for Cabo Verde. The scaling is non-uniform which gets thinner as the zoning gets higher (0-0.02, 0.02-0.06, 0.06-0.10, 0.10-0.14, **0.14-0.16.** This map that shows 20km isoline distance from the coast can be found in Appendix 13.

4.5.2. Suitable Energy Storage Zones and Resource for Onshore System (Case 1)

For the first case of the Onshore connected system that is interested in finding a trade-off between energy storage resource and cost, the amount of energy that can be stored for the identified optimal suitable locations in Santo Antão, São Vicente, and São Nicolau is between 2 and 6 kWh (Figure 42). A range between 6 and 8 kWh is also storable at a distance of about 20km from the coast around São Nicolau, and south of Santo Antão. Islands of Sal and Boa Vista generally have low potential, while storage capacity of 8 and 9 kWh are achievable in the southern and northern part of the southern islands of Santiago and Fogo at a distance of 20km. A value of 6 kWh can also be gotten from south Maio at this maximum distance of 20

km. Generally, most regions of the second and third classes fall outside of 20 km maximum distance from coast that we are considering.

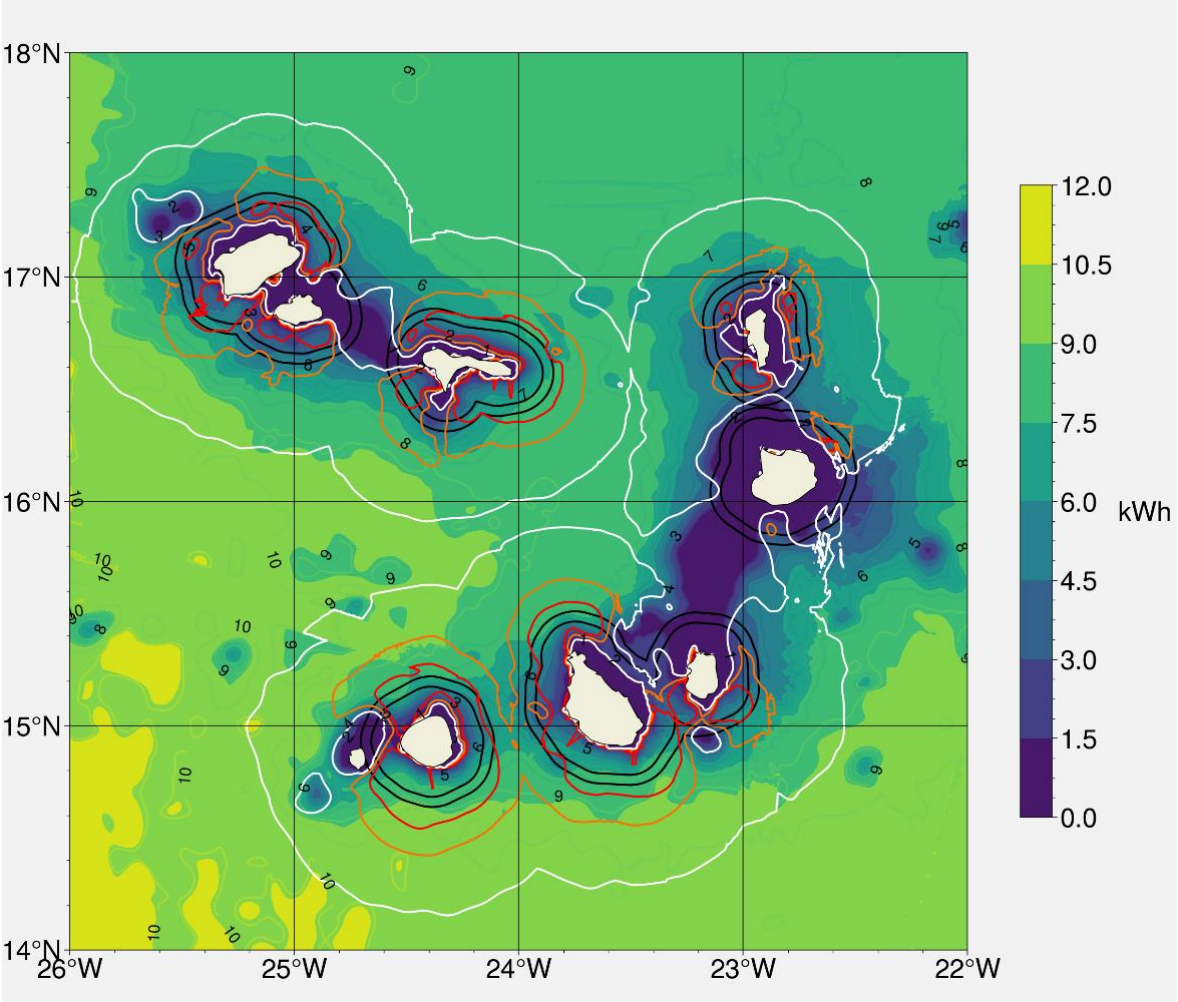

Figure 41. Marine gravitational energy storage resource potential per tonne of mass showing the optimally, most, and moderately suitable for two criteria model onshore connected system for Cabo Verde. Note: Areas encircled by the deep-red, orange and white respective are the zones representing optimally, most, and moderately suitable. The two black isolines represent 15, and 20 km distance from the coast respectively.

4.5.3. Suitable Energy Zones for Onshore system (Case 2): Considering the full defined criteria, Resource (~Depth), Cost (~closest distance), minimal impact of current (lowest Uv_max)

All the islands of Cabo Verde have coastal waters in their northern or southern region within the maximum 20 km distance from the nearest coast that fall in the optimally suitable domain except the island of Boa Vista. Fogo, Santiago, São Nicolau, and Santo Antão have

wide expanse of their neighboring waters that fall in this optimally suitable zone (Figure 43). Similarly, the portion of the aforementioned islands that did not fall within the first class but are within the 20 km maximum distance fall into the second class as obvious in all the islands although just a tiny fraction of Boa Vista. In a general sense, the 3 criteria model corresponds to an increase in the spatial expanse, and number of sites of two criteria.

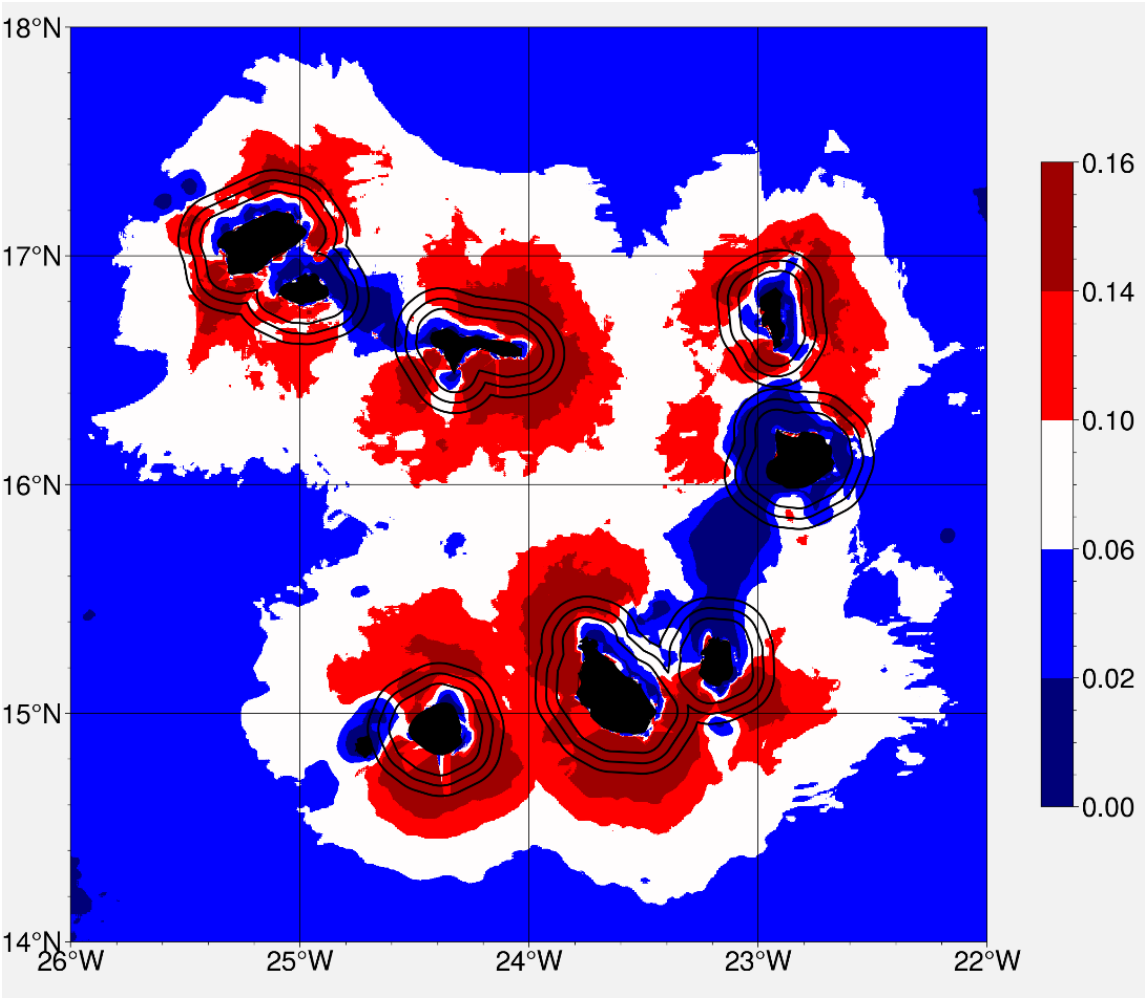

Figure 42. Marine gravitational energy storage suitability map for the full criteria model onshore connected system for Cabo Verde. The scaling is non-uniform which gets thinner as the zoning gets higher (0-0.02, 0.02-0.06, 0.06-0.10, 0.10-0.14, 0.14-0.16.

4.5.4. Suitable Energy Storage Zones and Resources for Onshore System (Case 2)

Within the 20km maximum zone, the energy capacity for the optimal suitable class of the full criteria model is around 3 to 7 kWh for the islands of Santo Antão and São Nicolau. Most neighboring coastal waters of São Vicente Island falls in the second class with earlier

mentioned capacity. An energy storage capacity range of 2 to 6 kWh is also achievable on the island of Sal in the eastern part, 5 kWh in Maio, and 3 to 8 kWh in the last three southern islands of Cabo Verde. The other two classes following the optimal class are mostly outside the 20 km distance (figure 37).

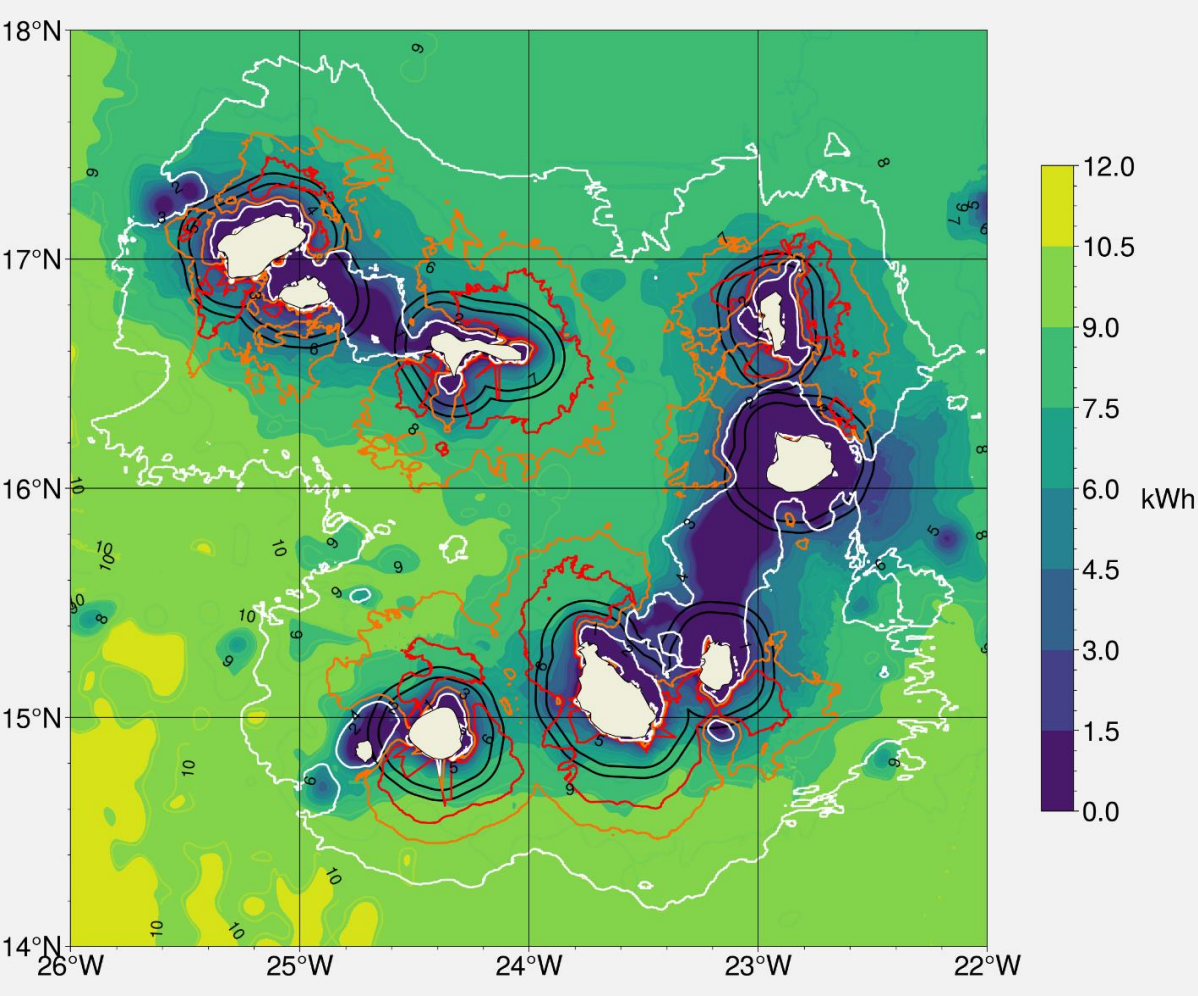

Figure 43. Marine gravitational energy storage resource potential per ton of mass showing the optimally, most, and moderately suitable for full criteria model onshore connected system for Cabo Verde. Areas encircled by the deep-red, orange and white respective are the zones representing optimally, most, and moderately suitable. The two black isolines represent 15, and 20 km distance from the coast respectively.

4.5.5. Linking Renewable potential with the Proposed Energy storage Capacity and potential Avoided CO_2

As presented in Figure 28, the total renewable energy production (from solar and wind) in Cabo Verde in 2018 is 100 GWh and corresponds to 20.3% of total energy consumption in

this same year (Appendix 6). Our results also illustrated that more than 9MW of OTEC energy is derivable at many locations around the coastal waters of Cabo Verde (Figure 32) especially in the southern island chain (Appendix 10). Further, wave power of above 10 kWm^{-1} (Figure 31) can be extracted in water bodies closer to the islands which can be extended to megawatts worth of extractable energy by making use of an array of wave floats. While ~ 8-12 kWh per ton of mass is storable for the optimally suitable zones of the Isolated MGES storage system, a range of energy storage capacity between 2 and 8 kWh can be stored by the Onshore-connected MGES storage system considering all the three limiting criteria. Hence, if 10 to 20 blocks were to be connected while increasing the mass to 10 tons for any of the two proposed storage systems, a single location will have the capacity to store 0.2 to 2.4 MWh which is extensible to 30 MWh by considering 50 to 100 blocks of 50 tons each running simultaneously. This implies that 10 to 15 stations running at the aforementioned capacity can store sufficient energy that can power the whole of Cabo Verde. In turn, this will avoid CO_2 emission contribution from the power industry, buildings, and other similar combustion activities in a value of half-million tons and above per year (Table 2, figure 33 and Appendix 7).

5. Discussion

5.1. Thermal Plants and Renewable Energy Penetration in Cabo Verde

The Cabo Verde archipelago is a country whose energy portfolio is majorly run on fossil fuel. Wood is the only primary energy resources in Cabo Verde in a limited amount due to poor quality of soil and little rainfall (ECREE, 2014). The country also lacks any reserves of oil and natural gas (REEEP, 2012). However, non-renewable sources of energy majorly thermal energy from imported fossil fuels has been covering the bulk of all energy sources in Cabo Verde. There was once a decline in the quantity of fossil fuels consumed as renewable grows but this did not last before it largely dominates again especially in 2017 and 2019. As an archipelago, each of the islands have at least one operational thermal plants and an electrical grid except the uninhabited island of Santa Luzia (ECREE, 2014; Costa, 2015). The most populous island of Santiago boasts the largest numbers of thermal plants and the largest plant in Cabo Verde (Secretariat, E. C. R. E. E. E., 2011). Thus, the amount of fossil fuel consumed varies from one island to another based on population and economic activities with some islands like Brava, Fogo and Maio totally running on fossil fuel.

Renewables is another contributor to the energy mix in Cabo Verde. Cabo Verde is among the 15 SIDS with ambition of attaining 100% electrification from renewables and has been setting several target years of achieving this, first 2020 and now 2025 (African Development Bank, 2014; Republic of Cabo Verde, 2016; Nordman *et al*., 2019). However, the trend in the amount of consumed renewables has rather been decreasing over the course of last decade. The major proportion of the renewables is from wind energy while solar contributes a small quota (Electra 2011, Electra 2018). The 25.5 MW Cabeolica wind farm was the first commercial scale in the whole region of sub-Saharan Africa (Auth *et al*., 2014) highlighting how Cabo Verde has positioned itself as a forerunner in wind power deployment in this region. Wind now accounts for 15% renewable penetration in 2019 produced on four of its islands (Cabeolica 2012-2019). Solar only accounted for 1.7% in 2017 (Electra, 2018; Taveres *et al*., 2019).

The heavy dependence on fossil fuel and the importation of all consumed fuel products are having a significant impact on the electricity prices which is high and unstable (Hove, 2018). It is hard to believe that the price of electricity in Cabo Verde is higher than many

European countries and other advanced nations. This price is in a fifth fold to that of countries like Nigeria and Ghana. According to Nordman *et al.* 2019, the electricity consumption per capital is ~727 kWh/person/year which almost doubles that of the Sub-Saharan Africa average of 488 kWh/person/year (World Bank, 2017). According to Tavares (2019), the variation of fuel prices does not benefit the energy sector and hence the national economy.

5.2. Harnessed Wind Resources, Cost and Resource Curtailment

Wind serves as the dominant renewable resource consumed in Cabo Verde. Its rate of production and generation have both increased over the years especially when compared to the last decade. It has also contributed immensely to electricity generation since its deployment in 2012, even though its penetration rate is now declining and does not keep pace with the increasing production rate as a result of rising energy need, population growth, and energy loss. For instance, Reiche *et al*. (2017) noted that the electricity production from wind between 2012 and 2017 avoided the consumption of about 15 million liters of imported fuel oil.

The dominance of wind energy for renewable energy consumption can strongly be related to wind power being envisioned as the most economical renewable resource that can be implemented on the islands of Cabo Verde (Gesto, 2011). The estimated energy production cost was 50 €/MWh which is less than half the cost of fuel oil at a price between 190 and 300 €/MWh, and far less than for solar photovoltaic resource with an estimated cost of 250 €/MWh in 2011 (Gesto, 2011; Heck *et al*. 2013). Additionally, wind is one of the easiest accessible renewable resources in Cabo Verde. The annual average speed far exceeds the minimum threshold (6–8 ms^{-1}) for energy generation on most of the islands. Hove (2018) reported an average wind speed of 9.8 ms^{-1} on the island of São Vicente. For the whole of Cabo Verde, the average wind speed is greater than 8 ms^{-1} and does exceed 9 ms^{-1} in some years.

Energy curtailment is a major setback facing many renewables. According to Bird *et al*. (2014), curtailment is the decrease in the output of an energy generator (wind or solar farm) from what it could otherwise produce from available resources (wind or solar energy), usually on an involuntary basis, to majorly maintain system energy balance, manage the grid system, and cater for transmission congestion or lack of transmission access or excess generation during low load periods (which is the case for Cabo Verde). In Cabo Verde, the amount of

wind energy that can be supplied to the grid has never gone beyond 78% and can be as low as 66% in some years. Out of the four generating islands, only Santiago can boast of attaining almost 100% efficiency while others battle under-consumption as energy demand and supply do not match, thus all the produced energy cannot be put on the grid. This curtailment is greatly pronounced on Sal Island to the extent of utilizing only 53% of produced energy until a recent improvement, yet more than 35% of produced energy was still wasted. Similarly, São Vicente is facing a massive energy curtailment issue despite the possession of very strong winds blowing throughout the year on this island (Hove, 2018). Although Boa Vista enjoys less than one-third of energy curtailment, the fact that more than 19% generated wind is wasted per year is also a concern.

The energy curtailment and intermittency are also reflected in the annual penetration rate of wind energy that keeps fluctuating over the years with a steep decline in 2018. Nordman *et al* (2019) directly linked the reduced penetration rate of wind energy in 2017 partly to technical restrictions imposed on electricity utility. Penetration rate can be inferred as the ratio of wind resources extracted to the total energy consumed in that year. To highlight the influence of curtailment on renewable energy industry of Cabo Verde, Cabeolica (2019) stated that power generation mostly does not reflect potential. Thus, only a fraction of the generated energy could be put on the grid.

In addition, the amount of revenue generated by Cabeolica through the sale of wind energy to Electra SA clearly highlights the monetary loss resulting from energy curtailment. A huge amount of money in the value of millions of euros is being paid for unused and wasted wind energy resources which if accumulated over the years could cover more ground for a more buoyant energy plan.

5.3. Renewable Energy Resource Potential and their Intermittency

5.3.1. Wind and Solar

Cabo Verde is an excellent candidate for wind energy development. The hourly, monthly, and yearly averages all favor the implementation of wind turbines for economic viability with a minimum of ~5 and 7.5 ms^{-1} for monthly and yearly average respectively. The wind climate explains the region where the country is situated which is typical of a subtropical region with

prevailing trade winds (Ranaboldo *et al*., 2014; Segurado, 2011). The nine islands have the potential to support a wind energy capacity of 241 MW at a Levelized Cost of electricity (LCOE) of around €0.05/kWh (Gesto Energy, 2011).

As stated, the geographic location of Cabo Verde places it in a suitable position for wind resources. Similarly, the amount of solar radiation received is promising. Gesto Energy (2011) estimated that 315 MW of solar PV projects are feasible in Cabo Verde with most of the potential development on Santiago. Currently, only 7.5 MW of solar PV capacity has been installed. The 315 MW of potential solar PV could produce as much as 471 GWh of electricity based on estimates using the PVGIS for Africa and Asia (Joint Research Centre, 2012).

However, the intermittency associated with both wind and solar energy is obvious. The amount of energy varies by the time of the day, season, and year. For solar, ~12 hours of the day could be without high energy, and months like January, February, November, and December often lack a high level of insolation. Similarly, wind also has a high level of hourly, daily, and seasonal variability.

5.3.2. Ocean Waves and OTEC

The mean wave power around Cabo Verde has a general value above 8 kwm^{-11}. The sides of the island have higher potential than the body of water that the islands surround. Northern Cabo Verde is generally the best site for ocean wave's plants. The eastern and southern parts outside the island are also some promising places. Generally, the 40 to 60 latitudinal range north and south are regions with concentrated high energy ocean waves especially off their western coasts as a result of the prevailing westerly winds (Rusu & Guedes-Soares, 2009). Although Cabo Verde falls outside this geographic space, ocean wave is a product of wind energy (Soukissian *et al*., 2017), and swells are created by distant windstorms which dominate over the locally generated waves explaining the reason for Northern Cabo Verde having huge wave power potential as a result of waves from the mid-latitude. Further, winds are stronger in the winter months than the summer months in the northern hemisphere where Cabo Verde falls within, and these strong winds generate stronger swells.

OTEC is another marine-based energy system that can be implemented in Cabo Verde. This technology works at its optimal when a temperature difference between the surface and

the deep water is around 20° C which ideally exists along equatorial latitudes (Vyawahare, 2015). Several locations around Cabo Verde are close to this threshold although detailed research would be needed to ascertain this fact. Nevertheless, the southern waters surrounding Cabo Verde are the best places to cite this energy generation technology as they possess the maximum potential.of more than 9 MW. As presented by Hamedi and Sadeghzadeh (2017), the expected LCOE of a 5 MW OTEC system with a 22° C temperature difference proposed in Oman Sea is US$0.12/kWh. For Cabo Verde, similar LCOE range could be economically feasible (Nordman *et al*., 2019).

Ocean waves and OTEC also showed some level of intermittency like winds and solar. Normally, these two marine-based are reflections of the land-based. Diurnal surface temperature is a function of solar irradiance while surface waves can be highly attributed to distant winds. Hence, while the summer months exhibit great OTEC power potential, the other months have average to low potential. For Wind, December through March have the greatest potential while the other months have low to average potential.

5.4. Ocean Current Analysis

The decision to select one of the ocean current statistical variables to use in this study is done after a thorough examination of individual variables. The goal is to select a variable that can completely represent the maximum impact of the ocean current in our study area. The selection problem lies in the fact that the weight will oscillate vertically during charge and discharge. Additionally, it will also stay in a fixed position either at the surface or at the bottom when no work is done. Hence, a variable that can give an account of all the highlighted conditions or to a larger extent must be considered.

The monthly mean of the standard deviation of the current amplitude (Uv_mstd) gives a full account of the impacts of tides with high Uv_mstd corresponding to tidal currents (Gomes *et al*., 2015). This current that is associated with tides will be sweeping across the structure with a daily-based impact. They are also more coastal, According to this study, the largest impact will be felt in January and December although several years of studies will be required to confirm this. The impact will be more pronounced between islands especially on the eastern side of São Vicente. Further, the eastern side of Boa Vista and the region between Boa Vista

and Maio are some of the hotspots. However, a major safe location is the eastern portion of Cabo Verde especially the eastern and southern part of Brava and southern Santiago.

The monthly and vertical maximum of the current amplitude gives a full account of the maximum current throughout the water column including the impacts of tides and eddies. These two major oceanic processes transfer momentum from one part of the ocean to another and are capable of impacting materials or structures along their path. In addition to tides, eddies are some of the oceanic processes pronounced in Cabo Verde's waters (Cardoso, *et al*., 2020). Several diverse physical processes can lead to their generation including current shear (Chelton *et al*., 2011; Schütte *et al*., 2016a); topography effects (Barkley, 1972; Heywood *et al*., 1990; Alpers *et al*., 2014); ocean-atmosphere interaction (Calil *et al*., 2008; Jiménez *et al*., 2008; Couvelard *et al*., 2012; Hogg *et al*., 2016); or even eddy-eddy interaction (Sangrà *et al*., 2009; Chelton *et al*., 2011).

Unlike the monthly and vertical mean of the daily standard deviation of the current amplitude, the monthly and vertical maximum of the current amplitude captures both major currents between, outside, and beyond the islands. A definite pattern can't really be seen from their monthly differences because of the irregularities in their spatial variability although several years of data will be needed to affirm this. The only thing that's more general is their strength and influence in the northern part of Cabo Verde, and between the islands of Santo Antão, São Vicente, Santa Luzia, and São Nicolau.

Other major variables analyzed for the purpose of this study are the monthly and vertical maximum of the current amplitude at the surface (uv_max_0), and the bottom (uv_max_bot). The amplitude of the maximum current at the surface is just half the one at the bottom and the whole vertical column of water which is why we ignore this variable although it also has similar pattern throughout the 12 months.

In conclusion, tides are important for the (on-shore grid system) because they will come back every day and are very coastal, while the strong currents associated with eddies are more occasional, not always in the same place as seen in our monthly result. But, eddies are common in Cabo Verde waters, and as such, we chose monthly and vertical maximum of the current amplitude and incorporated it in our model as our final choice for both on-shore and grid-connected systems. Nevertheless, it did not deter us from generating two different models for

the two most important statistical variables (Uv_max and Uv_mstd) and comparing their outputs. We realized their final outputs (suitability maps) are also similar.

5.5. MGES Resource Potential

One of the main advantages of the proposed method is its independency on weather variations but its dependency on water depth. The resource potential clearly illustrates the depth variation in Cabo Verde. The northern and eastern part of Cabo Verde have a low overall potential, especially regions closer to the coast. One of the most noticeable locations is found around one of the islets between Santa Luzia and São Nicolau with a value of 1kWh. This area corresponds to the shallow channels existing around one of the northern island chains which barely reaches 20 m depth (Ramalho, 2011). Nevertheless, a potential of 7-9 kwh is still storable in places a little further away from the coast at several locations.

Both the western and southern parts of Cabo Verde are regions with massive potential to implement this technology. Specifically, the southern offshore zones of all the islands are potentially some best locations. These regions constitute places with great depths to such an extent that the lowest storable energy is around 9 kwh. Further, a huge storage potential above 12kwh is derivable according to the baseline mass of 1 ton used in this study.

Some other interesting locations exist in the southern part of Cabo Verde. The area between the island of Fogo and Santiago is significantly deeper than other sites in-between the islands of Cabo Verde, and it is slightly above the 3,000 m isobaths (Remalho 2011). This area coincides with the zone having the maximum storage potential in-between two islands of Cabo Verde. Another noticeable location shown in the resource map is an area between Boa Vista and Maio which conforms to having a low energy storage potential of between 0 and 2 kWh. This area corresponds to a prominent feature in Cabo Verde's bathymetry known as the João Valente Bank or João Valente Shoals.

5.6. Suitable Energy Storage Zones and Resources 1 (Isolated System)

The energy storage system that focuses on consuming the stored energy offshore without transmitting it to the grid (offshore system) considers a trade-off between maximizing the achievable energy storage resources at the least possible impact of current. As highlighted in

the previous session, the regions with the maximum energy potential are located in the deep offshore of Cabo Verde in the west and south. Taking the offshore zone of Cabo Verde to start from the 20km maximum distance to the shoreline to the northern, southern, western, and eastern limit of Cabo Verde as defined in the Figures 38 – 44, only about 10% of the immediate offshore of Cabo Verde falls under the category of optimally suitable locations after considering the impacts of currents, and they are distributed around the west-central, and central Cabo Verde. A large spatial span is situated at the far west-central of Cabo Verde, and east of the south island chain. These areas are minimally impacted by currents with the amount of storable energy ranging between 8 and 11 kWh. However, most central Cabo Verde can store between 6 and 8 kWh.

Some sites also exist in the northern offshore Cabo Verde with a capacity to store between 6 and 8kWh. These locations are having the least impact of current in this region but the depth is not so great in comparison with the west central and southern Cabo Verde. The same can be said for the central waters of Cabo Verde discussed in the last paragraph.

However, an estimated 60% of waters in the offshore of Cabo Verde falls in the second class termed most suitable. The first thing to note is that the scale used for the classification under this heading (offshore system) was refined with the first two classes, optimally, and most suitable taking just 25% of the total scale of the five classes. This implies that the second class also has a high level of suitability as indicated in the derivable energy resource that is mostly greater than 9 kWh and can reach 12 kWh. Focusing on the highest energy resource, the northeast of Brava and Fogo Islands, and the south of Santiago and Maio are the best options.

The lower classes fall in region closer to the coast which is very intuitive because the impact of current is high, and the extractable energy resource is also low.

5.7. Suitable Energy Storage Zones and Resources 2 (On-shore Connected) with C02 Analysis

The onshore-connected aim at evaluating places with high enough potential, at a minimal distance to the coast with the possible impacts of current. A reference distance of 20km is set as the maximum distance from the nearest coast and the consideration is optimum suitability which takes 12.5% of the total scale of suitability.

Considering only distance and resources, all the islands of Cabo Verde have regions that are optimally suitable for the installation of this storage system near their coastal waters. This is particularly pronounced on the islands of São Nicolaus, Fogo, and Santiago. These three islands are almost completely surrounded by waters that are optimally suited for this storage system. The islands of Santo Antão, São Vicente, Sal and Maio also have some suitable places based on these two criteria, while Brava has few suitable places, although Brava shares proximity with the island of Fogo. The only island with a very tiny part based on these two conditions is the island of Boa Vista.

Intuitively, the distance from the islands increases as we move away from the shore and vice versa. Thus, all the aforementioned islands quickly get deep as we moved away from the coast such that the depth overcompensated the distance to attain an optimal suitability. However, the storage potential varies from 2-4 kWh in Boa Vista and Sal, 2-6 kWh in the north island chain, 6 kWh around Maio, to a maximum of between 8 and 9 kWh around the north and south of Fogo and Santiago.

Similar to the two criteria condition, all the islands of Cabo Verde are characterized by coastal waters that is optimally suitable for the installation of MGES within the 20km maximum distance except the tiny area around Boa Vista coastal waters. Broadly, the three criteria model corresponds to an increase in the spatial expanse, and number of sites of two criteria. Therefore, the energy capacity upper limit increases by a unit of 1 kWh. It seems that the two opposing criteria distance and maximum current tend to produce a net effect that improve the suitability of the area as opposed the two condition criteria that deals with only closest distance and resources.

The storable energy indicated that many of the islands with the largest population in Cabo Verde have great energy storage potential especially the two most populous islands of Santiago and São Vicente. With the addition of Sal, these three islands are also three of the four islands that have installed wind energy. The implication of this is to develop a swift approach of incorporating this proposed storage system into the existing renewable plants or as a part of any proposed renewable technology to reduce their associated curtailment, increase their rate of penetration, and put an end to the associated monetary loss. Additionally, these islands constitute the majority of the end-users, and the development of a storage system to meet the

energy demand of these islands is predominant to achieving a sustainable and secured energy outcome in Cabo Verde.

The CO2 burnt into the atmosphere is on the rise and has increased in a very steep manner recently as population and economic activities increase. The current emitted CO2 has surpassed that of the last decade in a multiple of 2.25. While buildings were one of the major contributors to CO2 emission in the past, power and transport constituted the dominant source of CO2 emission in Cabo Verde in recent years. As proven, the installation of wind turbines on four islands has prevented the emission of 0.8 million tons corresponding to avoiding ~17% of total CO2 that would have been released between 2012 and 2017 alone. This proves that 100% renewable in power, industry, and buildings will definitely largely reduce the tons of carbon released into the environment in a value of half a million tons.

We have established that Cabo Verde has massive potential for both land-based and marine renewables. These include the currently used renewable energies, wind and solar energy that are contributing about 10% (80 GWh) electricity generation. These two land-based RERs can be complemented with marine-based RERs by harnessing the greatest OTEC potential around the south to the central part of Cabo Verde of above 9MW, and waves power in the northern, and outward waters of Cabo Verde away from the islands around the center of the country with a potential exceeding 1 MW per 100 m. On this note, Cabo Verde can achieve 100% renewable penetration for electricity generation, and efficient utilization of fixed-cost resources in a similar suggestion of Veigas *et al*. (2014) in the Canary Islands. The asynchronous relationship of the renewable energies demand and supply can be solved through the Marine gravitational energy storage system by simultaneously running several individual blocks (50 to 100) of high magnitude of about 50 to 100 tons. Several such stations (10 -15) around Cabo Verde will have the capacity to store the consumed electricity which is around 400 GW. Toubeau *et al*. (2020) showed that 210 blocks can be connected to an induction coil for MGES and gave an estimation of the investment cost to be around 100 €/kWh which is cheaper than both battery and pump-hydro storage systems.

6. Conclusion

Cabo Verde is a country that can regionally and globally boast of high renewable penetration in electricity generation due to the significant progress made in the field of renewable energy supplies. However, major challenges still persist. The energy sector is characterized by a strong dependence on the imported petroleum products. Aside from the imported fossil fuel and associated CO_2 emissions, Cabo Verde is also witnessing high electricity tariff rates and energy curtailment. The economic development of a country is, to a certain extent, conditioned by the quantity and quality of energy it makes available to consumers and its associated value. The availability of affordable, and sustainable energy would go a long way in improving the sustainability of socio-economic development.

We have used this study to highlight some important concepts and theories, and at the same time support some previous research. Here, we have re-established Cabo Verde as a country with a massive renewable potential for both land-based and marine but undermining this potential. We have also shown that wind serves as the dominant renewable resource feeding the energy grid and has avoided the release of almost a metric ton of CO_2 into the atmosphere. The major reason behind resource underutilization is energy curtailment which many authors aren't aware of, and that's where storage comes in.

The potential for MGES is great. The storage resource is a function of depth and mass. Under a constant mass of 1 ton, the resource potential of 3 – 8 kWh is achievable for the optimally and most suitable zones of the onshore-connected system with around 8 kWh storable energy around the coastal waters of Santiago, Fogo, Sao Niolau, and Maio, and 6 kWh around São Vicente, Sal, Santo Antão. This capacity can reach 12 kWh for the aforementioned zones of the offshore system with 11 kWh around the coastal waters north of the four northern island chain (Santo Antão to São Nicolau), and 10-12 South of thesame chain, while 8-10 kWh is storable in the northwest and southeast offshore of the other six island chain (Sal to Brava). Any term used as 'tiny part' in this study is actually a large spatial extent in reality. Thus, MGES can be installed on the coastal or offshore zone of almost every island in Cabo Verde. Further, a deviation from the 1-ton constant mass by increasing the mass, for instance to 10 tons, will equally lead to ten times energy storage potential. Stacking up several masses strategically without an increase in depth will increase the storage potential to about several

megawatts and could possibly meet the energy consumed in Cabo Verde which is about 350 MW (Hove 2018).

Thus, solving curtailment by incorporating a storage mechanism like MGES will increase renewable penetration, investment into renewables, and reduce fossil fuel emission. A huge investment and focus on renewable technologies and storage technology like MGES will also improve grid stability and achieve the goal of cabo-verdean government of becoming a nation with 100% renewable.

This study was conducted based on placing the same weights on individual criterion. It would also be inquisitive to see the effect of prioritizing some of the criteria over another such as weighing resources twice the effect of ocean current. Further, the current data used is a seasonal cycle, many years of this high-resolution data will provide more information and might reveal the most suitable ocean current variable to use although it might not make so much difference. Lastly, a cost analysis of the implementation of this technology would also be an added value to this research in the future.

7. References

Abedin, A. H., & Rosen, M. A. (2012). Closed and open thermochemical energy storage: Energy-and exergy-based comparisons. *Energy*, *41*(1), 83-92.

Adesanya, A., Misra, S., Maskeliunas, R., & Damasevicius, R. (2020). Prospects of ocean-based renewable energy for West Africa's sustainable energy future. Smart and Sustainable Built Environment.

Adiputra, R., Utsunomiya, T., Koto, J., Yasunaga, T., & Ikegami, Y. (2020). Preliminary design of a 100 MW-net ocean thermal energy conversion (OTEC) power plant study case: Mentawai island, Indonesia. *Journal of Marine Science and Technology*, *25*(1), 48-68.

AFREC. (2015). AFREC Africa Energy Database. Algiers: African Energy Commission (AFREC).

African Development Bank. (2014). *Cabo Verde Country Strategy Paper 2014-2018* (No. ORWA Department/SNFO).

Ahuja, D., & Tatsutani, M. (2009). Sustainable energy for developing countries. *SAPI EN. S. Surveys and Perspectives Integrating Environment and Society*, (2.1).

Ajanovic, A., Hiesl, A., & Haas, R. (2020). On the role of storage for electricity in smart energy systems. *Energy*, *200*, 117473.

Akhil, A. A., Huff, G., Currier, A. B., Kaun, B. C., Rastler, D. M., Chen, S. B.... & Gauntlett, W. D. (2013). *DOE/EPRI 2013 electricity storage handbook in collaboration with NRECA* (Vol. 1, p. 340). Albuquerque, NM: Sandia National Laboratories.

Allen, M.R., O.P. Dube, W. Solecki, F. Aragón-Durand, W. Cramer, S. Humphreys, M. Kainuma, J. Kala, N. Mahowald, Y. Mulugetta, R. Perez, M.Wairiu, and K. Zickfeld, 2018: Framing and Context. In: Global Warming of 1.5°C. An IPCC Special Report on the impacts of global warming of 1.5°C above pre-industrial levels and related global greenhouse gas emission pathways, in the context of strengthening the global response to the threat of climate change, sustainable development, and efforts to eradicate poverty [Masson-Delmotte, V., P. Zhai, H.-O. Pörtner, D. Roberts, J. Skea, P.R. Shukla, A. Pirani, W. Moufouma-Okia, C. Péan, R. Pidcock, S. Connors, J.B.R. Matthews, Y. Chen, X. Zhou, M.I. Gomis, E. Lonnoy, T. Maycock, M. Tignor, and T. Waterfield (eds.)]. In Press.

Almeida, A. C. (2019). Multi actor multi criteria analysis (MAMCA) as a tool to build indicators and localize sustainable development goal 11 in Brazilian municipalities. *Heliyon*, *5*(8), e02128.

Alpers, W., Dagorne, D., Brandt, P. (2014). Satellite observations of oceanic eddies around Africa. In *Remote Sensing of the African Seas* (pp. 205-229). Springer Netherlands.

Alves, L. M. M., Costa, A. L., & da Graça Carvalho, M. (2000). Analysis of potential for market penetration of renewable energy technologies in peripheral islands. *Renewable energy*, *19*(1-2), 311-317.

Amante, C., & Eakins, B. W. (2009). ETOPO1 arc-minute global relief model: procedures, data sources and analysis.

Amirante, R., Cassone, E., Distaso, E., & Tamburrano, P. (2017). Overview on recent developments in energy storage: Mechanical, electrochemical and hydrogen technologies. *Energy Conversion and Management*, *132*, 372-387.

Amirante, R., & Tamburrano, P. (2015). Novel, cost-effective configurations of combined power plants for small-scale cogeneration from biomass: Feasibility study and performance optimization. *Energy Conversion and Management*, *97*, 111-120.

Andrijanovits, A., Hoimoja, H., & Vinnikov, D. (2012). Comparative review of long-term energy storage technologies for renewable energy systems. *Elektronika ir Elektrotechnika*, *118*(2), 21-26.

Aneke, M., & Wang, M. (2016). Energy storage technologies and real life applications–A state of the art review. *Applied Energy*, *179*, 350-377.

Anonymous. (2016). energy on the fly: Exploring the potential future of energy storage: bearingless flywheel motors. *Electronics Letters*, *52*(11), 890-890.

Antonio, F. D. O. (2010). Wave energy utilization: A review of the technologies. *Renewable and sustainable energy reviews*, *14*(3), 899-918.

Appiott, J.; Dhanju, A.; Cicin-Sain, B. Encouraging Renewable Energy in the Offshore Environment. Ocean Coast. Manag. 2014, 90, 58–64. [CrossRef] see also [Borthwick 2016, European commission 2014].

Ares. The Power of Gravity. 2019. Available online: https://www.aresnorthamerica.com/ (accessed on 1 July 2019).

Argonne National Laboratory (2009). Compressed air energy storage (CAES) in Salt Caverns.

Arnault, S. (1987). Tropical Atlantic geostrophic currents and ship drifts. *Journal of Geophysical Research: Oceans*, *92*(C5), 5076-5088.

Auth, K., Musolino, E., Thomas, T., Adebiyi, A., Reiss, K., Semedo, E., ... & Diarra, C. (2014). ECOWAS renewable energy and energy efficiency status report-2014.

Barkley, R. A. (1972). Johnston Atoll's Wake'. *Journal of Marine Research*, *30*(2), 201–216.

Barreira, I., Gueifão, C., & de Jesus, J. F. (2017, March). Off-stream Pumped Storage Hydropower plant to increase renewable energy penetration in Santiago Island, Cape Verde. In *Journal of Physics: Conference Series* (Vol. 813, No. 1, p. 012011). IOP Publishing.

Bassett, K., Carriveau, R., & Ting, D. S. K. (2016). Underwater energy storage through application of Archimedes principle. *Journal of Energy Storage*, *8*, 185-192.

Bassett, K. P., R. Carriveau, and DS-K. Ting. "Integration of buoyancy-based energy storage with utility scale wind energy generation." *Journal of Energy Storage* 14 (2017): 256-263.

BCV. Annual Report 2017 of the Bank of Cape Verde, Praia. Obtained on 22 January 2019, from http://www.bcv.cv/, 2017.

Becker, J. J., Sandwell, D. T., Smith, W. H. F., Braud, J., Binder, B., Depner, J. L., ... & Weatherall, P. (2009). Global bathymetry and elevation data at 30 arc seconds resolution: SRTM30_PLUS. *Marine Geodesy*, *32*(4), 355-371.

Belton, V., & Stewart, T. (2002). *Multiple criteria decision analysis: an integrated approach*. Springer Science & Business Media.

Bernardino, M., Rusu, L., & Soares, C. G. (2017). Evaluation of the wave energy resources in the Cape Verde Islands. *Renewable Energy*, *101*, 316-326.

Bird, L., Cochran, J., & Wang, X. (2014). *Wind and solar energy curtailment: experience and practices in the United States* (No. NREL/TP-6A20-60983). National Renewable Energy Lab.(NREL), Golden, CO (United States).

Blair C., Gravitricity – Storing Power as well as Energy [Online]. Available: http://www.all-energy.co.uk/Conference/Download-2016-Presentations/.

Book, I. I. G. C., & Contributors, O. D. GEBCO_2020 Grid.

BP. (2016). BP Statistical Review of World Energy June 2016. London: BP.

Borthwick, A. G. (2016). Marine renewable energy seascape. *Engineering*, *2*(1), 69-78.

Botha, C. D., & Kamper, M. J. (2019). Capability study of dry gravity energy storage. *Journal of Energy Storage*, *23*, 159-174.

Brancato, E. L. (1992). Estimation of lifetime expectancies of motors. *IEEE Electrical Insulation Magazine*, *8*(3), 5-13.

Bungane, B. - Gravitricity Sets Sights on South Africa to Test Green Energy Tech [Online]. Available: https://www.esi-africa.com/gravitricity-sets-sights-southafrica-test-green-energy-tech/ (accessed: March 2018).

Cabeolica (2021). Annual Reports. Retrieved January 19, 2021, from https://cabeolica.com/about-us/annual-reports/.

Caldeira, R. M. A., Stegner, A., Couvelard, X., Araújo, I. B., Testor, P., Lorenzo, A. (2014). Evolution of an oceanic anticyclone in the lee of Madeira Island: In situ and remote sensing survey. *Journal of Geophysical Research: Oceans*, *119*(2), 1195–1216.

Calil, P. H. R., Richards, K. J., Jia, Y., Bidigare, R. R. (2008). Eddy activity in the lee of the Hawaiian Islands. *Deep-Sea Research Part II: Topical Studies in Oceanography*, *55*(10–13), 1179–1194.

Cardoso, C., Caldeira, R. M., Relvas, P., & Stegner, A. (2020). Islands as eddy transformation and generation hotspots: Cabo Verde case study. Progress in Oceanography, 184, 102271.

Castillo, A., & Gayme, D. F. (2014). Grid-scale energy storage applications in renewable energy integration: A survey. *Energy Conversion and Management*, *87*, 885-894.

Cazzaniga, R., Cicu, M., Marrana, T., Rosa-Clot, M., Rosa-Clot, P., & Tina, G. M. (2017). DOGES: deep ocean gravitational energy storage. *Journal of Energy Storage*, *14*, 264-270.

Catalano, L. A., De Bellis, F., Amirante, R., & Rignanese, M. (2011). An immersed particle heat exchanger for externally fired and heat recovery gas turbines. *Journal of engineering for gas turbines and power*, *133*(3).

Cavanagh K, Ward J K, Behrens S, Bhatt A I, Ratnam E L, Oliver E and Hayward J. (2015). Electrical energy storage: technology overview and applications. CSIRO, Australia. EP154168.

Chan, C. W., Ling-Chin, J., & Roskilly, A. P. (2013). Reprint of "A review of chemical heat pumps, thermodynamic cycles and thermal energy storage technologies for low grade heat utilisation". *Applied thermal engineering*, *53*(2), 160-176.

Chauhan, A., & Saini, R. P. (2014). A review on Integrated Renewable Energy System based power generation for stand-alone applications: Configurations, storage options, sizing methodologies and control. *Renewable and Sustainable Energy Reviews*, *38*, 99-120.

Chelton, D. B., Schlax, M. G., Samelson, R. M. (2011). Global observations of nonlinear mesoscale eddies. *Progress in Oceanography*, *91*(2), 167–216.

Cheng, A. Y. C. (2005). *Economic modeling of intermittency in wind power generation* (Doctoral dissertation, Massachusetts Institute of Technology).

Chen, H., Cong, T. N., Yang, W., Tan, C., Li, Y., & Ding, Y. (2009). Progress in electrical energy storage system: A critical review. *Progress in natural science*, *19*(3), 291-312.

Chopin, P., Guindé, L., Causeret, F., Bergkvist, G., & Blazy, J. M. (2019). Integrating stakeholder preferences into assessment of scenarios for electricity production from locally produced biomass on a small island. *Renewable Energy*, *131*, 128-136.

Clement, A.; McCullen, P.; Falcao, A.; Fiorentino, A.; Gardner, F.; Hammarlund, K.; Lemonis, G.; Lewis, T.; Nielsen, K.; Petroncini, S.; *et al*. Wave Energy in Europe: Current Status and Perspectives. Renew. Sustain. Energy Rev. 2002, 6, 405–431. [CrossRef]

Climate and fundamentals of the energy offer in Cape Verde 2019. Jorge Tavares, Myriam Lopes, Fernando Netoa: 6th International Conference on Energy and Environment Research, ICEER 2019, 22–25 July, University of Aveiro, Portugal.

Com, E. C. (2018). Communication from the Commission to the European Parliament, the European Council, the Council, the European Economic and Social Committee, the Committee of the Regions and the European Investment Bank, A Clean Planet for all. *A European strategic long-term vision for a prosperous, modern, competitive and climate neutral economy. Brussels*, *28*, 2018.

Costa, A. (2015). Cabo Verde energy future: needs for innovation and strategic partnerships. Federal Ministry for Economic Affairs and Energy. https://www.germanenergysolutions.de/GES/Redaktion/DE/Audioslidehows/2015/Kap-Verden/Vortrag3/vortrag3_audio.html

Couch SJ, Bryden I. 2006. Tidal current energy extraction: Hydrodynamic resource characteristics. Proceedings of the Institution of Mechanical Engineers, Part M: Journal of Engineering for the Maritime Environment, 220(4), 185–194.

Couvelard, X., Caldeira, R. M. A., Araújo, I. B., Tomé, R. (2012). Wind mediated vorticity-generation and eddy-confinement, leeward of the Madeira Island: 2008 numerical case study. *Dynamics of Atmospheres and Oceans*, *58*, 128–149.

Crippa, M., Guizzardi, D., Muntean, M., Schaaf, E., Solazzo, E., Monforti-Ferrario, F., ... & Vignati, E. (2020). Fossil CO2 emissions of all world countries. *Luxembourg: European Commission*, 1-244.

Crippa, M., Oreggioni, G., Guizzardi, D., Muntean, M., Schaaf, E., Lo Vullo, E., ... & Vignati, E. (2019). Fossil CO2 and GHG emissions of all world countries. *Publication Office of the European Union: Luxemburg*.

Daoud, M. I., Abdel-Khalik, A. S., Massoud, A., Ahmed, S., & Abbasy, N. H. (2012, September). On the development of flywheel storage systems for power system applications: a survey. In *2012 XXth International Conference on Electrical Machines* (pp. 2119-2125). IEEE.

Daoud, M., Abdel-Khalik, A., Elserogi, A., Ahmed, S., & Massoud, A. (2015). Flywheel Energy Storage Systems. *Handbook of Clean Energy Systems*, 1-14.

Dehghani-Sanij, A. R., Tharumalingam, E., Dusseault, M. B., & Fraser, R. (2019). Study of energy storage systems and environmental challenges of batteries. *Renewable and Sustainable Energy Reviews*, *104*, 192-208.

Devis-Morales, A., Montoya-Sánchez, R. A., Osorio, A. F., & Otero-Díaz, L. J. (2014). Ocean thermal energy resources in Colombia. *Renewable Energy*, *66*, 759-769.

DGA, C. (2004). White Paper on the State of the Environment in Cape Verde.

Doorga, J. R. S., Chinta, D., Gooroochurn, O., Rawat, A., Ramchandur, V., Motah, B. A., & Samyan, C. (2018). Assessment of the wave potential at selected hydrology and coastal environments around a tropical island, case study: Mauritius. International Journal of Energy and Environmental Engineering, 9(2), 135-153.

D. Surroop, P. Raghoo. Renewable and Sustainable Energy Reviews 88 (2018) 176–183

Dragoon K. (2012, Feb. 12) "Energy storage opportunities and challenges: A West Coast perspective white paper," ECOFYS [Online]. Available: http://www.ecofys.com/files/files/ecofys-2014-energy?storage-white-paper.pdf [Accessed: 05 Feb. 2020].

Duić, N., Krajačić, G., & da Graça Carvalho, M. (2008). RenewIslands methodology for sustainable energy and resource planning for islands. *Renewable and Sustainable Energy Reviews*, *12*(4), 1032-1062.

ECREEE, (2014) "ECOWAS Renewable Energy and Energy Efficiency Facility (EREF)", Retrievd from http://www.ecowrex.org/reee_initiative/ecowas-renewableenergy-and-energy-efficiency-facility-eref.

EDGAR - Emissions Database for Global Atmospheric Research. (n.d.). Retrieved March 10, 2021, from Global Greenhouse Gas Emissions: https://edgar.jrc.ec.europa.eu/index.php/dataset_ghg60

Electra (2011). Relatorio e Contas 2010. Annual Report. Praia.

Electra (2013). Relatorio e Contas 2012. Annual Report. Praia.

Electra 2018. Management report. Cape Verde. Obtained on 20 December 2018, from http://www.electra.cv/.

EMODnet Bathymetry Consortium. (2018). EMODnet Digital Bathymetry (DTM 2018).

Energy Vault (2019). Enabling a Renewable World. Retrieved from: https://energyvault.com/

Energy Storage Association. Compressed Air Energy Storage (CAES). 2017:1-3.

Energiasrenovaveis (2020). Retrieved January 10, 2021, from https://www.energiasrenovaveis.cv/copia-estatisticas

Estévez, R. A., Espinoza, V., Ponce Oliva, R. D., Vásquez-Lavín, F., & Gelcich, S. (2021). Multi-Criteria Decision Analysis for Renewable Energies: Research Trends, Gaps and the Challenge of Improving Participation. *Sustainability*, *13*(6), 3515.

Estévez, R. A., & Gelcich, S. (2015). Participative multi-criteria decision analysis in marine management and conservation: Research progress and the challenge of integrating value judgments and uncertainty. *Marine Policy*, *61*, 1-7.

E.U. CMEMS, 2020. Retrieved November 10, 2020, from https://resources.marine.copernicus.eu/?option=com_csw&view=details&product_id=GLOBAL_REANALYSIS_PHY_001_030

European Commission (2017). Retrieved 1 MArch 2021 from https://ec.europa.eu/energy/sites/ener/files/documents/swd2017_61_document_travail_service_part1_v6.pdf

Eurostat (2018), Electricity price statistics - Statistics Explained, European Commission. Retrieved 10 March,2021 from http://ec.europa.eu/eurostat/statistics-explained/index.php?title=Electricity_price_statistics

Fatemi, M., & Rezaei-Moghaddam, K. (2019). Multi-criteria evaluation in paradigmatic perspectives of agricultural environmental management. *Heliyon*, *5*(2), e01229.

Faye, S., Lazar, A., Sow, B. A., Gaye, A. T. (2015). A model study of the seasonality of sea surface temperature and circulation in the Atlantic North-eastern Tropical Upwelling System. *Frontiers in Physics*, *3*(September), 1–20.

Faraji, F., Majazi, A., & Al-Haddad, K. (2017). A comprehensive review of flywheel energy storage system technology. *Renewable and Sustainable Energy Reviews*, *67*, 477-490.

Fernandes, M. J., Lázaro, C., Santos, A. M. P., Oliveira, P. (2005). Oceanographic characterisation of the Cabo Verde region using multisensor data. *Proceedings of the ENVISAT and ERS Symposium, Salzburg, 6–10 September* 2004.

Fernandez, E., & Lellouche, J. M. (2018). Product User Manual for the Global Ocean Physical Reanalysis product GLOBAL_REANALYSIS_PHY_001_030. Report CMEMS-GLO-PUM, (001-030), 15.

Fiedler, B., Grundle, D. S., Schütte, F., Karstensen, J., Löscher, C. R., Hauss, H., … Körtzinger, A. (2016). Oxygen utilization and downward carbon flux in an oxygen-depleted eddy in the eastern tropical North Atlantic. *Biogeosciences*, *13*(19), 5633–5647.

Frantantoni, D.M. (2001). North Atlantic surface circulation during the 1990s observed with satellite-tracked drifters. *Journal of Geophysical Research* 106, 22067–22093.

Freeport LNG. The Freeport LNG project, 2014. Available at: www.freeportlng.com.

Fyke, A. (2019). The fall and rise of gravity storage technologies. *Joule*, *3*(3), 625-630.

GEBCO Bathymetric Compilation Group 2019 (2019). The GEBCO_2019 Grid - a continuous terrain model of the global oceans and land. British Oceanographic Data Centre, National Oceanography Centre, NERC, UK. doi:10/c33m. doi:10.5285/836f016a-

33be-6ddc-e053-6c86abc0788e
https://www.gebco.net/data_and_products/gridded_bathymetry_data/gebco_2020/

Geometrica. Coal storage domes, 2008. Available at: Available from: www.geometrica.com.

Gesto Energy. (2011). 50% Renewable Cape Verde Renewable Action Plan. http://gestoenergy.com/en/project/50-renewable-cape-verde-renewable-action-plan/ Global CCS Institute (2015). Cape Verde.

Gomes, N., Neves, R., Kenov, I. A., Campuzano, F. J., & Pinto, L. (2015). Tide and tidal currents in the Cape Verde Archipelago. *Revista de Gestão Costeira Integrada-Journal of Integrated Coastal Zone Management*, *15*(3), 395-408.

GOPA International Energy Consultants, "Mali - Support Project to the Energy Sector (PASE): Consulting Services for Preparatory Studies for the Implementation of the 'Energy Efficiency and Demand-Side Management,' Component," http://www.gopa-intec.de/Mali-Support- Project-to-the-Energy-Sec.1694.0.html, viewed 14 April 2014.

Gravitricity. (n.d.). *Fast, long-life energy storage*. Retrieved March 10, 2021, from https://gravitricity.com/technology/ .

Gravitypower, 2011.Gravity Power Module. Energy Storage. Grid-Scale Energy Storage. Available at: http://www.gravitypower.net/

Greaves, D. (2018). Epilogue: The Future of Wave and Tidal Energy. *Wave and Tidal Energy*, 659-661.

Gregory, R., & Keeney, R. L. (1994). Creating policy alternatives using stakeholder values. *Management Science*, *40*(8), 1035-1048.

Gregory, R., Failing, L., Harstone, M., Long, G., McDaniels, T., & Ohlson, D. (2012). *Structured decision making: a practical guide to environmental management choices*. John Wiley & Sons.

Guezgouz, M., Jurasz, J., Bekkouche, B., Ma, T., Javed, M. S., & Kies, A. (2019). Optimal hybrid pumped hydro-battery storage scheme for off-grid renewable energy systems. *Energy Conversion and Management*, *199*, 112046.

Guney, M. S., & Tepe, Y. (2017). Classification and assessment of energy storage systems. *Renewable and Sustainable Energy Reviews*, *75*, 1187-1197.

Guo, H., Xu, Y., Chen, H., & Zhou, X. (2016). Thermodynamic characteristics of a novel supercritical compressed air energy storage system. *Energy conversion and management*, *115*, 167-177.

Gür, T. M. (2018). Review of electrical energy storage technologies, materials and systems: challenges and prospects for large-scale grid storage. *Energy & Environmental Science*, *11*(10), 2696-2767.

Hai Alami, A. (2014). Analytical and experimental evaluation of energy storage using work of buoyancy force. *Journal of Renewable and Sustainable Energy*, *6*(1), 013137.

Hall, C. A., & Klitgaard, K. A. (2011). *Energy and the wealth of nations: understanding the biophysical economy*. Springer Science & Business Media.

Hamedi, A.S., & Sadeghzadeh, S. (2017). Conceptual design of a 5 MW OTEC power plant in the Oman Sea. *Journal of Marine Engineering and Technology*, 16(2), 94-102. https://doi.org/10.1080/20464177.2017.1320839.

Harper, M., Anderson, B., James, P., & Bahaj, A. (2019). Assessing socially acceptable locations for onshore wind energy using a GIS-MCDA approach. *International Journal of Low-Carbon Technologies*, *14*(2), 160-169.

Heck, P., Knaus, M., Flesch, F., Grabowski, M., Keller, T., Martinez, J., & Synwoldt, C. (2013). Cape Verde 100% Renewable: a roadmap to 2020 - development of energy optimization strategies for Cape Verde. Institute for Applied Material Flow Management

Hendl Energy. (n.d.). *A new solution for large scale energy storage.* Retrieved from https://heindl-energy.com/

Heindl, E. (2014). Hydraulic Hydro Storage system for self-sufficient cities. *Energy Procedia*, *46*, 98-103.

Hersbach, H., Bell, B., Berrisford, P., Biavati, G., Horányi, A., Muñoz Sabater, J., Nicolas, J., Peubey, C., Radu, R., Rozum, I., Schepers, D., Simmons, A., Soci, C., Dee, D., Thépaut, J-N. (2018): ERA5 hourly data on single levels from 1979 to present. Copernicus Climate Change Service (C3S) Climate Data Store (CDS). (Accessed on < 10-05-2021 >), 10.24381/cds.adbb2d47.

Hersbach, H., & Dee, D. J. E. N. (2016). ERA5 reanalysis is in production. *ECMWF newsletter*, *147*(7), 5-6.

Heywood, K. J., Barton, E. D., Simpson, J. H. (1990). The effects of flow disturbance by an oceanic island. *Journal of Marine Research*, *48*, 55–73.

Hove, K. (2018). Cabeolica annual report 2017. Cabeolica. http://www.cabeolica.coms-1ite1/about-us/annual-reports/

Hsueh, J. T., & Lin, C. Y. (2015). Constructing a network model to rank the optimal strategy for implementing the sorting process in reverse logistics: case study of photovoltaic industry. *Clean Technologies and Environmental Policy*, *17*(1), 155-174.

Htut, A. Y., Shrestha, S., Nitivattananon, V., & Kawasaki, A. (2014). Forecasting climate change scenarios in the Bago River Basin, Myanmar. *J. Earth Sci. & Clim. Change*, *5*(9).

Huang, I. B., Keisler, J., & Linkov, I. (2011). Multi-criteria decision analysis in environmental sciences: Ten years of applications and trends. *Science of the total environment*, *409*(19), 3578-3594.

Huang, Y., Keatley, P., Chen, H. S., Zhang, X. J., Rolfe, A., & Hewitt, N. J. (2018). Techno-economic study of compressed air energy storage systems for the grid integration of wind power. *International Journal of Energy Research*, *42*(2), 559-569.

Huckerby, J., Jeffrey, H., de Andres, A. and Finlay, L., 2016. An International Vision for Ocean Energy. Version III. Published by the Ocean Energy Systems Technology Collaboration Programme: www.ocean-energy-systems.org.

Huisman. (2018, March 21). *Gravitricity teams up with worldwide lifting, drilling and subsea specialists Huisman to build prototype energy store*. Retrieved February 23, 2021, from https://www.huismanequipment.com/

Hussain, A., Arif, S. M., & Aslam, M. (2017). Emerging renewable and sustainable energy technologies: State of the art. *Renewable and Sustainable Energy Reviews*, *71*, 12-28.

Ibrahim, H., Ilinca, A., & Perron, J. (2008). Energy storage systems—Characteristics and comparisons. *Renewable and sustainable energy reviews*, *12*(5), 1221-1250.

Instituto Nacional de Estatistica (2016). Projecções demográficas da população por concelho e faixa etária, 2010-2030. http://ine.cv/quadros/resumo-das-projeccoes-demograficas-da-populacao-concelho-2010-2030/

International Energy Agency, I. E. A., and World Bank. (2014). *Sustainable Energy for All 2013-2014: Global Tracking Framework Report*. The World Bank.

International Monetary Fund (IMF). IMF Country Information. Available online: https://www.imf.org/en/ Countries (accessed on 1 June 2019).

IPCC, 2017: Meeting Report of the Intergovernmental Panel on Climate Change Expert Meeting on Mitigation, Sustainability and Climate Stabilization Scenarios. [Shukla, P.R., J. Skea, R. Diemen, E. Huntley, M. Pathak, J. PortugalPereira, J. Scull, and R. Slade (eds.)]. IPCC Working Group III Technical Support Unit, Imperial College London, London, UK, 44 pp.

IRENA (International Renewable Energy Agency). (2016). The Power to Change: Solar and Wind Cost Reduction Potential to 2025.

Jia, Y., Calil, P. H. R., Chassignet, E. P., Metzger, E. J., Potemra, J. T., Richards, K. J., & Wallcraft, A. J. (2011). Generation of mesoscale eddies in the lee of the Hawaiian Islands. *Journal of Geophysical Research: Oceans*, *116*(C11).

Jiménez, B., Sangrà, P., Mason, E. (2008). A numerical study of the relative importance of wind and topographic forcing on oceanic eddy shedding by tall, deep water islands. *Ocean Modelling* (Vol. 22).

Jonathan, R. (2013). Energy storage technologies. *Ingenia*, *2013*, 27-32.

Joint Research Centre (2012). Photovoltaic Geographical Information System (PVGIS). http://re.jrc.ec.europa.eu/pvgis/apps4/pvest.php?lang=en&map=africa

Karstensen, J., Fiedler, B., Schütte, F., Brandt, P., Körtzinger, A., Fischer, G., ... Wallace, D. W. (2015). Open ocean dead-zone in the tropical North Atlantic Ocean. *Biogeosciences (BG), 12(8),* 2597-2605.

Keeney, R. L., & Gregory, R. S. (2005). Selecting attributes to measure the achievement of objectives. *Operations Research*, *53*(1), 1-11.

Kelso, N. V., & Patterson, T. (2010). Introducing natural earth data-naturalearthdata. com. *Geographia Technica*, *5*(82-89), 25.

Khan, N., Kalair, A., Abas, N., & Haider, A. (2017). Review of ocean tidal, wave and thermal energy technologies. *Renewable and Sustainable Energy Reviews*, *72*, 590-604.

Kim, S., Usman, M., Park, C., & Hanif, A. (2021). Durability of slag waste incorporated steel fiber-reinforced concrete in marine environment. *Journal of Building Engineering*, *33*, 101641.

Klar, R., Steidl, B., Sant, T., Aufleger, M., & Farrugia, R. N. (2017). Buoyant Energy—Balancing wind power and other renewables in Europe's oceans. *Journal of Energy Storage*, *14*, 246-255.

Kostianoy, A. G. and Zatsepin, A. G. (1996). The West African coastal upwelling filaments and cross-frontal water exchange conditioned by them. *Journal of Marine Systems*, *7*(2–4), 349–359. https://doi.org/10.1016/0924-7963(95)00029-1.

Kousksou, T., Bruel, P., Jamil, A., El Rhafiki, T., & Zeraouli, Y. (2014). Energy storage: Applications and challenges. *Solar Energy Materials and Solar Cells*, *120*, 59-80.

Koyuncu, D. (2007). *Inquiry into the underwater structures: architectural approaches to design considerations* (Master's thesis, Middle East Technical University).

Krishan, O., & Suhag, S. (2019). An updated review of energy storage systems: Classification and applications in distributed generation power systems incorporating renewable energy resources. *International Journal of Energy Research*, *43*(12), 6171-6210.

Lange, C. B., Romero, O. E., Wefer, G., Gabric, A. J. (1998). Offshore influence of coastal upwelling off Mauritania, NW Africa, as recorded by diatoms in sediment traps at 2195 m water depth. *Deep-Sea Research Part I: Oceanographic Research Papers*, *45*(6), 985–1013.

Lázaro, C., Fernandes, M. J., Santos, A. M. P., Oliveira, P. (2005). Seasonal and interannual variability of surface circulation in the Cabo Verde region from 8 years of merged T/P and ERS-2 altimeter data. *Remote Sensing of Environment*, *98*(1), 45–62.

Le Bas, T.P.; Masson, D.G.; Holtom, R.T.; Grevemeyer, I.. 2007. Slope failures of the flanks of the southern Cape Verde Islands. In: Lykousis, V.; Sakellariou, D.; Locat, J., (eds.) Submarine mass movements and their consequences: 3rd International Symposium. Dordrecht, Netherlands, Springer, 337-345, 424pp. (Advances in Natural and Technological Hazards Research, 27).

Lellouche, J. M., Bourdalle-Badie, R., Greiner, E., Garric, G., Melet, A., Bricaud, C., ... & Drevillon, M. (2021, April). The Copernicus global 1/12° oceanic and sea ice reanalysis. In *EGU General Assembly Conference Abstracts* (pp. EGU21-14961).

Lellouche, J. M., Greiner, E., Le Galloudec, O., Garric, G., Regnier, C., Drevillon, M., ... & Le Traon, P. Y. (2018). Recent updates to the Copernicus Marine Service global ocean monitoring and forecasting real-time 1⁄ 12° high-resolution system. *Ocean Science*, *14*(5), 1093-1126.

Letcher, T. M., Law, R., & Reay, D. (2016). *Storing energy: with special reference to renewable energy sources* (Vol. 86). Amsterdam: Elsevier.

Lewis, A.; Estefen, S.; Huckerby, J.; Lee, K.S.; Musial,W.; Pontes, T.; Torres-Martinez, J. Ocean energy. In IPCC Special Report on Renewable Energy Sources and Climate Change Mitigation; Edenhofer, O., Pichs-Madruga, R., Sokona, Y., Seyboth, K., Matschoss, P., Kadner, S., Zwickel, T., Eickemeie, P., Hansen, G., Schlömer, S., *et al*., Eds.; Cambridge University Press: Cambridge, UK; New York, NY, USA, 2011; pp. 497–534.

Li, J., Zhang, R., Liu, C., & Fan, H. (2012). Modeling of ocean mesoscale eddy and its application in the underwater acoustic propagation.

Li, X., Anvari, B., Palazzolo, A., Wang, Z., & Toliyat, H. (2017). A utility-scale flywheel energy storage system with a shaftless, hubless, high-strength steel rotor. *IEEE Transactions on Industrial Electronics*, *65*(8), 6667-6675.

Löscher, C. R., Fischer, M. A., Neulinger, S. C., Fiedler, B., Philippi, M., Schütte, F., … Schmitz, R. A. (2015). Hidden biosphere in an oxygen-deficient Atlantic open-ocean eddy: Future implications of ocean deoxygenation on primary production in the eastern tropical North Atlantic. *Biogeosciences*, *12*(24), 7467–7482.

Lovell J. (2013). Biofuels: Europe's 2nd-biggest coal-fired power plant will turn to wood from North America. E & E Publishing, LLC. Available at: Available from: www.eenews.net.

Lund, P. D., Lindgren, J., Mikkola, J., & Salpakari, J. (2015). Review of energy system flexibility measures to enable high levels of variable renewable electricity. *Renewable and sustainable energy reviews*, *45*, 785-807.

Luo, X., Wang, J., Dooner, M., & Clarke, J. (2015). Overview of current development in electrical energy storage technologies and the application potential in power system operation. *Applied energy*, *137*, 511-536.

Luo, X., Wang, J., Krupke, C., Wang, Y., Sheng, Y., Li, J., ... & Chen, H. (2016). Modelling study, efficiency analysis and optimisation of large-scale Adiabatic Compressed Air Energy Storage systems with low-temperature thermal storage. *Applied energy*, *162*, 589-600.

Luomi, M. (2014). Sustainable Energy in Brazil–Reversing Past Achievements or Realizing Future Potential.

LUSA. (2021, October 7). *Cabo Verde: State plans renewable electricity production of 250 MW by 2030*. Retrieved December 04, 2021, from https://www.macaubusiness.com/cabo-verde-state-plans-renewable-electricity-production-of-250-mw-by-2030/

Mahdy, M., & Bahaj, A. S. (2018). Multi criteria decision analysis for offshore wind energy potential in Egypt. *Renewable energy*, *118*, 278-289.

Mahlia, T. M. I., Saktisahdan, T. J., Jannifar, A., Hasan, M. H., & Matseelar, H. S. C. (2014). A review of available methods and development on energy storage; technology update. *Renewable and sustainable energy reviews*, *33*, 532-545.

Mahmoud, M., Ramadan, M., Olabi, A. G., Pullen, K., & Naher, S. (2020). A review of mechanical energy storage systems combined with wind and solar applications. *Energy Conversion and Management*, *210*, 112670.

Marcello, J., Hernández-Guerra, A., Eugenio, F., Fonte, A. (2011). Seasonal and temporal study of the northwest African upwelling system. *International Journal of Remote Sensing*, *32*(7), 1843–1859.

Mardiana, A., & Riffat, S. B. (2015). Building Energy Consumption and Carbon dioxide Emissions: Threat to Climate Change. J Earth Sci Climat Change S3: 001. doi: 10.4172/2157-7617. S3-001 Page 2 of 3 J Earth Sci Climat Change ISSN: 2157-7617

JESCC, an open access journal Environmental Challenges of energy consumption in buildings which is more than 60% of total consumption [21, 22]. Whilst, lighting accounts for approximately 11 to 20% of total building energy demand [17]. In the UK, energy consumption for space heating contributes to about .... *China, the air-conditioning and heating system account for, 65*.

Marques Antonio Cardoso. (2018) Challenges, public intervention and demand management of electricity. Energy economics, first ed.. Silabo, Editions.

Marrasso, E., Roselli, C., & Sasso, M. (2019). Electric efficiency indicators and carbon dioxide emission factors for power generation by fossil and renewable energy sources on hourly basis. *Energy Conversion and Management*, *196*, 1369-1384.

Masutani, S. M., & Takahashi, P. K. (2001). Ocean thermal energy conversion (OTEC). Oceanography, 22(609), 625.

Masson, D. G., Le Bas, T. P., Grevemeyer, I., & Weinrebe, W. (2008). Flank collapse and large-scale landsliding in the Cape Verde Islands, off West Africa. *Geochemistry, Geophysics, Geosystems*, *9*(7).

Melikoglu, M. (2018). Current status and future of ocean energy sources: A global review. *Ocean Engineering*, *148*, 563-573.

Meunier, T., Barton, E. D., Barreiro, B., Torres, R. (2012). Upwelling filaments off cap blanc: Interaction of the NW African upwelling current and the Cape Verde frontal zone eddy field? *Journal of Geophysical Research: Oceans*, *117*(8), 1–18.

MGH (2015)– *Deep Sea Energy Storage*. Retrieved March 2021 from: http://www.mgh-energy.com/ .

Mittelstaedt, E. (1983). The upwelling area off Northwest Africa - A description of phenomena related to coastal upwelling. *Progress in Oceanography*, *12*(3), 307–331.

Mittelstaedt, E. (1991). The ocean boundary along the northwest African coast: Circulation and oceanographic properties at the sea surface. *Progress in Oceanography*, *26*(4), 307– 355.

Mofor, L., Goldsmith, J., & Jones, F. (2014). Ocean energy: Technology readiness, patents, deployment status and outlook. *Abu Dhabi*.

Mork, G., Barstow, S., Kabuth, A., & Pontes, M. T. (2010, January). Assessing the global wave energy potential. In *International Conference on Offshore Mechanics and Arctic Engineering* (Vol. 49118, pp. 447-454).

Morstyn, T., Chilcott, M., & McCulloch, M. D. (2019). Gravity energy storage with suspended weights for abandoned mine shafts. *Applied Energy*, *239*, 201-206.

Mukhedkar, R. (2019). Technology Choices for an Evolving Power System.

Nakagawa, T (2013). 3 impressive storage tank facilities. Castagra, Nevada (USA)

Natural Earth (2021). Retrieved January 30, 2021, from www.naturalearthdata.com

Nielsen, P. (2009)Coastal and Estuarine Processes. Advanced Serieson Ocean Engineering, vol. 29, World Scientific, Singapore.

Nihous, G. C. (2007). A preliminary assessment of ocean thermal energy conversion resources.

Nikolaidis, P., & Poullikkas, A. (2017). A comparative review of electrical energy storage systems for better sustainability. *Journal of power technologies*.

NOAA National Centers for Environmental Information. 2004: Multibeam Bathymetry Database (MBBDB). NOAA National Centers for Environmental Information. https://doi.org/doi:10.7289/V56T0JNC. Accessed [01/04/2021].

Nordman, E., Barrenger, A., Crawford, J., McLaughlin, J., & Wilcox, C. (2019). Options for achieving Cape Verde's 100% renewable electricity goal: a review. *Island Studies Journal*, *14*(1).

Nye, J. S. (2011). The future of power. Public Affairs.

Okokpujie, I. P., Okonkwo, U. C., Bolu, C. A., Ohunakin, O. S., Agboola, M. G., & Atayero, A. A. (2020). Implementation of multi-criteria decision method for selection of suitable material for development of horizontal wind turbine blade for sustainable energy generation. *Heliyon*, *6*(1), e03142.

OES (2020), Ocean Energy in Islands and Remote Coastal Areas: Opportunities and Challenges. IEA Technology Collaboration Programme for Ocean Energy Systems, www.ocean-energy-systems.org

Ozdemir, E., Ozdemir, S., Erhan, K., & Aktas, A. (2016, March). Energy storage technologies opportunities and challenges in smart grids. In *2016 International Smart Grid Workshop and Certificate Program (ISGWCP)* (pp. 1-6). IEEE.

Øvergaard, S. (2008). Issue paper: Definition of primary and secondary energy. *Statistics Norway, Oslo*.

Pardo, P., Deydier, A., Anxionnaz-Minvielle, Z., Rougé, S., Cabassud, M., & Cognet, P. (2014). A review on high temperature thermochemical heat energy storage. *Renewable and Sustainable Energy Reviews*, *32*, 591-610.

Pena-Alzola, R., Sebastián, R., Quesada, J., & Colmenar, A. (2011, May). Review of flywheel based energy storage systems. In *2011 International Conference on Power Engineering, Energy and Electrical Drives* (pp. 1-6). IEEE.

Perruche, C., Hameau, A., Paul, J., Régnier, C., & Drévillon, M. (2016). Quality Information Document (CMEMS-GLO-QUID-001-014).

Pérez-Rodríguez, P., Pelegrí, J. L., Marrero-Díaz, A. (2001). Dynamical characteristics of the Cape Verde frontal zone. *Scientia Marina*, 65(S1), 241–250.

Pickard, W. F. (2011). The history, present state, and future prospects of underground pumped hydro for massive energy storage. *Proceedings of the IEEE*, *100*(2), 473-483.

Plebmann, G., Erdmann, M., Hlusiak, M., & Breyer, C. (2014). Global energy storage demand for a 100% renewable electricity supply. *Energy Procedia*, *46*, 22-31.

Ramalho, R. A. S. (2011). The Cabo Verde archipelago. In *Building the Cabo Verde Islands*. Berlin, Heidelberg: Springer Berlin Heidelberg, pp. 13–26.

Ranaboldo, M., Lega, B. D., Ferrenbach, D. V., Ferrer-Martí, L., Moreno, R. P., & García-Villoria, A. (2014). Renewable energy projects to electrify rural communities in Cape Verde. *Applied energy*, *118*, 280-291.

REEEP (2012) Country Profile: Cape Verde Vienna Renewable Energy and Energy Efficiency Partnership (REEEP).

Rehman, S., Al-Hadhrami, L. M., & Alam, M. M. (2015). Pumped hydro energy storage system: A technological review. *Renewable and Sustainable Energy Reviews*, *44*, 586-598.

Reiche, K., Hille, G., Mayer-Tasch, L., Sokona, M.Y., & Semedo, E. (2017). *Cabeólica Wind Project, Cabo Verde: case study RE flagship projects in the ECOWAS Region*. http://www.ecowrex.org/document/cabeolica-wind-project-cabo-verde-case-study-re-flagship-projects-ecowas-region.

Ren, G., Liu, J., Wan, J., Guo, Y., & Yu, D. (2017). Overview of wind power intermittency: Impacts, measurements, and mitigation solutions. *Applied Energy*, *204*, 47-65.

Republic of Cabo Verde (2016). Intended nationally determined contribution of Cape Verde. https://www4.unfccc.int/sites/ndcstaging/Pages/Home.aspx

Ressurreição, A., Gibbons, J., Dentinho, T. P., Kaiser, M., Santos, R. S., & Edwards-Jones, G. (2011). Economic valuation of species loss in the open sea. *Ecological Economics*, *70*(4), 729-739.

Richardson, P. L. (1983). Eddy kinetic energy in the North Atlantic from surface drifters. *Journal of Geophysical Research: Oceans*, *88*(C7), 4355-4367.

Römer, B., Reichhart, P., Kranz, J., & Picot, A. (2012). The role of smart metering and decentralized electricity storage for smart grids: The importance of positive externalities. *Energy Policy*, *50*, 486-495.

Ruoso, A. C., Caetano, N. R., & Rocha, L. A. O. (2019). Storage gravitational energy for small scale industrial and residential applications. *Inventions*, *4*(4), 64.

Rusu, E., & Soares, C. G. (2009). Numerical modelling to estimate the spatial distribution of the wave energy in the Portuguese nearshore. *Renewable Energy*, *34*(6), 1501-1516.

Saaty, T. L. (1980). The Analytic Hierarchy Process: Planning, Priority Setting, Resource Allocation: McGraw-Hill. *New York*.

Saaty, T. L. (2008). Decision making with the analytic hierarchy process. *International journal of services sciences*, *1*(1), 83-98.

Sandru, O. (2012). Gravel energy storage system funded by Bill Gates. *Green Optimist*. Available online: www.greenoptimistic.com (accessed on 1 July 2019).

Sawin, J. L., Sverrisson, F., Rutovitz, J., Dwyer, S., Teske, S., Murdock, H. E., ... & Arris, L. (2018). Renewables 2018-Global status report. A comprehensive annual overview of the state of renewable energy. Advancing the global renewable energy transition-Highlights of the REN21 Renewables 2018 Global Status Report in perspective.

SBC (2011). SBC energy institute analysis based on US DOE energy storage program planning document.

Schüth F. Energy storage strategies. In: Schlögl R, editor. Chemical energy storage. Göttingham (Berlin): Hubert & Co. GmbH & Co. KG; 2013. p. 35–47.

Schütte, F., Brandt, P., Karstensen, J. (2016a). Occurrence and characteristics of mesoscale eddies in the tropical northeastern Atlantic Ocean. *Ocean Science*, *12*(3), 663–685.

Schütte, F., Karstensen, J., Krahmann, G., Hauss, H., Fiedler, B., Brandt, P., … Körtzinger, A. (2016b). Characterization of "dead-zone" eddies in the eastern tropical North Atlantic. *Biogeosciences*, *13*(20), 5865–5881.

Sebastián, R., and Alzola, R. P. (2012). Flywheel energy storage systems: Review and simulation for an isolated wind power system. *Renewable and Sustainable Energy Reviews*, *16*(9), 6803-6813.

Secretariat, E. C. R. E. E. E. (2011). Summary of Cape Verde Renewable Energy Plan.

Secretariat of the Pacific Applied Geoscience Commission (2009). A SOPAC Desktop Study of Ocean-Based Renewable Energy Technologies. SOPAC Community Lifelines Programme.

Segurado, R., Krajačić, G., Duić, N., & Alves, L. (2011). Increasing the penetration of renewable energy resources in S. Vicente, Cape Verde. *Applied energy*, *88*(2), 466-472.

Segurado, R., Costa, M., Duić, N., & Carvalho, M. G. (2015). Integrated analysis of energy and water supply in islands. Case study of S. Vicente, Cape Verde. *Energy*, *92*, 639-648.

Sgobbi, A., Simoes, S. G., Magagna, D., & Nijs, W. (2016). Assessing the impacts of technology improvements on the deployment of marine energy in Europe with an energy system perspective. *Renewable Energy*, *89*, 515-525.

Shadman, M., Silva, C., Faller, D., Wu, Z., de Freitas Assad, L. P., Landau, L., ... & Estefen, S. F. (2019). Ocean renewable energy potential, technology, and deployments: A case study of Brazil. Energies, 12(19), 3658.

Siedler, G., Zangenberg, N., Onken, R. (1992). Seasonal changes in the tropical Atlantic circulation - observation and simulation of the Guinea Dome. *Journal of Geophysical Research-Oceans*, *97*(C1), 703–715.

Singh, Shakti; Singh, Mukesh; Kaushik, Subhash Chandra (2016). *Feasibility study of an islanded microgrid in rural area consisting of PV, wind, biomass and battery energy storage system. Energy Conversion and Management, 128(), 178–190.* doi:10.1016/j.enconman.2016.09.046.

SInkFloatSolutions. (n.d.). *A sustainable future with intermittent solutions*. Retrieved from Our Technology: http://sinkfloatsolutions.com/our-technology/

Slocum, A. H., Fennell, G. E., Dundar, G., Hodder, B. G., Meredith, J. D., & Sager, M. A. (2013). Ocean renewable energy storage (ORES) system: Analysis of an undersea energy storage concept. *Proceedings of the IEEE*, *101*(4), 906-924.

Soares C. 2002. Tidal power: The next wave of electricity. Pollution Engineering 34(7),6–9.

Soukissian, T. H., Denaxa, D., Karathanasi, F., Prospathopoulos, A., Sarantakos, K., Iona, A., & Mavrakos, S. (2017). Marine renewable energy in the Mediterranean Sea: status and perspectives. Energies, 10(10), 1512.

Stramma, L. and Schott, F. (1999). The mean flow field of the tropical Atlantic Ocean. *Deep Sea Research. II*, *46*(1–2), 279–303.

Stramma, L. and Siedler, G. (1988). Seasonal changes in the North Atlantic subtropical gyre. *Journal of Geophysical Research*, *93*(C7), 8111.

Stramma, L., Hüttl, S., Schafstall, J. (2005). Water masses and currents in the upper tropical northeast Atlantic off northwest Africa. *Journal of Geophysical Research: Oceans*, *110*(12), 1–18.

StratoSolar. (n.d.). *Gravity Energy Storage: Integrated with StratoSolar PV generation.* Retrieved May 2, 2021, from http://www.stratosolar.com/gravity-energy-storage.html

Succar, S., & Williams, R. H. (2008). Compressed air energy storage: theory, resources, and applications for wind power. *Princeton environmental institute report*, *8*, 81.

Syamsuddin, M. L., Attamimi, A., Nugraha, A. P., Gibran, S., Afifah, A. Q., & Oriana, N. (2015). OTEC potential in the Indonesian seas. *Energy Procedia*, *65*, 215-222.

Tan, X., Li, Q., & Wang, H. (2013). Advances and trends of energy storage technology in microgrid. *International Journal of Electrical Power & Energy Systems*, *44*(1), 179-191.

Tavares, J., Lopes, M., & Neto, F. (2020). Climate and fundamentals of the energy offer in Cape Verde. *Energy Reports*, *6*, 370-377.

Toubeau, J. F., Ponsart, C., Stevens, C., De Grève, Z., & Vallée, F. (2020). Sizing of underwater gravity storage with solid weights participating in electricity markets. *International Transactions on Electrical Energy Systems*, *30*(10), e12549.

Tozer, B, Sandwell, D. T., Smith, W. H. F., Olson, C., Beale, J. R., & Wessel, P. (2019). Global bathymetry and topography at 15 arc sec: SRTM15+. Earth and Space Science. 6. https://doi.org/10.1029/2019EA00065.

Uehara H, Ikegami Y (1990) Optimization of a closed-cycle OTEC system. J Sol Energy Eng 112:247–256

UNEP, A. (2017). Atlas of Africa energy resources. *United Nations Environment Programme, Nairobi*.

UNIDO; ECREE (n.d.). ECOWAS Centre for Renewable Energy and Energy Efficiency. CAPE VERDE : ENERGY ANALYSIS AND RECOMMENDATION. Retrieved January 3, 2015, from http://www.ecreee.org/sites/default/files/unido-ecreee_report_on_cape_verde.pdf

Union, I. (2014). Communication from the Commission to the European Parliament, the Council, the European Economic and Social Committee and the Committee of the Regions. *A new skills agenda for europe. Brussels*.

Van Camp, L., Nykjaer, L., Mittelstaedt, E., Schlittenhardt, P. (1991). Upwelling and boundary circulation off Northwest Africa as depicted by infrared and visible satellite observations. *Progress in Oceanography*, *26*(4), 357–402.

Varela-Lopes, G. E. and Molion, L. C. B. (2014). Precipitation Patterns in Cabo Verde Islands: Santiago Island Case Study. *Atmospheric and Climate Sciences*, *4*(December), 854–865.

Vega, L. A., & Nihous, G. C. (1994, March). Design of a 5 MWe OTEC pre-commercial plant. In *Proceedings Oceanology International'94 Conference*.

Veigas, M., Carballo, R., & Iglesias, G. (2014). Wave and offshore wind energy on an island. *Energy for Sustainable Development*, *22*, 57-65.

Von Winterfeldt, D. and Edwards, W. (1986). Decision analysis and behavioral research. Cambridge University Press, Cambridge.

Vyawahare, M. (2015). Hawaii first to harness deep-ocean temperatures for power. Scientific American, 27 August. https://www.scientificamerican.com/article/hawaii-first-to-harness-deep-ocean-temperatures-for-power

Wang, J. J., Jing, Y. Y., Zhang, C. F., & Zhao, J. H. (2009). Review on multi-criteria decision analysis aid in sustainable energy decision-making. *Renewable and sustainable energy reviews*, *13*(9), 2263-2278.

Wang, S., Yuan, P., Li, D., & Jiao, Y. (2011). An overview of ocean renewable energy in China. *Renewable and Sustainable Energy Reviews*, *15*(1), 91-111.

Wang, Z., Ting, D. S. K., Carriveau, R., Xiong, W., & Wang, Z. (2016). Design and thermodynamic analysis of a multi-level underwater compressed air energy storage system. *Journal of Energy Storage*, *5*, 203-211.

Weinstein, A.; Fredrikson, G.; Parks, M.J.; Nielsen, K. AquaBuOY-the offshore wave energy converter numerical modeling and optimization. In Proceedings of the Oceans '04 MTS/IEEE Techno-Ocean '04, Kobe, Japan, 9–12 November 2004; pp. 1988–1995.

Wicki, S., & Hansen, E. G. (2017). Clean energy storage technology in the making: An innovation systems perspective on flywheel energy storage. *Journal of cleaner production*, *162*, 1118-1134.

WorldAtlas. (2021, Febraury 21). *Countries In Africa With The Longest Coastlines*. Retrieved from https://www.worldatlas.com/articles/countries-in-africa-with-the-longest-coastlines.html

World Bank Group. "Lighting Africa," http://lightingafrica.org/, viewed 24 April 2014.

World Bank. (2015). World Development Indicators 2015. Washington D.C.: World Bank.

World Energy Council. World energy resources—e-storage. 2016;1. http://www.worldenergy.org/wpcontent/uploads/2013/09/Complete_WER_2013_Survey.pdf

World Bank (2017). Electric power consumption (kWh per capita) 2016 https://data.worldbank.org/indicator/EG.USE.ELEC.KH.PC.

Yang, C. J., & Jackson, R. B. (2011). Opportunities and barriers to pumped-hydro energy storage in the United States. *Renewable and Sustainable Energy Reviews*, *15*(1), 839-844.

Yang, Y., Bremner, S., Menictas, C., & Kay, M. (2018). Battery energy storage system size determination in renewable energy systems: A review. *Renewable and Sustainable Energy Reviews*, *91*, 109-125.

Yang, Y., Wu, K., Long, H., Gao, J., Yan, X., Kato, T., & Suzuoki, Y. (2014). Integrated electricity and heating demand-side management for wind power integration in China. *Energy*, *78*, 235-246.

Yergin, D., Gross, S., & Meyer, N. (2013). Energy Vision 2013-Energy Transitions: Past and Future. In *World Economic Forum*.

Yoon, K. P., & Hwang, C. L. (1995). *Multiple attribute decision making: an introduction*. Sage publications.

Yoshida, S., Qiu, B., Hacker, P. (2010). Wind-generated eddy characteristics in the lee of the island of Hawaii. *Journal of Geophysical Research: Oceans*, *115*(3), 1–15.

Zakeri, B., & Syri, S. (2016). Corrigendum to "Electrical energy storage systems: A comparative life cycle cost analysis"[Renew. Sustain. Energy Rev. 42 (2015) 569–596]. *Renewable and Sustainable Energy Reviews*, *100*(53), 1634-1635.

Zavadskas, E. K., & Turskis, Z. (2011). Multiple criteria decision making (MCDM) methods in economics: an overview. *Technological and economic development of economy*, *17*(2), 397-427.

Zenk, W., Klein, B., Schroder, M. (1991). Cape Verde Frontal Zone. *Deep Sea Research Part A. Oceanographic Research Papers*, *38*, S505–S530.

Zhang, D., McPhaden, M. J., Johns, W. E. (2003). Observational Evidence for Flow between the Subtropical and Tropical Atlantic: The Atlantic Subtropical Cells. *Journal of Physical Oceanography*, *33*, 1783–1797.

Zhang, R., Zhang, S., Luo, J., Han, Y., & Zhang, J. (2019). Analysis of near-surface wind speed change in China during 1958–2015. *Theoretical and Applied Climatology*, *137*(3), 2785-2801.

Zhou, Z., Benbouzid, M., Charpentier, J. F., Scuiller, F., & Tang, T. (2013). A review of energy storage technologies for marine current energy systems. *Renewable and Sustainable Energy Reviews*, *18*, 390-400.

Appendix

Appendix 1: Cape Verde's estimated population, by island (Instituto Nacional de Estatistica, 2016)

Island	Island population (2019 est.)	Percent of total population	Percent urban (based on 2010 census)
Boa Vista	18,795	3.41	58.88
Brava	5,463	0.99	18.81
Fogo	35,015	6.36	33.40
Maio	7,351	1.34	42.91
Sal	39,696	7.21	92.49
Santiago (São Tiago)	309,633	56.25	60.82
Santo Antão	38,194	6.94	34.92
São Nicolau	12,107	2.20	44.14
São Vicente	84,229	15.30	92.65
Total	**550,483**	**100**	**61.79**

Appendix 2: Seasonal mean speed and direction for scatterometer-derived ocean winds (a–d) and currents (e–g) in the region of Cabo Verde, within the years 2003–2014. Seasons are grouped as follows: Winter (December, January, and February); Spring (March, April, and May); Summer (June, July, and August); and Autumn (September, October, November) as adapted from Cardoso, *et al* 2020.

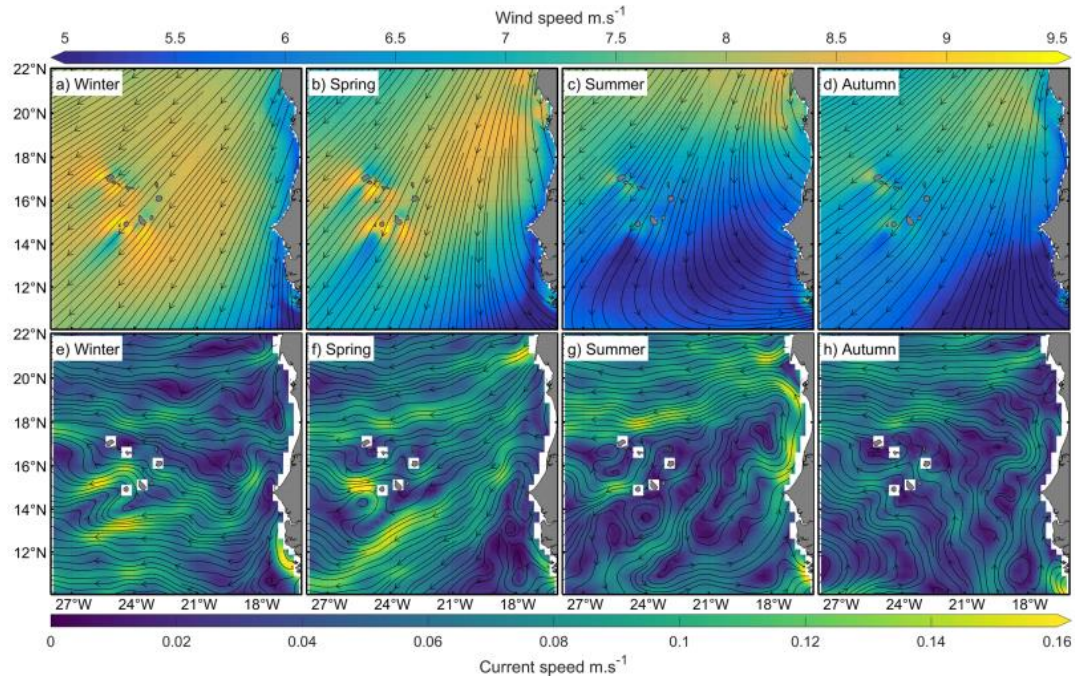

Appendix 3: Technical characteristics of some selected energy storage technologies. Adapted from Aneke and Wang 2016.

Technology	Energy density Wh/kg(Wh/L)	Power density W/kg(W/L)	Power rating	Discharge time	Suitable storage duration	Life time (years)	Cycle life (cycles)	Capital Cost			Round trip efficiency (%)	Technological maturity
								$/kW	$/kWh	$/kWh-per cycle		
Flywheel	10–30(20–80)	400–1500(1000–2000)	0–250 kW	ms–15 min	s–min	~15	20,000+	250–350	1000–5000	3–25	85–95	Commercial
PHES	0.5–1.5(0.5–1.5)		100–5000 MW	1–24 h+	h–months	40–60		600–2000	5–100	0.1–1.4	65–87	Matured
CAES	30–60(3–6)		5–300 MW	1–24 h+	h–months	20–60		400–800	2–50	2–4	50–89	Developed
GES												
GPM	1.06(1.06)	3.13(3.13)	40–150 MW		h–months	30+		1000			75–80	Concept
ARES			100–3000 MW	34 s	h–months	40+		800			75–86	Concept
HES												
Fuel cell	800–10,000(500–3000)	500+(500+)	0–50 MW	s–24+ h	h–months	5–15	1000	10,000+		6000–20,000	20–35	Developing
Gas engine	33,300(530–750)		0–50 MW	s–24+ h	h–months						40–50	Developing
Super-capacitor	2.5–15	500–5000	0–300 kW	ms–60 min	s–h			100–300	300–2000	2–20	90–95	Developed
Batteries												Commercial
NaS	150–240(150–250)	150–230	50 kW–8 MW	s–h	s–h	10–15	2500	1000–3000	300–500	8–20	80–90	Commercial
NaNiCl	100–120(150–180)	150–200(220–300)	0–300 kW	s–h	s–h	10–14	2500+	150–300	100–200	5–10	85–90	Commercial
VRB	10–30		30 kW–3 MW	s–10 h	h–months	5–10	12,000+	600–1500	150–1000	5–80	85–90	Demonstration
FeCr	10–50	16–33	5–250 kW	s12+h	h–months				250		70–80	Commercial
ZnBr	30–50(30–60)		50 kW–2 MW	s–10 h	h–months	5–10	2000+	700–2500	150–1000	5–80	70–80	Demonstration
Zn–air	150–3000(500–10,000)	100	0–10 kW	s–24h+	h–months			100–250	10–60		50–55	Demonstration
Li-ion	75–200(200–500)	500–2000	0–100 kW	min–h	min–days			1200–4000	600–2500	15–100	85–90	Demonstration
SMES	0.5–5(0.2–2.5)	500–2000(1000–4000)	100 kW–10 MW	m–8 s	min–h	20+	100,000+	200–300	1000–10,000		95–98	Demonstration
LAES	97		350 kW–5 MW	1–24 h+	h–months	20+		1000–2000			50–70	Demonstration

Note: PHES = PSH (Pumped Hydropower)

Appendix 4: Statosolar Energy storage System (Adapted from Stratosolar)

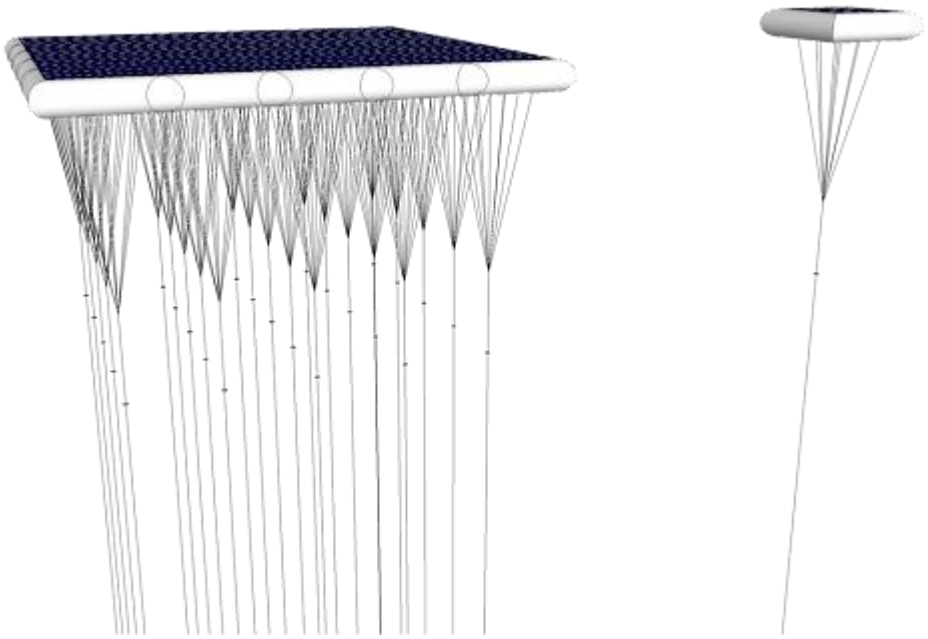

Appendix 5: Multibeam Bathymetric Data Sources

- NOAA/National Ocean Service (NOS)
- UNOLS/Rolling Deck to Repository (R2R) Program
- NOAA/Office of Exploration and Research (OER)
- Marine Geoscience Data System (MGDS - IEDA - LDEO)
- US Geological Survey (USGS)
- US Navy (NAVO)
- Scripps Institution of Oceanography (SIO)
- Woods Hole Oceanographic Institution (WHOI)
- University of New Hampshire Center for Coastal and Ocean Mapping (UNH/CCOM)
- University of Hawaii (SOEST)
- California State University at Monterey Bay Seafloor Mapping Laboratory (CSUMB/SFML)
- Geological Survey of Ireland (GSI)
- Bundesamt für Seeschiffahrt und Hydrographie (BSH)
- US Interagency Elevation Inventory

Appendix 6: Final Energy Consumption in Cabo Verde according to sources in 2018 (Data from energiasrenovaveis, 2020).

	2018	2019	2020
Thermal Production (GWh)	393	414	370.2
Total Production (GWh)	493	507	447.63
Renewable-Production (GWh)	100	93	77.43
Renewable Penetration (%)			
Cabo Verde	20.3	18.4	17.29
Santo Antao	7.8	8.6	11.7
Sao Vicente	29.4	27	25.1
Sao Nicolau	0	0	2.05
Sal	26.4	27.6	28.3
Boa Vista	21.8	18.3	21.9
Maio	0	0	4.25
Santiago	17.9	15	15.8
Fogo	0	0	4.17
Brava	0	0	0.95

Appendix 7: C02 Emission by sector (Data from Edgar 2020)

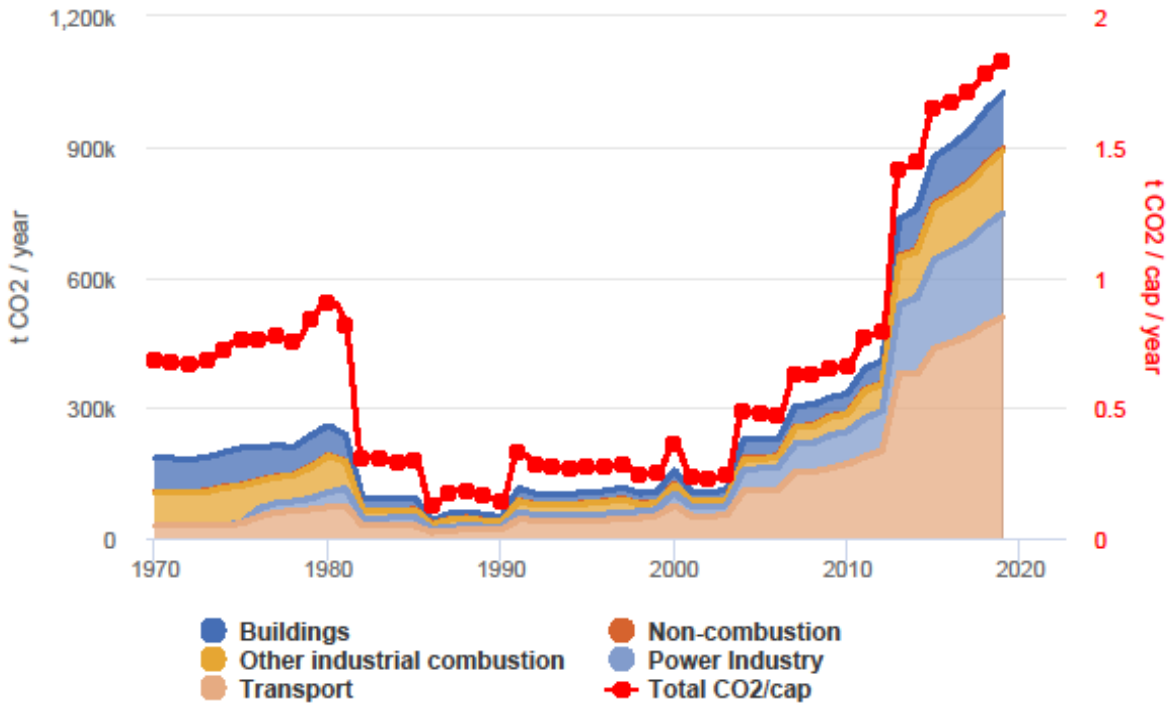

Appendix 8: Distance to the coast contoured.

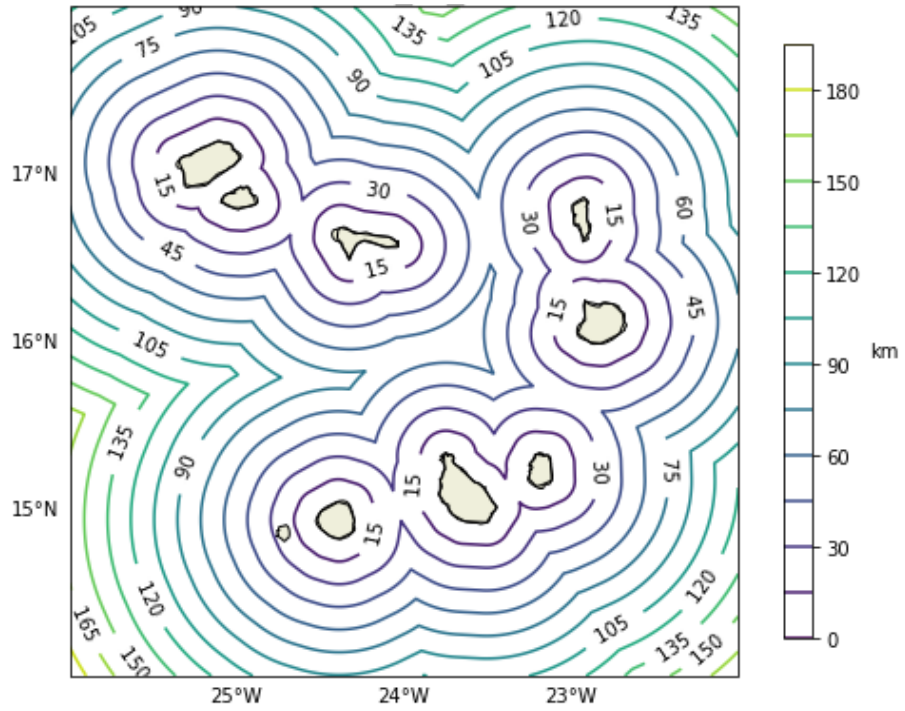

Appendix 9: 1996 to 2021 monthly variation of mean wave power (kW/m) in Cape Verde.

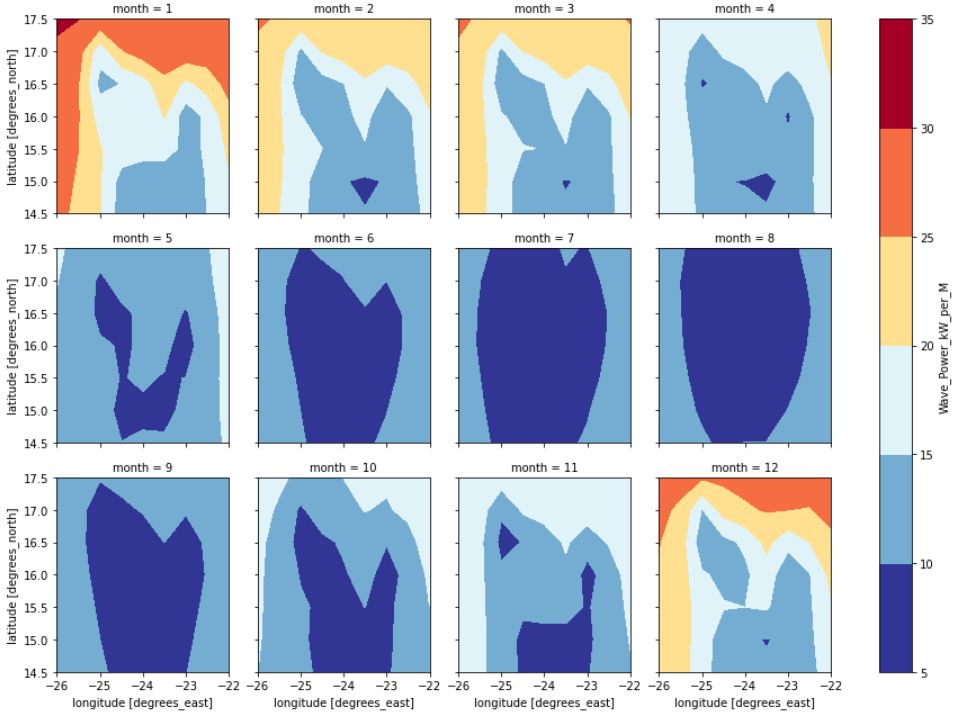

Appendix 10: 2000 – 2020 Average monthly temperature difference between the surface and 1000m depth in Cabo Verde

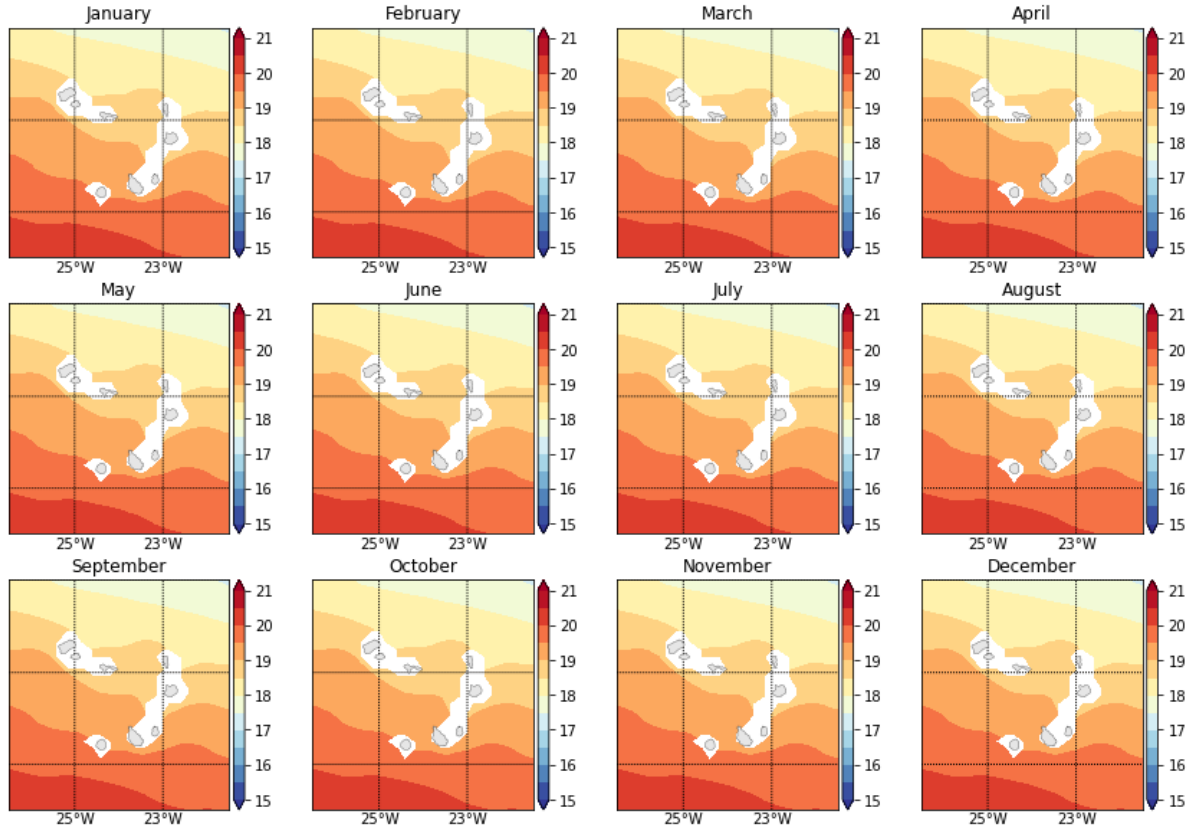

Appendix 11: One year monthly and vertical maximum of the current amplitude at the bottom (Uvmax_0)

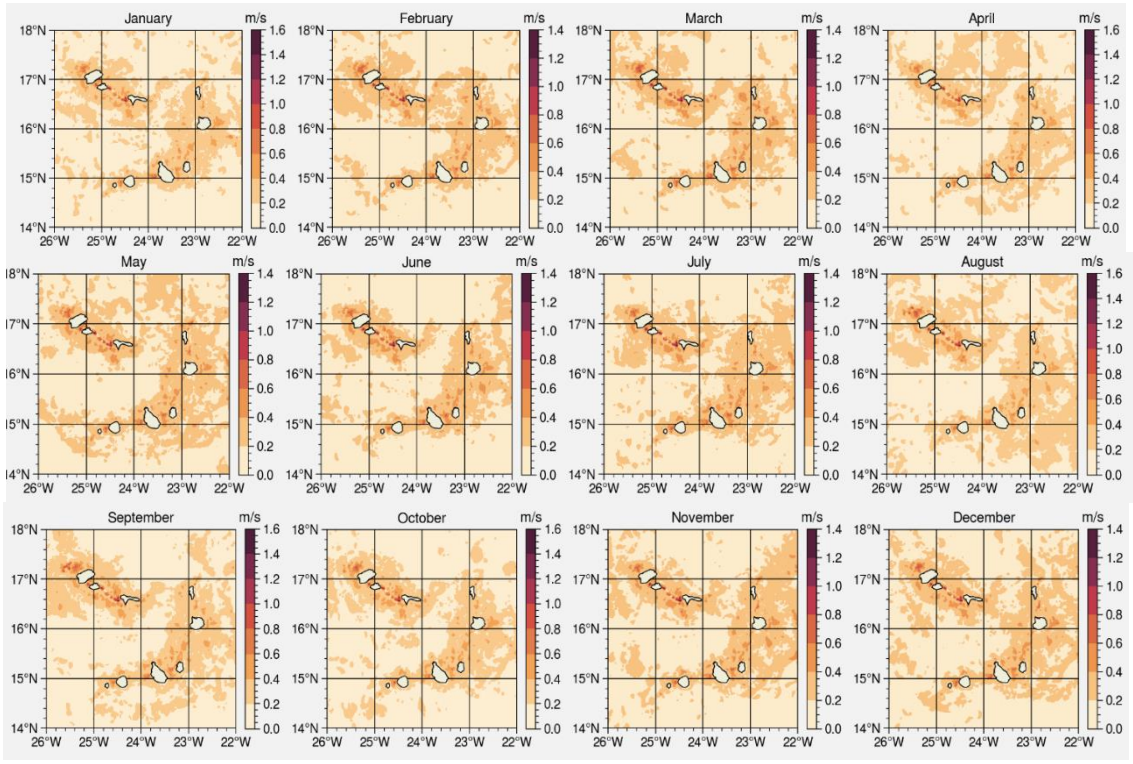

Appendix 12: MGES resource potential highlighting 5, 10, and 15 km distance from coast in red isolines and 1000m depth in black dotted line.

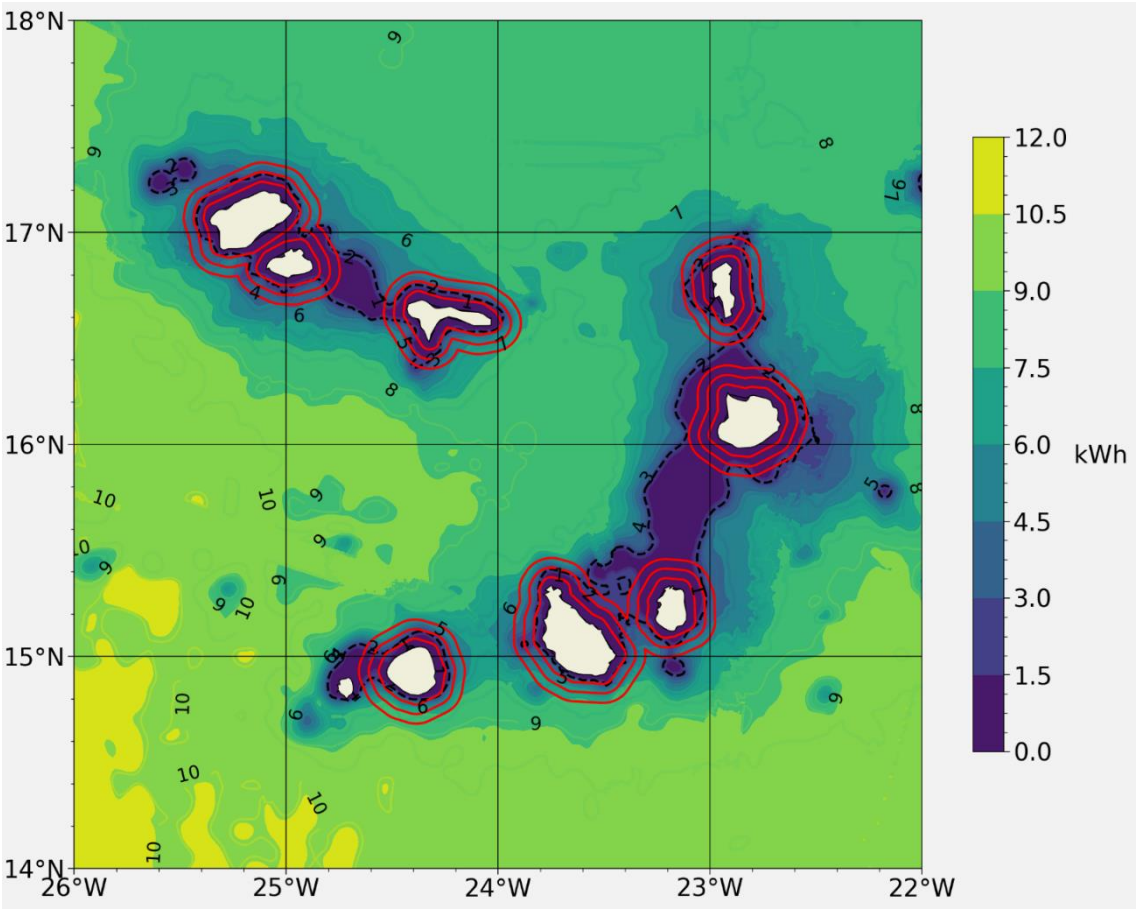

Appendix 13: Economic Interest Zone showing the 10, 15, and 20 km distance from shore.